



## Dynamics of spin charge carriers in polyaniline

V. I. Krinichnyi

Citation: [Applied Physics Reviews](#) **1**, 021305 (2014); doi: 10.1063/1.4873329

View online: <http://dx.doi.org/10.1063/1.4873329>

View Table of Contents: <http://scitation.aip.org/content/aip/journal/apr2/1/2?ver=pdfcov>

Published by the AIP Publishing

---

### Articles you may be interested in

The role of spin exchange in charge transfer in low-bandgap polymer: Fullerene bulk heterojunctions  
J. Chem. Phys. **141**, 044906 (2014); 10.1063/1.4890995

Low-temperature carrier dynamics in high-mobility organic transistors of alkylated dinaphtho-thienothiophene as investigated by electron spin resonance  
Appl. Phys. Lett. **105**, 033301 (2014); 10.1063/1.4890962

Transport properties of CdS nanowire embedded poly(3-hexyl thiophene) nanocomposite  
J. Chem. Phys. **125**, 174717 (2006); 10.1063/1.2370928

Quadrimeric recombination kinetics of photogenerated charge carriers in regioregular poly(3-alkylthiophene)/fullerene composites  
Appl. Phys. Lett. **84**, 1317 (2004); 10.1063/1.1650910

Charge carrier mobility in doped semiconducting polymers  
Appl. Phys. Lett. **82**, 3245 (2003); 10.1063/1.1572965

---

**NEW Special Topic Sections**

**NOW ONLINE**  
Lithium Niobate Properties and Applications:  
Reviews of Emerging Trends

AIP | Applied Physics  
Reviews

# APPLIED PHYSICS REVIEWS

## Dynamics of spin charge carriers in polyaniline

V. I. Krinichnyi<sup>a)</sup>

*Institute of Problems of Chemical Physics, Russian Academy of Sciences, 142432 Chernogolovka, Moscow Region, Russian Federation*

(Received 3 January 2014; accepted 7 April 2014; published online 9 May 2014)

The review summarizes the results of the study of emeraldine forms of polyaniline by multifrequency (9.7–140 GHz, 3-cm and 2-mm) wavebands Electron Paramagnetic Resonance (EPR) spectroscopy combined with the spin label and probe, steady-state saturation of spin-packets, and saturation transfer methods. Spin excitations formed in emeraldine form of polyaniline govern structure, magnetic resonance, and electronic properties of the polymer. Conductivity in neutral or weakly doped samples is defined mainly by interchain charge tunneling in the frames of the Kivelson theory. As the doping level increases, this process is replaced by a charge thermal activation transport by molecular-lattice polarons. In heavily doped polyaniline, the dominating is the Mott charge hopping between well-conducting crystalline ravelles embedded into amorphous polymer matrix. The main properties of polyaniline are described in the first part. The theoretical background of the magnetic, relaxation, and dynamics study of nonlinear spin carriers transferring a charge in polyaniline is briefly explicated in the second part. An original data obtained in the EPR study of the nature, relaxation, and dynamics of polarons as well as the mechanism of their transfer in polyaniline chemically modified by sulfuric, hydrochloric, camphorsulfonic, 2-acrylamido-2-methyl-1-propanesulfonic, and *para*-toluenesulfonic acids up to different doping levels are analyzed in the third part. Some examples of utilization of polyaniline in molecular electronics and spintronics are described. © 2014 AIP Publishing LLC.

[<http://dx.doi.org/10.1063/1.4873329>]

### TABLE OF CONTENTS

|   |    |   |    |
|---|----|---|----|
| I. INTRODUCTION .....   | 2  | III. MAGNETIC, RELAXATION, AND DYNAMICS PARAMETERS OF CHARGE CARRIERS IN POLYANILINE AS FUNCTION OF STRUCTURE AND CONCENTRATION OF DOPAND ..... | 14 |
| A. Electronic properties of polyaniline (PANI) ..   | 2  | A. Polyaniline chemically modified by sulfuric and hydrochloric acids .....   | 15 |
| B. Magnetic properties of polyaniline .....   | 4  | B. Polyaniline chemically modified by camphorsulfonic and 2-acrylamido-2-methyl-1-propanesulfonic acids .....                                   | 20 |
| II. THEORETICAL BACKGROUNDS OF SPIN RESONANCE AND SPIN TRANSFER IN CONDUCTING POLYANILINE .....   | 5  | C. Polyaniline chemically modified by <i>para</i> -toluenesulfonic acid .....   | 24 |
| A. Magnetic parameters of polarons stabilized in PANI directly obtained by EPR spectroscopy ..... | 5  | IV. UTILIZATION OF POLYANILINE IN MOLECULAR ELECTRONICS .....   | 26 |
| 1. Lande factor .....   | 5  | A. Polyaniline-based sensors for solution components .....  | 26 |
| 2. Spin susceptibility .....  | 5  | 1. Ethanol in hexane .....  | 26 |
| 3. Line shape and width .....   | 5  | 2. Citric acid in ethanol .....   | 27 |
| 4. Electron spin-spin and spin-lattice relaxation of spin-packets .....                           | 8  | 3. Nitroxide radical ATPO in ethanol .....  | 27 |
| 5. Saturation transfer EPR (ST-EPR) of paramagnetic centers in polymer semiconductors .....       | 9  | B. Spin-assisted charge transfer in polyaniline composites .....  | 27 |
| B. Spin diffusion in conducting polymers .....  | 10 | 1. EPR and light-induced EPR (LEPR) spectra of PANI-ES/P3DDT/PCBM composite .....   | 28 |
| C. Mechanisms of charge carrier transfer in conjugated polymers .....                             | 12 | 2. EPR linewidth of charge carriers in PANI-ES/P3DDT/PCBM composites .....  | 29 |

<sup>a)</sup>E-mail: kivirus@gmail.com. Fax: +7(496) 515 3588.

|  |    |
|--|----|
| 3. Spin susceptibility of charge carriers in PANI-ES/P3DDT/PCBM composites . . . . . | 30 |
| 4. Electron relaxation of polarons in PANI-ES/P3DDT/PCBM composites . . . . .        | 32 |
| V. CONCLUDING REMARKS . . . . .  | 33 |

## I. INTRODUCTION

Various low-dimensional compounds can be attributed to organic conductors, such as molecular crystals based on charge transfer complexes and ion-radical salts,<sup>1–5</sup> modified fullerenes,<sup>6–8</sup> phthalocyanine metal complexes,<sup>9</sup> dyes,<sup>10</sup> metal-filled polymers,<sup>11,12</sup> etc. These compounds are interesting from the scientific standpoint, concerning the fundamentals of charge transfer processes. Polymers<sup>13</sup> and their composites with carbon nano-materials<sup>14–18</sup> can also be classified to organic conductors. Of a particular interest are organic conducting polymers as a new class of electronic materials.<sup>3,19–31</sup> The interest to such systems was initiated at 1964 by the Little hypothesis<sup>32</sup> on the possibility of synthesis of high-temperature superconductors based on conducting polymers. They have also attracted considerable attention, since the investigation of these systems has generated entirely new scientific conceptions and a potential for their perspective application as active material for creation of components of organic molecular electronics.<sup>23–26,33</sup> Another main scientific goal is to reinforce human brain with computer ability. However, a convenient modern computer technology is based on three-dimensional silicon crystals, whereas human organism consists of low-dimensional biological systems. So, the combination of a future computer based on organic conducting polymers of lowed dimensionality with biopolymers is expected to increase considerably a power of human apprehension.

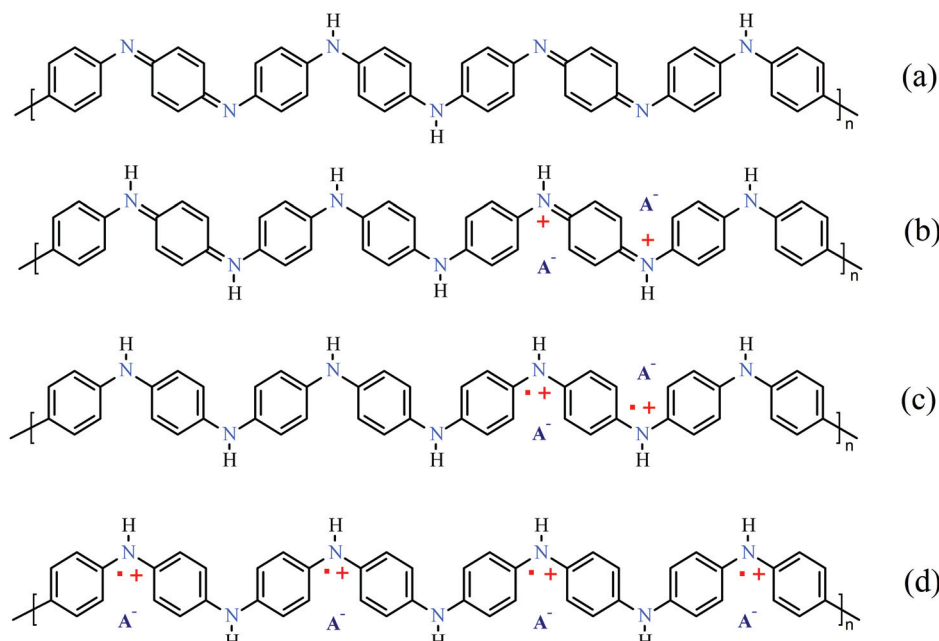


FIG. 1. Chemical structures of emeraldine base form of polyaniline (PANI-EB) (a) and its full (50%) protonation with formation of single bipolarons  $+Ph=+$  (b), polaron pairs  $+•-Ph-•+$  (c) followed by their separation in more stable emeraldine salt form (PANI-ES) with maximum doping level  $y = 0.5$  (d). Anion radicals  $A^-$  are shown.

## A. Electronic properties of polyaniline (PANI)

Within the class of conducting polymers, PANI (Fig. 1) is of particular interest because of its excellent stability under ambient conditions and well perspective of utilization in molecular electronics.<sup>34,35</sup> The PANI family is known for its remarkable insulator-to-conductor transition as a function of doping (protonation or oxidation) level  $y$  ( $y$  implies a number of dopant molecules per a repeating polymer unit, monomer).<sup>36</sup> Depending on the doping level  $y$  it can be in leucoemeraldine (LE), pernigraniline (PN), emeraldine base (EB), or emeraldine salt (ES) forms (Fig. 1). PANI-LE is fully reduced state. PANI-PN is fully oxidized state with imine links instead of amine links. These two forms are poor conductors, even when doped with an acid. PANI-EB is neutral form, whereas PANI-ES is a *p*-type semiconductor with hole charge carriers.<sup>37</sup> It is semicrystalline, heterogeneous system with a crystalline (ordered) region embedded into an amorphous (disordered) matrix.<sup>38</sup> When PANI is doped with an acid, intermediate bipolaron, and more stable polaron structures form as shown in Fig. 1. Such charge carriers transfer elemental charges during their intrachain and inter-chain diffusion as well as hopping inside and between well-ordered crystallites.<sup>39</sup> In polaron structure, a cation radical of one nitrogen acts as a hole which can transfer an elemental positive charge. The electron from the adjacent nitrogen (neutral) jumps to this hole and it becomes electrically neutral initiating motion of the holes (Fig. 1). However, in bipolaron structure, this type of movement is not possible since two holes are adjacently located (Fig. 1). This polymer differs from polyacetylene (PA), poly(*para*-phenylene) (PPP), other PPP-like organic conjugated polymers in several important aspects. In contrast with these polymers, it has no charge conjugation symmetry. Besides, both carbon rings and nitrogen atoms are involved in the conjugation. The phenyl rings of PANI can rotate or flip, significantly altering the nature of electron-phonon interaction. So, an additional

mobility of macromolecular units can modulate sufficient electron-phonon interactions and, therefore, lead to more complex mechanism of electron transfer in PANI.<sup>40,41</sup> These results are somewhat different in magnetic and charge-transport properties of PANI compared with other conducting polymers. It was shown theoretically and experimentally<sup>42</sup> that charges in PANI, as in case of other conducting polymers, are transferred by polarons moving along individual polymer chains. At low  $y$  a hopping charge transfer between polarons and bipolarons predominates in PANI. In modified polymer, a number of such charge carriers increases and their energy levels merge and form metal-like band structure, so called polaron lattice.<sup>39,43</sup> Stronger spin-orbit and spin-lattice interactions of the polarons diffusing along the chains is also characteristic of PANI. Upon protonation of PANI-EB or oxidation of PANI-LE, insulating forms of PANI their conductivity increase by more than 10 orders of magnitude whereas a number of electrons on the polymer chains remain constant in the ES form of PANI.<sup>44</sup> Such a doping is accompanied by appearance of the Pauli susceptibility,<sup>45,46</sup> characteristic for classic metals, due to formation of high-conductive completely protonated or oxidized clusters with the characteristic size about 5 nm in amorphous polymer. While doping of PANI-EB films with the sulfonated dendrimers gives direct current (*dc*) macroconductivity ( $\sigma_{dc}$ ) up to ca. 10 S/cm, the hydrogensulfated fullerenol-doped materials show metallic characteristics with room temperature (RT)  $\sigma_{dc}$  as high as<sup>47</sup> 100 S/cm that is about 6 orders of magnitude higher than the typical value for fullerene-doped conducting polymers. In some cases diamagnetic bipolarons<sup>39</sup> and/or anti-ferromagnetic interacting polaron pairs<sup>48</sup> each possessing two elemental charges can also be formed in heavily doped polymer. The effective crystallinity of polymer increases up to  $\sim$ 50%–60%. The lattice constants of the PANI-EB and PANI-ES forms are presented in Table I.

Crystallinity and, therefore, conducting properties of PANI essentially depend on structure of a dopant introduced. The mechanism of charge transfer in heavily doped PANI is also dependent sufficiently on the nature of a dopant as well as on the method of the polymer synthesis. For instance, the Fermi level in PANI doped with sulfuric (PANI-SA) or hydrochloric (PANI-HCA) acid lies in the region of localized states, therefore, is considered as a Fermi glass with localized electronic states,<sup>49</sup> whereas the Fermi level energy

TABLE I. Lattice constants (in nm) determined for PANI. Abbreviations: e.b. — emeraldine base; e.s. — emeraldine salt; p.o.r. — pseudo-orthogonal cell; o.r. — orthorhombic cell; HCA — hydrochloric acid; SA — sulfuric acid; CSA — camphorsulphonic acid; DBSA — dodecylbenzenesulphonic acid; PTSA — *p*-toluenesulfonic acid.

| Polymer                | <i>a</i> | <i>b</i> | <i>c</i> | References |
|------------------------|----------|----------|----------|------------|
| PANI (e.b.)            | 0.765    | 0.575    | 1.020    | 38         |
| PANI-HCA (e.s.)        | 0.705    | 0.860    | 0.950    | 38         |
| PANI-SA (e.s., p.o.r.) | 0.430    | 0.590    | 0.960    | 43         |
| PANI-CSA               | 0.590    | 0.100    | 0.720    | 49         |
| PANI-DBSA (o.r.)       | 1.178    | 1.791    | 0.716    | 50         |
| PANI-PTSA              | 0.440    | 0.600    | 1.100    | 51         |

$\varepsilon_F$  of PANI highly doped with camphorsulphonic acid (PANI-CSA) lies in the region of extended states governing metal behavior of the latter near the metal-insulator boundary.<sup>52,53</sup> On the other hand, optical (0.06–6 eV) reflectance measurements of e.g., in PANI-CSA<sup>49,54–56</sup> suggest that this polymer is a disordered Drude-like metal near the metal-insulator boundary due to improved homogeneity and reduced degree of structural disorder. From optical measurements, it was determined that the effective charge carrier mass  $m^* \approx 2m_e$ , the mean free path  $l^* \approx 0.7$  nm, and the density of states at the Fermi level  $n(\varepsilon_F) \approx 1$  state per eV per two ring repeat units.<sup>49,54</sup> Studies of the effect of doping level on both the electronic transport and film morphology of PANI-CSA shown a direct correlation between the degree of crystallinity (induced by hydrogen bonding with the CSA counter ion) and the metallic electronic properties.<sup>57–59</sup> This leads to the improvement of crystallinity and metallic conductivity of the polymer in the series PANI-HCA → PANI-SA → PANI-CSA at comparable modification levels. However, this deduction is not always conformed to results obtained at PANI study by other methods and other authors.<sup>3</sup>

Typical *dc* conductivity is frequently a result of various electronic transport processes and is ca.  $10 - 10^2$  S/cm for disoriented and oriented PANI-ES (see Fig. 1).<sup>36,44,52,60–67</sup> For example, this value has been determined for PANI-CSA to vary in the range  $\sigma_{dc} \approx 1.0 \times 10^2 - 3.5 \times 10^2$  S/cm at room temperature.<sup>66,68</sup> The variety of conducting properties makes difficult to investigate completely and correctly by usual experimental methods true charge dynamics along a polymer chain, which can be masked by interchain, interglobular, and other charge transfer processes. The inhomogeneity of distribution of the counter-ion molecules results in an additional complexity of experimental data interpretation.

The electronic structure of PANI-ES has been described theoretically by the metallic polaron lattice model<sup>39,69</sup> with a finite  $n(\varepsilon_F)$  value.<sup>70</sup> An analysis of experimental data on the temperature dependencies of *dc* conductivity, thermoelectric power, and Pauli-like susceptibility allowed MacDiarmid, Epstein *et al.*<sup>60,63,71–74</sup> to declare that PANI-EB is completely amorphous insulator in which quasi-three-dimensional (Q3D) granular metal-like domains of characteristic size of 5 nm are formed during its doping and transformation into PANI-ES. A more detailed study of the complex microwave (MW) dielectric constant, paramagnetic resonance linewidth, and electric field dependence of conductivity of PANI-ES<sup>38,43,60,61,63,75</sup> allowed them to conclude that both chaotic and oriented PANI-ES consist of some parallel chains strongly coupled into “metallic bundles” between which quasi-one-dimensional (Q1D) Variable Range Hopping (VRH) charge transfer occurs and in which Q3D electron delocalization takes place. The intrinsic Q3D alternating current (*ac*) conductivity of the domains was evaluated using Drude model<sup>76</sup> as  $\sigma_{ac} \cong 10^7$  S/cm at 6.5 GHz,<sup>77</sup> which was very close to the value expected by Kivelson and Heeger for the metal-like clusters in highly doped Naarmann *trans*-PA.<sup>78</sup> However, this value of the sample does not exceed  $\sigma_{ac} \cong 7 \times 10^2$  S/cm.<sup>77</sup> It means that other processes, which make difficult its determination, mask the true process of electron transfer by usual experimental methods.

## B. Magnetic properties of polyaniline

The polaronic charge carriers in PANI and other conducting polymers are characterized by electron spin  $S = 1/2$ , so then the direct Electron Paramagnetic Resonance (EPR) spectroscopy<sup>79–84</sup> is widely used for the study of relaxation and dynamics properties of such paramagnetic centers (PC) in these systems.<sup>85–88</sup> The oxidation or protonation of PANI-EB leads to the monotonically increase in PC concentration accompanied with strong line narrowing.<sup>89,90</sup> Lapkowski and Genies<sup>90</sup> and MacDiarmid and Epstein<sup>91</sup> showed the initial creation of Curie spins in EB, indicating a polaron formation, followed by a conversion into Pauli spins, which indicates the formation of the polaron lattice in high conductive PANI-ES.<sup>92,93</sup> The method enables to determine electron relaxation and diffusion of spin charge carriers even in PANI with chaotically oriented chains in scale from several macromolecular units.<sup>85,86</sup> These parameters are important to understand how relaxation and transport properties of spin charge carriers depend on the structure and dynamics of their microenvironment (lattice, anion, etc.). It should be noted that diffusion of electron spin effects nuclear relaxation of protons in PANI, so in principle the Nuclear Magnetic Resonance (NMR) spectroscopy can additionally be used for the study of electron spin dynamics in PANI.<sup>94</sup> Such investigations were mainly carried out for highly doped PANI-HCA.<sup>95–99</sup> It was noted,<sup>86</sup> however, that the data on PANI proton relaxation experimentally obtained by NMR method,<sup>95–97</sup> reflect an electron spin dynamics indirectly and consequently cannot give a correct enough conception of charge transfer in polymer. On the other hand, EPR method registers electron relaxation of spin charge carriers, which allows more precisely to determine relaxation and dynamic parameters of polarons in PANI and in other conducting polymers.

The method takes a possibility to determine both the longitudinal (spin-lattice) and the transverse (spin-spin) relaxation occurring with characteristic times  $T_1$  and  $T_2$ , respectively, as well as the diffusion of spin charge carriers along and between chains with appropriate coefficients  $D_{1D}$  and  $D_{3D}$ , respectively, even in PANI with chaotically oriented chains in scale from several macromolecular units.<sup>85,86</sup> Both relaxation times of polarons govern their peak-to-peak EPR linewidth  $\Delta B_{pp}$ , whereas the dependencies  $T_1 \propto \omega_p^{1/2}$  and  $\Delta B_{pp} \propto \omega_e^{1/2}$  (here  $\omega_p$  and  $\omega_e$  are the angular frequency of nuclear and electron spin precession, respectively) obtained by comparatively low-frequency magnetic resonance methods for highly protonated PANI-ES were interpreted in terms of their Q1D diffusion and Q3D hopping in polymer backbone.  $D_{1D}$  value was obtained to be, respectively, near to  $10^{14}$  and  $10^{12}$  rad/s and weakly depends on the doping level, while  $D_{3D}$  value strongly depends on  $y$  and correlated with both *dc* and *ac* conductivities of PANI-HCA.<sup>95</sup> The anisotropy of such motion  $A = D_{1D}/D_{3D}$  varies at room temperature from  $10^4$  in PANI-EB down to 10 in PANI-ES. This fact was interpreted in favor of existence of single high-conductive chains even in highly protonated PANI, between which Q1D charge transfer is realized.<sup>100</sup> Such an interpretation differs from the alternate model of formation

of Q3D metal-like clusters in amorphous phase of the polymer.<sup>71,72</sup> Besides, the diffusion constants were determined from EPR linewidth which may reflect different processes carrying out in PANI. Indeed, at registration frequencies less than 10 GHz, the lines of multicomponent spectra or spectra of different radicals with close magnetic resonance parameters overlap due mainly to low spectral resolution. So, linewidth of PANI at these frequencies generally represents a superposition of various contributions of localized and delocalized PC.

The presence in the PANI of oxygen molecules can also affect its magnetic resonance parameters. In this case, the change in linewidth of organic systems is normally explained by dipole-dipole interaction of polarons with spin  $S = 1/2$  with the oxygen molecules possessing sum spin  $S = 1$ . It was found<sup>101–105</sup> that oxygen can reversibly broad EPR spectrum of PANI without remarkable change of its conductivity. Initial pumping of the sample leads to more promising effect of spin-spin interaction on spin relaxation.<sup>105–108</sup> However, Kang *et al.* have shown<sup>109</sup> that the contact of PANI-HCA with air leads to reversible decrease in the intensity and increase in the width of the EPR spectrum of PANI at simultaneous decrease in its conductivity. Such change in the polymer properties was explained by the decrease of the polaron mobility at its interaction with air. The opposite effect, however, was registered in the study of polypyrrole<sup>110</sup> and PANI-HCA.<sup>111</sup> In the latter case, the diffusion of the oxygen into the polymer bulk was proposed to lead to reversible increase in the polymer linewidth and conductivity due to acceleration of a polaron motion along the polymer chain.

As in case of convenient conductors and conducting polymers, some highly doped PANI samples demonstrate EPR spectra with Dyson contribution<sup>112</sup> as a result of interaction of MW field with both the spin and spineless charge carriers.<sup>113,114</sup> This additionally results in ambiguous interpretation of the data obtained on electron relaxation and dynamics, and also on mechanism of charge transport in conducting polymers.

In the present review described the data of multifrequency (9.7 – 140 GHz), EPR study of magnetic and charge transport properties of PANI-EB and PANI-ES doped with SA, HCA, CSA as well as 2-acrylamido-2-methyl-1-propanesulfonic (AMPSA) and *para*-toluenesulfonic (PTSA) acids up to  $y \leq 0.60$  carried out in the Russian Institute of Problems of Chemical Physics in collaboration with UK and German labs.<sup>87,115–131</sup> High-Frequency EPR spectroscopy of other systems is excluded from consideration and is described in various reviews.<sup>132–137</sup> It starts with brief theoretical background necessary for the interpretation of magnetic, relaxation, and dynamics parameters of nonlinear spin carriers transferring a charge in polyaniline backbone. The main results obtained by the EPR spectroscopy in combination with the steady-state saturation of spin-packets, spin label, and probe, and saturation transfer methods in the study of the nature, relaxation, and dynamics of polarons as well as the mechanism of their transfer in polyaniline chemically modified by different dopants are summarized and analyzed in Sec. III. Some examples of utilization of polyaniline in molecular electronics finalized the review.

## II. THEORETICAL BACKGROUNDS OF SPIN RESONANCE AND SPIN TRANSFER IN CONDUCTING POLYANILINE

### A. Magnetic parameters of polarons stabilized in PANI directly obtained by EPR spectroscopy

Spin Hamiltonian of PANI can be written as

$$\begin{aligned} H = & \gamma_e \hbar m \mathbf{B}_0 - \gamma_e \hbar S \sum_{i=1} a \mathbf{I}_i \\ & - \gamma_e \gamma_p \hbar^2 \mathbf{S} \mathbf{I}_i \int \psi * (x) \frac{1 - 3 \cos^2 \theta}{r^3} \psi(x) d\tau, \end{aligned} \quad (1)$$

where  $\gamma_e$  and  $\gamma_p$  are the hyromagnetic ratio for electron and proton, respectively,  $\hbar = h/2\pi$  is the Planck constant,  $S$  is the electron spin operator,  $\mathbf{I}_i$  is  $i$ -th term of nuclear spin operator,  $= 1/3 (A_{xx} + A_{yy} + A_{zz})$  is an isotropic hyperfine interaction (HFI) constant,  $A_{ij}$  is an anisotropic HFI constants,  $\theta$  is the angle between the external magnetic field  $\mathbf{B}_0$  vector and  $\mathbf{r}$  vector, which is the vector between dipole moments of electron spin and the  $i$ -th nucleus,  $x$  is the electron spin coordinate,  $\psi(0)$  is a wave function proportional to a probability of the localization (or the density) of an unpaired electron near the interacting nucleus. The  $a$  value is not equal to zero only for the electrons, possessing a nonzero spin density  $\rho(0) = [\psi(0)]$ ,<sup>2</sup> that is, for  $s$ -electrons.

#### 1. Lande factor

The first term of Eq. (1) characterizes the Zeeman interaction of an unpaired electron characterizing by the splitting factor  $g$  with external magnetic field. If the resonance condition,

$$\hbar \omega_e = \gamma_e \hbar B_0 = g \mu_B B_0 \quad (2)$$

is fulfilled (here  $\mu_B$  is the Bohr magneton), an unpaired electron absorbs an energy quantum and is transferred to a higher excited state. It can be seen that the higher  $B_0$  (or  $\omega_e$ ) value, the higher excited state an electron can reach and the higher spectral resolution can therefore be realized. The second term of Eq. (1) defines the nuclear interaction and the third one is the contribution of nuclear Zeeman interaction.

One of the most significant characteristics of a polaron is its  $g$ -factor (Lande-factor), which is the ratio of electron mechanic momentum to a magnetic moment. It is stipulated by the distribution of spin density in PANI unit, the energy of exited configurations and its interaction with N and C nuclear. If polaron weakly interacts with own environments, its Lande-factor lies near  $g$ -factor of free electron,  $g_e = 2.00232$ . The nuclei of C and N atoms in PANI induce an additional magnetic field resulting tensoric character of its Lande-factor as<sup>81,138–140</sup>

$$\mathbf{g} = \begin{vmatrix} g_{xx} & & \\ & g_{yy} & \\ & & g_{zz} \end{vmatrix} = \begin{vmatrix} 2 \left( 1 + \frac{\lambda \rho(0)}{\Delta E_{n\pi^*}} \right) & & \\ & 2 \left( 1 + \frac{\lambda \rho(0)}{\Delta E_{\sigma\pi^*}} \right) & \\ & & 2 \end{vmatrix}, \quad (3)$$

where  $\lambda$  is the spin-orbit coupling constant,  $\rho(0)$  is the spin density,  $\Delta E_{n\pi^*}$  and  $\Delta E_{\sigma\pi^*}$  are the energies of the unpaired electron  $n \rightarrow \pi^*$  and  $\sigma \rightarrow \pi^*$  transitions, respectively. Polaron in PANI with nitrogen atom requires a small energy of  $n \rightarrow \pi^*$  transition. This leads to deviation of its  $g_{xx}$  and  $g_{yy}$  values from  $g_e$ . The inequality  $g_{xx} > g_{yy} > g_{zz} \approx g_e$  always holds for such PC in PANI and other organic conducting polymers. Thus, the  $g$ -factor anisotropy is a result of inhomogeneous distribution of additional fields along the  $x$  and  $y$  directions within the plane of the polymer  $\sigma$ -skeleton rather than along its perpendicular  $z$  direction. Multifrequency EPR spectroscopy allows to resolve some PC with near  $g$ -factors or spectral components of a PC with anisotropic  $g$ -factor.<sup>81</sup>

#### 2. Spin susceptibility

The temperature dependence of spin susceptibility  $\chi$  is also important to reveal mobile or localized character of spins and their possible interaction. For non-interacting and localized (or slightly delocalized) electrons in disordered phase, susceptibility follows the Curie law  $\chi_C \propto 1/T$ , whereas polarons delocalized in the conduction band of ordered crystallites cause temperature-independent Pauli behavior,  $\chi_P$ . However, such simple picture can be questioned for PANI and some other disordered conducting polymers because most of the spins are expected to be localized.<sup>86,141</sup> Disorder localizes electron spins and conducting polymer systems exhibit significant disorder. In this case, the additional term  $\chi_{ST}$  follows due to a possible singlet-triplet spin equilibrium in the system appears<sup>142–144</sup>

$$\begin{aligned} \chi(T) = & \chi_P + \chi_C + \chi_{ST} = N_A \mu_{\text{eff}}^2 n(\varepsilon_F) + \frac{N \mu_{\text{eff}}^2}{3k_B T} \\ & + \frac{k_1}{T} \left[ \frac{\exp(-J_{af}/k_B T)}{1 + 3 \exp(-J_{af}/k_B T)} \right]^2, \end{aligned} \quad (4)$$

where  $N_A$  is the Avogadro's number,  $\mu_{\text{eff}} = \mu_B g \sqrt{S(S+1)}$  is the effective magneton,  $k_B$  is the Boltzmann constant,  $n(\varepsilon_F)$  is the density of states per unit energy for both spin orientations per PANI monomer unit at the Fermi level  $\varepsilon_F$ ,  $N \mu_{\text{eff}}^2 / 3k_B = C$  is the Curie constant per mole-C/mol-monomer,  $k_1$  is a constant, and  $J_{af}$  is the antiferromagnetic exchange coupling constant. The contributions of the  $\chi_c$  and  $\chi_p$  terms to the total paramagnetic susceptibility depend on various factors, for example, on the nature and mobility of charge carriers can vary at the system modification. In some cases the Kahol-Clark model<sup>145,146</sup> can be more suitable for interpretation of magnetic susceptibility of PANI with couple exchanged spin pairs. According to this approach,  $N_s/2$  spin pairs randomly distributed in a polymer matrix can interact with the exchange coupling coefficient  $J$ . A small value of  $J$  corresponds to spin localization in a strongly disordered matrix. Higher value of  $J$  arises at overlapping of wave functions of spin pairs in more ordered regions. In this case effective spin susceptibility of such interacting spins should depend on temperature as<sup>145</sup>

$$\chi(T) = \frac{Ca_d}{3k_B T} \left[ 3 + \exp\left(-\frac{2J}{k_B T}\right) \right]^{-1} + \frac{C(1-a_d)}{3} \times \left\{ \frac{J}{3k_B T} + \ln\left[ 3 + \exp\left(-\frac{2J}{k_B T}\right) \right] \right\}, \quad (5)$$

where  $a_d$  is a fraction of spin pairs interacting in disordered polymer regions.

### 3. Line shape and width

In contrast with a solitary and isolated spin characterized by  $\delta$ -function absorption spectrum, the spin interaction with own environment in a real system leads typically to the change in line shape and increase of linewidth. By analyzing the shape and intensity of experimental spectral line, it is possible to get direct information about electronic processes taking part in the system under study. It is known that an electron spin is affected by local magnetic fields, induced by another nuclear and electron  $n r_{ij}$ -distanced spins<sup>147</sup>

$$B_{\text{loc}}^2 = \frac{1}{4n} \gamma_e^2 \hbar^2 S(S+1) \sum_{ij} \frac{(1 - 3 \cos^2 \theta_{ij})}{r_{ij}^6} = \frac{M_2}{3\gamma_e^2}, \quad (6)$$

where  $M_2$  is the second moment of a spectral line. If a line broadening is stipulated by local magnetic field fluctuating faster than the rate of interaction of a spin with nearest environment, the Lorentzian line with a width between positive and negative peaks  $\Delta B_{\text{pp}}^L$  and maximum intensity between these peaks  $I_L^{(0)}$  is registered at resonance frequency  $\omega_e^{(0)}$ <sup>148,149</sup>

$$I_L = \frac{16}{9} I_L^{(0)} \frac{(B - B_0)}{\Delta B_{\text{pp}}^L} \left[ 1 + \frac{4}{3} \frac{(B - B_0)^2}{(\Delta B_{\text{pp}}^L)^2} \right]^{-2}. \quad (7)$$

At slower fluctuation of an additional local magnetic field, the line is defined by Gaussian function of distribution of spin packets<sup>148,149</sup>

$$I_G = \sqrt{e} I_G^{(0)} \frac{(B - B_0)}{\Delta B_{\text{pp}}^G} \exp\left[-\frac{2(B - B_0)^2}{(\Delta B_{\text{pp}}^G)^2}\right]. \quad (8)$$

The EPR line shape due to dipole or hyperfine broadening is normally Gaussian. An exchange interaction between the spins, realized in some real paramagnetic system, may result in the appearance of more complicated line shape, described by a convolution of Lorentzian and Gaussian distribution function. This takes a possibility from the analysis of such a line shape to define the distribution, composition, and local concentrations of spins in the system. For example, if equivalent paramagnetic centers with concentration  $n$  are arranged chaotically or regularly in the system, their line shape is described by the Lorentzian and Gaussian distribution functions, respectively, with the width  $\Delta B_{\text{pp}}^L = \Delta B_{\text{pp}}^G = 4\gamma_e \hbar n$ .<sup>150</sup> In the mixed cases, the line shape transforms to Lorentzian at a distance from the center  $\delta B \leq 4\gamma_e \hbar / r^3$  (here  $r$  is a distance between magnetic dipoles) and with the width  $\Delta B_{\text{pp}}^L = 4\gamma_e \hbar n$  in the center and it becomes a Gaussian type on the tails at  $\delta B \geq \gamma_e \hbar / r^3$  and with the width of

$\Delta B_{\text{pp}}^G = \gamma_e \hbar \sqrt{n/r^3}$ . An exchange between spin-packets separated by  $\Delta \omega_{ij}$  distance with frequency  $\omega_{\text{ex}}$  should lead to an additional line broadening as<sup>138</sup>

$$\Delta B_{\text{pp}} = \Delta B_{\text{pp}}^0 + \frac{\Delta \omega_{ij}^2}{8\gamma_e \omega_{\text{ex}}}, \quad (9)$$

where  $\Delta B_{\text{pp}}^0$  is the linewidth at the absence of an interaction between PC. EPR line can additionally be broadened due to Q1D diffusion of one of the exchange interacting spins. The collision of these PC should to broad EPR spectrum by<sup>111,151</sup>

$$\delta(\Delta B_{\text{pp}}) = p \omega_{\text{hop}} C_g = k \omega_{\text{hop}} C_g \left( \frac{\alpha^2}{1 + \alpha^2} \right), \quad (10)$$

where  $p$  is the flip-flip probability during a collision of both spins,  $\omega_{\text{hop}}$  is the angular frequency of the polaron Q1D hopping along a polymer chain,  $C_g$  is the number of guest PC per each aniline ring,  $k$  is constant equal to  $1/2$  and  $16/27$  for  $S = 1/2$  and  $S = 1$ , respectively,  $\alpha = (3/2)2\pi J_{\text{ex}}/\hbar\omega_{\text{hop}}$ , and  $J_{\text{ex}}$  is a constant of spin exchange interaction. In this case, the guest spin acts as a nanoscopic probe of the polaron dynamics. If the ratio  $J_{\text{ex}}/\hbar$  exceeds the frequency of collision of both types of spins, the condition of strong interaction is realized in the system leading to a direct relation of spin-spin interaction and polaron diffusion frequencies, so  $\lim(p) = 1/2$ . In the opposite case  $\lim(p) = 9/2(\pi/\hbar)^2 (J_{\text{ex}}/\omega_{\text{hop}})^2$ . According to the spin exchange fundamental concepts<sup>151</sup> if exchange interaction changes between these limits, an appropriate  $\delta(\Delta \omega)(T)$  dependency may demonstrate extremal dependence with characteristic temperature  $T_c$ . This should evidence the realization of high and low of spin-spin interaction at  $T \leq T_c$  and  $T \geq T_c$ , respectively, as it realized in the PANI-PTSA sample (see below). An additional reason of the line broadening can be spin localization with the temperature decrease at  $T \geq T_c$ . Supposing activation character of spin-spin interaction with activation energy  $E_a$ , when  $\omega_{\text{hop}} = \omega_{\text{hop}}^0 \exp(-E_a/k_B T)$ , effective linewidth can be written as

$$\Delta B_{\text{pp}}(T) = \Delta B_{\text{pp}}^0 + \frac{k C \omega_{\text{hop}}^0 \exp(-E_a/k_B T)}{\gamma_e \left[ 1 + \left( \frac{\hbar \omega_{\text{hop}}^0 \exp(-E_a/k_B T)}{3\pi J_{\text{ex}}} \right)^2 \right]}. \quad (11)$$

Except fast electron spin diffusion, EPR line can also be broadened by the acceleration of molecular dynamics processes, for example, oscillations or slow torsion librations of the polymer macromolecules. The approach of random walk treatment provides<sup>152</sup> that such Q1D, Q2D, and Q3D spin diffusion with respective diffusion coefficients  $D_{1\text{D}}$ ,  $D_{2\text{D}}$ , and  $D_{3\text{D}}$  in the motionally narrowed regime changes the respective linewidth of a spin-packet as<sup>153</sup>

$$\Delta B_{\text{pp}} \approx \frac{\gamma_e^{1/3} (\Delta B_{\text{pp}}^0)^{4/3}}{D_{1\text{D}}^{1/3}}, \quad (12)$$

$$\Delta B_{\text{pp}} \approx \frac{\gamma_e (\Delta B_{\text{pp}}^0)^2}{\sqrt{D_{1\text{D}} D_{3\text{D}}}}, \quad (13)$$

$$\Delta B_{\text{pp}} \approx \frac{\gamma_e (\Delta B_{\text{pp}}^0)^2}{D_{3D}}, \quad (14)$$

where  $\Delta B_{\text{pp}}^0$  is an initial linewidth when the spin mobility is frozen. In accordance with this theory, at the transition from Q1D to Q2D and then to Q3D spin motion the shape of the EPR line should transform from Gaussian to Lorentzian. This approach takes a possibility to evaluate a dimension of the system under study, say from an analysis of temperature dependence of its EPR spectrum linewidth. For spin Q3D motion or exchange, the line shape becomes close to Lorentzian shape, corresponding to an exponential decay of transverse magnetization with time  $t$ , proportional to  $\exp(-\eta t)$ ; for a Q1D spin motion, this value is proportional to  $\exp(-\rho t^{3/2})$  (here  $\eta$  and  $\rho$  are constants).<sup>154</sup> So, in order to determine the type of spin dynamics in Q1D system the anamorphosis<sup>154</sup>  $I_0/I(B)$  vs.  $[(B - B_0)/\Delta B_{1/2}]^2$  (here  $\Delta B_{1/2}$  is the half-width of an integral line) is usually analyzed.<sup>61,63,155</sup> It, however, requires integrating of first derivative of signal absorption that leads to an additional error. Besides, at millimeter waveband, EPR charge carriers frequently show EPR spectrum with integral-like and derivative lines due to the anisotropy of  $g$ -factor. So, in order to analyze what line of such spectra reflects the spin motion both the anamorphoses  $I_0/I(B)$  vs.  $[(B - B_0)/\Delta B_{1/2}]^2$  and  $I_0/I(B)$  vs.  $[(B - B_0)/\Delta B_{\text{pp}}]^2$  is appeared to be more suitable. Figure 2 demonstrates how the shape of a single line changes at the defrosting of spin Q1D and Q3D mobility.

EPR line of PC in conducting solids is complicated by the fact that the magnetic term  $B_1$  of MW field used to excite resonance sets up eddy currents in the material bulk. These currents effectively confine the magnetic flux to a surface layer of thickness of order of the “skin depth.” This phenomenon affects the absorption of MW energy incident upon a sample and results in the less intensity of electron absorption

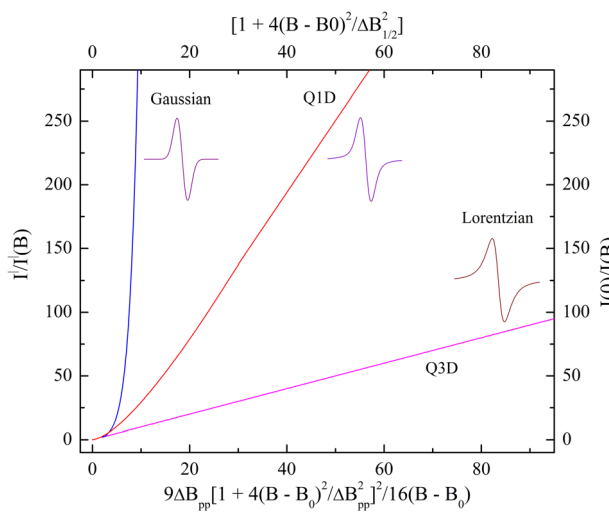


FIG. 2. The  $I_0/I(B)$  vs.  $[(B - B_0)/\Delta B_{1/2}]^2$  and  $I_0/I(B)$  vs.  $[(B - B_0)/\Delta B_{\text{pp}}]^2$  anamorphoses for EPR liner in case of spin localization and Q1D and Q3D diffusion. The Q3D spin diffusion gives Lorentzian line shape and localized spin gives Gaussian line shape. Localized spins is characterized by Gaussian line shape, Q3D spin dynamics originates EPR spectrum with Lorentzian line shape, whereas the convolution of these spectra happens at the Q1D spin diffusion. EPR spectra are shown at appropriate curves.

per unit volume of material for large particles than for small ones. This leads also to the appearance of asymmetric EPR spectra, so-called Dyson-like line<sup>112</sup> in some high-conducting inorganic substances,<sup>156</sup> organic conducting ion-radical salts,<sup>1</sup> highly doped PANI,<sup>87,88,113,114,119,121,122,124,125,129</sup> and other organic conducting polymers.<sup>85,86,88,118,157</sup>

Such effect appears when the skin-layer thickness  $\delta$  becomes comparable or thinner than a characteristic size of a sample, e.g., due to the increase of conductivity. In this case the time of charge carrier diffusion through the skin-layer becomes essentially less than a spin relaxation time and the Dysonian line with characteristic asymmetry factor  $A/B$  (the ratio of intensities of the spectral positive peak to negative one) is registered as it is shown in the inset of Fig. 3. Such line shape distortion is accompanied by the line shift into higher magnetic fields and the drop of sensitivity of EPR technique.

Generally, the Dysonian line consists of dispersion  $\chi^l$  and absorption  $\chi^u$  terms; therefore, one can write for its first derivative the following equation:

$$\frac{d\chi}{dB} = A \frac{2x}{(1+x^2)^2} + D \frac{1-x^2}{(1+x^2)^2}, \quad (15)$$

where  $x = 2(B-B_0)/\sqrt{3}\Delta B_{\text{pp}}^L$ . Organic polymers are usually studied as powder and film. Appropriate coefficients of absorption  $A$  and dispersion  $D$  in Eq. (15) for skin-layer on the surface of a spherical powder particle with radius  $R$  and intrinsic conductivity  $\sigma_{ac}$  can be calculated from the below equations,<sup>158</sup>

$$\begin{aligned} \frac{4A}{9} &= \frac{8}{p^4} - \frac{8(\sinh p + \sinh p)}{p^3(\cosh p - \cos p)} + \frac{8 \sinh p \sinh p}{p^2(\cosh p - \cos p)^2} \\ &+ \frac{(\sinh p - \sinh p)}{p(\cosh p - \cos p)} - \frac{(\sinh^2 p - \sinh^2 p)}{(\cosh p - \cos p)^2} + 1, \end{aligned} \quad (16)$$

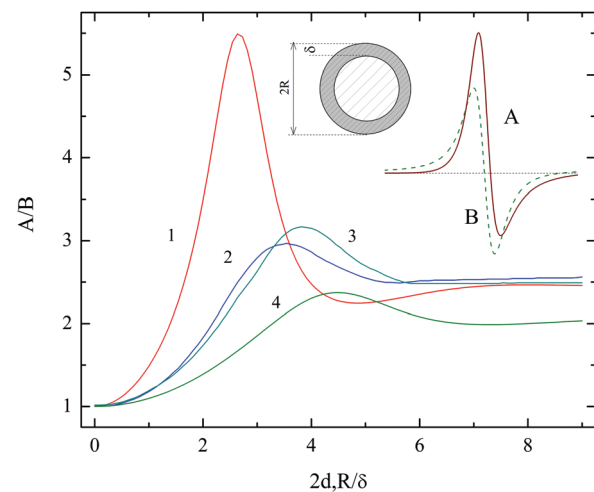


FIG. 3. The dependence of the spectrum asymmetry factor  $A/B$  on the thickness of skin-layer formed on the conducting plate (1), shank with square (2) and circular (3) section, and sphere (4). In the inset is shown a sample with characteristic size of  $2R$  and skin-layer with the thickness  $\delta$  covering its surface. EPR spectra of PC in insulating (dashed line,  $D/A = 0$ ,  $A/B = 1$ ) and conducting (solid line,  $D/A = 0.8$ ,  $A/B = 2.2$ ) materials are shown as well.

$$\frac{4D}{9} = \frac{8(\sinh p - \sin p)}{p^3(\cosh p - \cos p)} - \frac{4(\sinh^2 p - \sin^2 p)}{p^2(\cosh p - \cos p)^2} + \frac{(\sinh p + \sin p)}{p(\cosh p - \cos p)} - \frac{2 \sinh p \sin p}{(\cosh p - \cos p)^2}, \quad (17)$$

where  $p = 2R/\delta$ ,  $\delta = \sqrt{2/\mu_0\omega_e\sigma_{ac}}$ , and  $\mu_0$  is the magnetic permeability for vacuum. In case of the formation of skin-layer on the flat plate with a thickness of  $2d$  the above coefficients can be determined from relations,<sup>158</sup>

$$A = \frac{\sinh p + \sin p}{2p(\cosh p + \cos p)} + \frac{1 + \cosh p \cos p}{(\cosh p + \cos p)^2}, \quad (18)$$

$$D = \frac{\sinh p - \sin p}{2p(\cosh p + \cos p)} + \frac{\sinh p \sin p}{(\cosh p + \cos p)^2}, \quad (19)$$

where  $p = 2d/\delta$ .

From the analysis, it was determined that the line asymmetry parameter  $A/B$  is correlated with the coefficients  $A$  and  $D$  of Eq. (13) simply as  $A/B = 1 + 1.5 D/A$  independently on the linewidth. Figure 3 shows dependence of the  $A/B$  ratio on the thickness of skin-layer formed on surface of different shape. This allows to determine directly *ac* conductivity of a conducting solid from its Dysonian spectrum.

#### 4. Electron spin-spin and spin-lattice relaxation of spin-packets

According to the Boltzmann's law, electron spins being in the thermal equilibrium in an external magnetic field are distributed between ground and excited states. If this equilibrium is somehow disturbed for a certain time, e.g., by the increase of MW field, the magnetic moments of the spins relax with appropriate relaxation times  $T_1$  and  $T_2$ . These values are described by well-known Bloch's equations for a slow resonance passage and absence of MW saturation.<sup>138,150,159</sup>

A spin-packet shape is assigned by the following set of time characteristics:  $T_1$ ,  $T_2$ ,  $(\gamma_e \Delta B_{1/2})^{-1}$ ,  $\omega_m^{-1}$ ,  $(\gamma_e B_m)^{-1}$ ,  $(\gamma_e B_1)^{-1}$ , and  $B_1/(dB/dt)$ , where  $\omega_m$  and  $B_m$  are the angular frequency and intensity of a modulation field. The first three of them are stipulated by the origin of the substance and the remaining ones are the instrumental parameters. If the parameters of a spectrum registration satisfy certain inequalities, it becomes possible to analyze the behavior of a magnetization vector  $\mathbf{M}$  qualitatively. If the saturation factor  $s = \gamma_e B_1 \sqrt{T_1 T_2} = \gamma_e B_1 \tau \ll 1$  (here  $\tau$  is the effective relaxation time),  $\tau$  does not exceed precession time  $(\gamma_e B_1)^{-1}$  of  $\mathbf{M}$  vector near  $\mathbf{B}_1$  one, so then the line of spin-packet can be described by the classic analytical expressions (7) and (8). For this case, the analysis of the possible line shape distortion is sufficiently elucidated in literature (see, e.g., Refs. 160 and 161).

The saturation of spin-packets is realized as the opposite condition  $s \geq 1$  holds. In this case the intensity  $I^{(0)}$  and linewidth  $\Delta B_{pp}^{(0)}$  of their non-saturated spectrum increase non-linearly with the increase of  $B_1$  value as<sup>160</sup>

$$I = I^{(0)} B_1 (1 + \gamma_e^2 B_1^2 T_1 T_2)^{-3/2}, \quad (20)$$

$$\Delta B_{pp} = \Delta B_{pp}^{(0)} \sqrt{1 + \gamma_e^2 B_1^2 T_1 T_2}, \quad (21)$$

and the qualitative characteristics of passage effects are defined by the time of resonance passage  $B_1/(dB/dt)$  to the effective relaxation time  $\tau$  ratio. If  $B_1/(dB/dt) > \tau$ , the spin system comes to equilibrium when the sinusoidal modulation field is at one end of its excursion with a sweep rate going to zero.  $\mathbf{M}$  and  $\mathbf{B}_0$  vectors are parallel and remain unchanged during a sweep, assuming that adiabatic condition  $\gamma_e \omega_m B_m \ll \gamma_e^2 B_1^2$  holds. In this case the spectrum exhibiting the integral function of spin-packets distribution is observed at modulation method of spectra registration instead of the traditional first derivative of absorption signals or dispersion. This phenomenon was called as passage effect and is widely considered in literature<sup>162–167</sup> in terms of fast passage of saturated spin-packets. In real solids the interaction between spin-packets can be realized. The probability  $P_{cr}$  of cross-relaxation decreases strongly with the increase of a polarizing MW frequency  $\omega_e \propto B_0$  according to<sup>168</sup>

$$P_{cr} = 2\pi\sqrt{M_2} \exp\left(-\frac{\omega_e^2}{8\pi^2 M_2}\right). \quad (22)$$

This value decreases strongly with the  $\omega_e$  increase, so then the spin-packets become non-interacting and therefore can be saturated at lower  $B_1$  values. Besides, the electron relaxation time of PC in some solids can increase with the increase in  $\omega_e$ . This is the other reason for an appearance of fast passage effects at 2-mm waveband,<sup>169–171</sup> than at lower operation frequency wavebands EPR, on registering PC in different solids of lowed dimensionality.

The dispersion or absorption signal is detected as the projection of  $\mathbf{M}$  on  $+x$ -axis. If the system comes to equilibrium again at the other end of the sweep, then  $\mathbf{M}$  is initially oriented along  $+z$ -axis,  $\mathbf{M}$  and  $\mathbf{B}_{eff}$  become antiparallel during the passage, and the signal appears as the projection of  $\mathbf{M}$  on  $-x$ -axis. Thus, the signal from a single spin-packet is registered with  $\pi/2$ -out-of-phase shift with respect to the field modulation. Between two extremes,  $\omega_m T_1 \ll 1$  and  $\omega_m T_1 \gg 1$ , the first derivative of, e.g., dispersion signal  $U$  is followed from Eqs. (35) and (36) of Ref. 172 to be generally written as

$$U(\omega_e t) = u_1 g(\omega_e) \sin(\omega_e t) + u_2 g(\omega_e) \sin(\omega_e t - \pi) + u_3 g(\omega_e) \sin(\omega_e t \pm \pi/2), \quad (23)$$

where  $u_1$ ,  $u_2$ , and  $u_3$  are, respectively, the in-phase and quadrature dispersion terms.

It is obvious that  $u_2 = u_3 = 0$  without MW saturation of a spin-packets. The saturation being realized, the relative intensity of  $u_1$  and  $u_3$  components is defined by the relationship between the relaxation time of a spin-packet and the rate of its resonance field passage. If the rate of resonance passage is high and the modulation frequency is comparable or higher than effective relaxation rare  $\tau^{-1}$ , the magnetic field change is too fast and the magnetization vector of spin system does not in time for reorientation of the  $\mathbf{B}_1$  vector. At adiabatic condition,  $\omega_m B_m \ll \gamma_e B_1^2$  such delay leads to that

spin can “see” only an average applied magnetic field, and the first derivative of a dispersion signal is mainly defined by the integral  $u_2g(\omega_e)$  and  $u_3g(\omega_e)$  terms of Eq. (23) with  $u_2 = M_0\pi\gamma_e^2B_1B_mT_2/2$  and  $u_3 = M_0\pi\gamma_e^2B_1B_mT_2/(4\omega_mT_1)$ .

When the effective relaxation time is less than the modulation period,  $\tau < \omega_m$ , but exceeds the passage rate,  $\tau > B_1/(dB/dt)$ , the magnetization vector have time to relax to equilibrium state during one modulation period; therefore, the dispersion signal of a spin-packet is independent on the relationship of its resonant field and an external field  $\mathbf{B}_0$ . The sign of a signal is defined by which side the resonance is achieved. In this case the  $\pi/2$ -out-of-phase term of a dispersion signal is also registered as integral function of spin-packets distribution, and the first derivative of a dispersion signal is mainly defined by  $u_1g'(\omega_e)$  and  $u_3g(\omega_e)$  terms of Eq. (23), with  $u_1 = M_0\pi\gamma_e^2B_1B_m$  and  $u_3 = M_0\pi\gamma_e^2B_1B_mT_1T_2/2$ . Thus, the times of electron relaxation of a spin system can be estimated by registering the components of a dispersion spectrum of saturated spin-packets at appropriate phase tuning at a phase detecting.

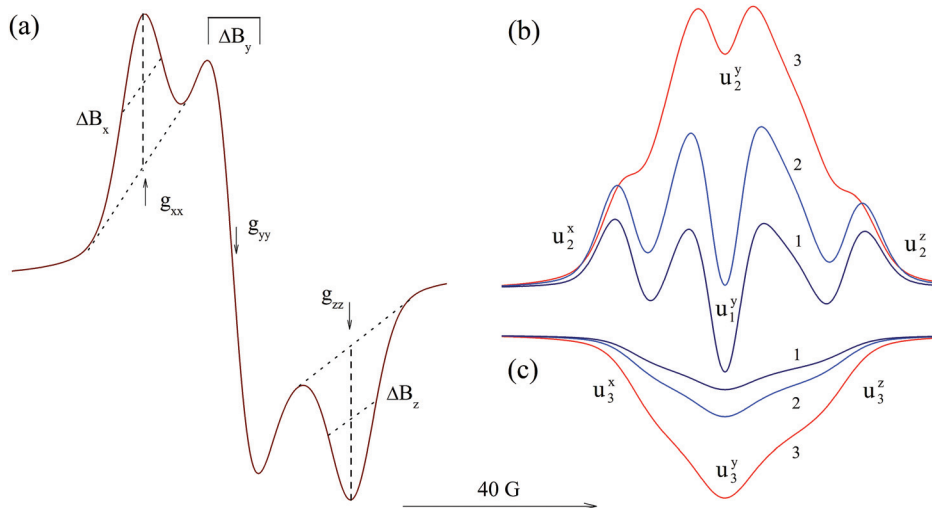
EPR spectra of saturated PC appear as an integral (almost always Gaussian) distribution function of spin-packets. Figure 4 shows the change of the shape of the in-phase and quadrature components of the 2-mm waveband dispersion signal obtained for anisotropic PC at the  $B_1$  increase. The relaxation times of adiabatically saturated PC in  $\pi$ -conducting polymers can be determined separately from the analysis of the  $u_1-u_3$  components of its dispersion spectrum as<sup>173,174</sup>

$$T_1 = \frac{3\omega_m(1+6\Omega)}{\gamma_e^2 B_{10}^2 \Omega(1+\Omega)}, \quad (24)$$

$$T_2 = \frac{\Omega}{\omega_m} \quad (25)$$

(here  $\Omega = u_3/u_2$ ,  $B_{10}$  is the polarizing field at which the condition  $u_1 = -u_2$  is valid, in-phase dispersion spectrum 2 at Fig. 4) at  $\omega_m T_1 > 1$  and

$$T_1 = \frac{\pi u_3}{2\omega_m u_1}, \quad (26)$$



at  $\omega_m T_1 < 1$ . The amplitudes of  $u_i$  components are measured in the central point of the spectra, when  $\omega = \omega_e$ . It derives from the formulas, that the determination of  $B_1$  value in the cavity center is not required for the evaluation of relatively short relaxation times.

### 5. Saturation transfer EPR (ST-EPR) of paramagnetic centers in polymer semiconductors

For the study of structurization, destruction, orientation, interdiffusion, crystallization as well as dynamics of PC and their nearest microenvironment in convenient<sup>79,175,176</sup> and conducting<sup>177</sup> polymers are widely used methods of spin label and probe based on the introduction to the polymer of reporter various radical groups, e.g., nitroxide radicals, nitrogen oxide, paramagnetic ions of transition metals, lanthanide ions, and peroxide radicals with anisotropic magnetic resonance parameters. If, e.g., PC motion is stipulated by a thermal activation with the energy  $E_a$ , the temperature dependence of correlation time of a paramagnetic probe rotation is well described by the Arrhenius equation,

$$\tau_c = \tau_c^{(0)} \exp\left(\frac{E_a}{k_B T}\right). \quad (28)$$

In high-viscous systems, PC moves with  $E_a \sim 0.08$ – $0.16$  eV with preexponential factor  $\tau_c^{(0)}$  varying within  $10^{-12}$ – $10^{-13}$  s region that is close to the times of orientation swings of molecules in condensed phase.<sup>81,139,140,175</sup> These parameters obtained for polymer systems vary in 0.19–0.76 eV and  $10^{-13}$ – $0^{-20}$  s ranges, respectively.<sup>81,139,140,147</sup> A linear dependency of  $\ln(\tau_c^{(0)})$  vs.  $E_a$  can hold for polymers, indicating the possible compensation effect and a cooperative character of molecular motion in these systems.

The method of spin label and probe enabled the study of molecular dynamics in condensed media, occurring with  $10^{-7} > \tau_c > 10^{-11}$  s. However, as in high-viscous compounds, in most low-dimensional polymer systems the molecular processes often take place with characteristic

FIG. 4. In-Phase absorption (a) and in-phase (b) and  $\pi/2$ -out-of-phase (c) dispersion spectra of paramagnetic centers with  $g_{xx} = 2.00401$ ,  $g_{yy} = 2.003126$ ,  $g_{zz} = 2.002322$ ,  $\Delta B_x = \Delta B_y = \Delta B_z = 6.2$  G obtained for  $B_1 = 0.005$  G (1),  $B_1 = B_{10}$  (2), and  $B_1 = 0.1$  G (3) at 2-mm waveband EPR. The positions of magnetic resonance parameters are shown.

correlation time  $\tau_c \geq 10^{-7}$  s. Such dynamics is studied by the ST-EPR method,<sup>162</sup> which is based on the fast passage of saturated spin-packets and broadens the correlation time range up to  $10^{-3}$  s. The literature concerning the effect of the motion of  $\pi$ -conjugated chains onto interchain charge transfer is sparse.

Both of these methods are frequently used for the study at  $\omega_e/2\pi \leq 10$  GHz,<sup>81,139,140,175</sup> which limits the method in the study of PC moving and localized on polymer chains. Robinson and Dalton showed<sup>178</sup> that the sensitivity of ST-EPR spectra to the anisotropic molecular rotations can be increased at 8-mm waveband EPR. However, the anisotropy of a resonance field stipulated by  $\mathbf{g}$  tensor is comparable to that of HFI at this waveband; therefore, the overlapping of lines attributed to different main radical orientations remains almost unchanged and, consequently, the difficulties of a registration of anisotropic superslow molecular processes and the separation of dynamic and relaxation processes are not eliminated in condensed media.

Earlier, it was demonstrated<sup>170,171,179</sup> that all terms of anisotropic  $\mathbf{g}$  and  $\mathbf{A}$  tensors of nitroxide radicals can be registered separately at 2-mm waveband EPR. This allowed to determine subtle features of structure, conformation, dynamics, etc., parameters of PC in different biological,<sup>169–171</sup> model<sup>132</sup> systems as well as macromolecular mobility in different conducting polymers.<sup>85,88,118,180</sup>

The introduction of such groups is respect not to disturb a radical microenvironment in the object under study. In the practice, however, PC usually used as labels and probes can misrepresent data obtained at  $\omega_e/2\pi \leq 10$  GHz. In contrast with nitroxide radical, the polaron with weak anisotropic magnetic parameters being native and localized on the chains of conjugated polymers becomes themselves as stable spin label. Therefore, the closest environment of such PC remains undisturbed and the results obtained on structure or spin and molecular motion become more accurate and complete. As a spectral resolution at 2-mm waveband EPR is enhanced, the opportunities of this method in more detailed study of superslow molecular motion was proved to be widened. The method allows to determine anisotropic molecular motions of the polymer macromolecules near its main axes and then to find possible correlations (modulation) involving the anisotropic spin-charge carrier's transfer and macromolecular dynamics in the system under study.

Let us introduce three critical frequencies,  $\Delta\omega$ ,  $\tau_c^{-1}$ , and  $T_1^{-1}$  (here  $\Delta\omega$  is the magnitude of the anisotropy of the magnetic interaction), then the region of the superslow tumbling domain is characterized by the inequalities  $\Delta\omega\tau_c \gg 1$  and  $100T_1 > \tau_c > 0.01T_1$ . The first inequality shows that the EPR absorption spectrum is the same as that obtained by using a rigid powder. The second inequality determines a condition for a diffusion of saturation across the spectrum, since rotational diffusion is comparable to spin-lattice relaxation rate. For nitroxide radicals, this inequality is valid in the range of  $10^{-3} > \tau_c > 10^{-7}$  s. The most sensitive to such molecular motions are the  $\pi/2$ -out-of-phase first harmonic dispersion and second harmonic absorption spectra. According to the ST-EPR method,<sup>162</sup> if the inequality,

$$\tau_c \leq \frac{2}{3\pi^2 T_1 \gamma_e^2 B_1^4} \frac{\sin^2 \vartheta \cos^2 \vartheta (B_\perp^2 - B_\parallel^2)^2}{B_\perp^2 \sin^2 \vartheta + B_\parallel^2 \cos^2 \vartheta}, \quad (29)$$

holds for a correlation time of radical rotation near, e.g.,  $x$ -axis, the adiabatic condition  $dB/dt \ll \gamma_e B_1^2$  can be realized for the radicals oriented by  $x$ -axis along  $\mathbf{B}_0$  and cannot be realized for the radicals with other orientations. This results in the elimination of the saturation of the spectra of radicals, whose  $y$  and  $z$  axes are oriented parallel to the field  $\mathbf{B}_0$  and consequently to the decrease of their contribution to the total ST-EPR spectrum. Therefore, slow spin motion should lead to an exchange of  $y$  and  $z$  spectral components and to the diffusion of saturation across the spectrum with the average transfer rate<sup>162</sup>

$$\left\langle \frac{d(\delta B)}{dt} \right\rangle = \sqrt{\frac{2}{3\pi^2 T_1 \tau_c}} \frac{\sin \vartheta \cos \vartheta (B_\perp^2 - B_\parallel^2)}{\sqrt{(B_\perp^2 \sin^2 \vartheta + B_\parallel^2 \cos^2 \vartheta)}}, \quad (30)$$

where  $\delta B$  the average spectral diffusion distance,  $B_\perp$  and  $B_\parallel$  are the anisotropic EPR spectrum components arrangement along the field,  $\vartheta$  is the angle between  $\mathbf{B}_0$  and a radical axis. One can expect to obtain more detailed information on motion when  $T_1/\tau_c \leq 1$ . Fast motion causes rapid averaging over all angles, and the details of individual random walk process are lost, whereas the motion near the rigid lattice limit the particle does not walk far enough to give much insight into the random walk process. It already has been argued<sup>162</sup> that anisotropic motions are better studied from the analysis of second-harmonic absorption  $\pi/2$ -out-of-phase spectra at  $T_1/\tau_c \leq 1$ . However, as we have showed,<sup>85,181</sup> at millimeter wavebands EPR, the first-harmonic dispersion  $\pi/2$ -out-of-phase spectra seem also to be informative for the registration of anisotropic superslow radical and spin-modified macromolecule fragments rotations, provided that a separate registration of all components of their ST-EPR spectra is carried out.<sup>136</sup> Figure 5 demonstrates how changes the ratio of an appropriate term amplitudes of  $\pi/2$ -out-of-phase dispersion signal (see Eq. (23)) with the correlation time  $\tau_c^{x,y}$  of superslow anisotropic motion near  $x$ - and  $y$ -axis at different spin-lattice relaxation time.<sup>85,181</sup> This means that registering at 2-mm waveband EPR, both terms of adiabatically saturated dispersion signal of PC with anisotropic magnetic parameters, one can determine separately first both the relaxation times and then all the parameters of superslow macromolecular dynamics. The correlation time of such anisotropic motion can be calculated from simple equation<sup>85,88</sup>

$$\tau_c^{x,y} = \tau_{c0}^{x,y} (u_3^{x,y}/u_3^{y,x})^{-\alpha}, \quad (31)$$

where  $\alpha$  is a constant determining by an anisotropy of  $g$ -factor. As in the case of other conjugated polymers with heteroatoms, this method can also be used for the study of relaxation and dynamics of polarons stabilized on chains of the PANI-EB and slightly doped PANI-ES.

## B. Spin diffusion in conducting polymers

Spin relaxation can be accelerated by molecular and spin dynamics taking part in the system. Indeed, the diffusion of

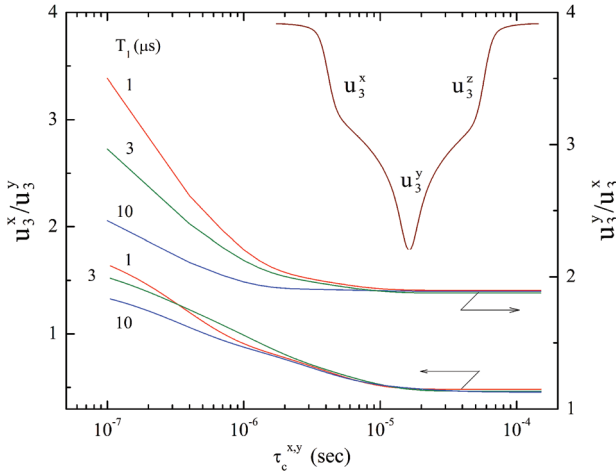


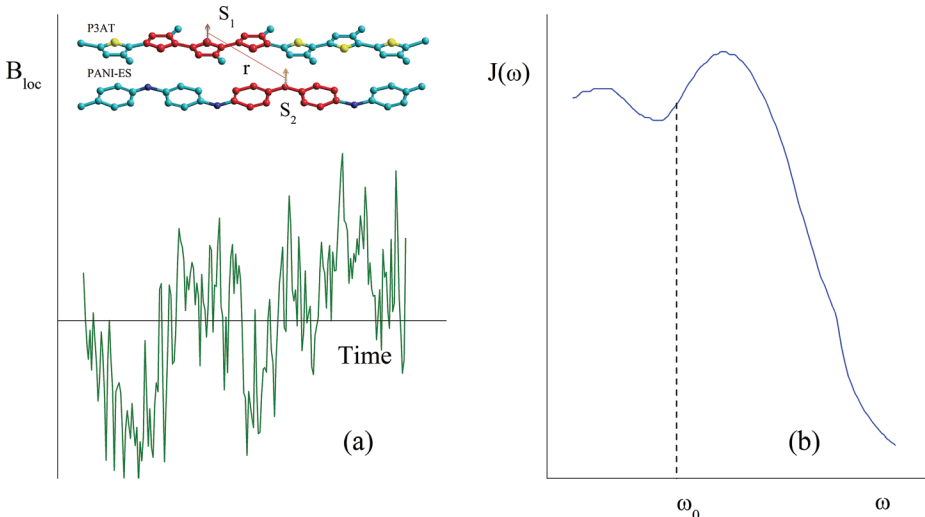
FIG. 5. Logarithmic plots of  $u_3^i/u_3^j$  ratio calculated from the  $\pi/2$ -out-of-phase first harmonic dispersion spectrum of paramagnetic centers shown in the inset with  $g_{xx}=2.00401$ ,  $g_{yy}=2.003126$ ,  $g_{zz}=2.002322$ ,  $A_{xx}=A_{yy}=A_{zz}=6.2$  G rotating near  $x$ - and  $y$ -axis versus an appropriate correlation time  $\tau_c^{xy}$  at different spin-lattice relaxation time. In the inset are also shown respective amplitudes  $u_3^i$  of components of the dispersion spectrum.

electron spin  $S_1$  shown in the inset of Fig. 6(a) along and between polymer chains induces a local magnetic field  $B_{loc}(t)$ , fluctuating rapidly with time in the situation of another electron, e.g., spin  $S_2$  (or/and nuclear) due to their dipole (and/or hyperfine) interaction. According to the theory of magnetic resonance, such spin diffusion is characterized by a translating motion propagator  $P(r, r_0, t)$ . Its  $P_{tr}(r, r_0, t)dr$  value characterizes the probability of that if the  $j$ -th particle is located in  $r_0$  point with respect to the  $i$ -th particle at the initial moment  $t=0$ , then it is located in  $r+dr$  range with respect to a new location of the  $i$ -th particle at  $t=\tau$  moment.

An analytical form of the motion propagator depends on the diffusion dynamics model, applied to condensed systems.<sup>182</sup> This parameter is a solution of a well known Brownian diffusion equation,

$$\frac{dP(r, r_0, \tau)}{dt} = \mathbf{D} \Delta P(r, r_0, \tau), \quad (32)$$

with the initial condition  $P(r, r_0, t)=\delta(r-r_0)$ , where  $\mathbf{D}=[D_i]$ ,  $D_i=\nu_i c_i$  is the diffusion coefficient,  $\nu_i$  is a



diffusion rate, and  $c_i$  is a proportionality constant, considering the discreteness of a real polymer system,  $i$  is unit vector of molecular coordinate system. The solution of Eq. (32) for the case of Q1D spin diffusion is the following:

$$P(r, r_0, \tau) = \frac{1}{\sqrt{4D_{1D}\tau}} \exp\left[-\frac{(r-r_0)^2}{4D_{1D}c_{1D}^2\tau}\right] \exp(-D_{3D}\tau), \quad (33)$$

where  $D_{1D}$  and  $D_{3D}$  are, respectively, the coefficients of spin diffusion along and between polymer chains and  $c_{1D}$  is the appropriate lattice constant. The latter exponent multiplier of Eq. (33) is introduced because of spin interaction hopping probability.

The diffusion motion has an ordered character in solids and is realized over crystal lattice centers. For this case, the motion propagator is estimated with lattice sums and depends on the symmetry and parameters of a lattice. The relationship between electron relaxation times and parameters of molecular mobility is defined by the Hamiltonian of interaction and the accepted model of molecular mobility. This relationship can be generally written as  $T_{1,2}=fJ(\omega)$ , where  $J(\omega)$  is a function of spectral density, which is of significance in EPR relaxation theory.

Let the general relationships for relaxation times be written assuming dipole-dipole interaction between equal unpaired electrons and neglecting HFI in polymer system. This yields for electron relaxation rates in polycrystalline system,<sup>138,182</sup>

$$T_1^{-1} = \langle \Delta\omega^2 \rangle [2J(\omega_e) + 8J(2\omega_e)], \quad (34)$$

$$T_2^{-1} = \langle \Delta\omega^2 \rangle [3J(0) + 5J(\omega_e) + 2J(2\omega_e)], \quad (35)$$

where  $\langle \Delta\omega^2 \rangle = \frac{1}{10} \gamma_e^4 \hbar^2 S(S+1) n \sum \sum (1 - 3 \cos^2 \theta)^2 r_1^{-3} r_2^{-3}$  is the averaged constant of the spin dipole interaction in a powder-like sample,  $n=n_1+n_2/\sqrt{2}$ ,  $n_1$  and  $n_2$  are the concentration of mobile and localized spins, respectively,

FIG. 6. Schematic explanation of the fluctuating local field  $B_{loc}$  (a) and the spectral density function  $J(\omega)$  (b) produced by spin  $S_2$  stabilizing on the PANI-ES chain and diffusing near spin  $S_1$  localized on neighboring chain of the same polymer or, e.g., P3AT and separated by the distance  $r$  (inset in a).

$$J_{1D}(\omega) = \frac{1}{\sqrt{4D_{1D}^1 D_{3D}}} \sqrt{\frac{1 + \sqrt{1 + (\omega/2D_{3D})^2}}{1 + (\omega/2D_{3D})^2}}$$

$$= \begin{cases} (2D_{1D}^1 \omega)^{-1/2}, & \text{at } D_{1D}^1 \gg \omega \gg D_{3D} \\ (2D_{1D}^1 D_{3D})^{-1/2}, & \text{at } \omega \ll D_{3D}, \end{cases} \quad (36)$$

$D_{1D}^1 = 4D_{1D}/L^2$ , and  $L$  is the number of monomer units along which a spin is delocalized. The latter value obtained for polarons and bipolarons in conjugated polymers is 4–5 and 5–5.5 monomer units, respectively.<sup>183–185</sup> In real polymer systems with “random” population of sites, one can expect distribution of interspin distances. If one propose for the simplicity that the spins are situated near the units of the cubic lattice with concentration of the monomer units  $N_c$  and constant  $r_0 = (8/3N_c)^{-1/3}$ , then  $\sum \sum (1 - 3 \cos^2 \theta)^2 r_1^{-3} r_2^{-3} = 6.8r_0^{-6}$ .<sup>150</sup> Note that for 2D spin motion  $J_{2D}(\omega) = \ln(4\pi^2 D_2/\omega)/2\pi\sqrt{D_1 D_2}$ .<sup>94</sup> If solid matrix contains spin nano-adducts pseudorotating due to interconversion between Jahn-Teller states near own main axis with correlation time  $\tau_c$ ,<sup>186–191</sup> dynamics parameters of such PC can be determined by using appropriate spin density function  $J_r(\omega_e) = 2\tau_c/(1 + \tau_c^2 \omega_e^2)$ .

### C. Mechanisms of charge carrier transfer in conjugated polymers

A superposition of different charge transfer mechanism can be realized in conducting polymers whose conductivity varies by 12–15 orders of magnitude upon doping,<sup>192</sup> e.g., Q1D diffusion and Q3D hopping of charge carriers along and between polymer chains through amorphous phase, and tunneling between high-conductive crystallites embedded into amorphous matrix. It is quite obvious, that the contributions of these processes to the total conductivity depend on the structure, the method of synthesis, and doping level of a polymer.<sup>193</sup> As polarons and bipolarons can have a major effect on the electronic states accessible for electrons, traversing a polymer, they can dramatically affect transport properties.

Despite the numerous reports on transport properties of electrically conducting polymers, no general agreement on the charge transport mechanism prevails. This is largely due to the complex structural and morphological forms that conducting polymers are characterized. Generally there are disordered systems, whose charge transport can usually be considered by a percolation phenomenon. The specific nature of (bi)polaronic charge carriers in these systems reflects the importance of electron-phonon interaction; however, their Coulomb interaction may additionally play significant role. A conjugated carbon chain is a Q1D conductor; therefore, the dimensionality is an important factor effecting an electronic properties of conducting polymers. Dimensionality plays a role when the film thickness becomes comparable to the charge carrier hopping length. Another factor strongly influencing the structure and electronic properties of the polymer characteristics is the doping. Intrinsic conductivity and mechanism of charge transfer in PANI with doping level

lying above the percolation threshold depend on the structure and number of counter-ion introduced into a polymer. At high doping level, the saturation of spin-packets decreases significantly due to the increase in direct and cross spin-spin and spin-lattice interactions. Besides, Dysonian term appears in EPR spectra of such polymers due to the formation of skin-layer on their surface. In contrast with the saturated dispersion EPR signal, the Dyson-like line shape “feels” both types of charge carriers, spin polarons, and spinless bipolarons, as effective charge ensemble, diffusing through a skin layer. The number and dynamics of each type of charge carriers can differ; thus the electronic dynamics properties of the sample should depend on its doping level. In order to determine this correctly the analysis of both the *dc* and *ac* conductivities is required.

The temperature dependence of conductivity gives important information about the electrical conduction mechanism. In both insulators and semiconductors, there is an energy gap between a low-lying completely filled valence band (VB) formed by  $\sigma$ -bonds and a partially filled conducting band (CB) formed by  $\pi$  bonds. In the absence of thermal energy, no electrons are excited to the CB and these systems become insulators. Undoped or slightly doped polymers show strong temperature dependence of the conductivity. Charge transport in such insulators and semiconductors is described as occurring via hopping between the states of the localized charge carriers. The electronic properties of moderately doped polymers are typically more difficult to interpret, because there may be several transport processes acting in parallel. In disordered systems, there are tunneling and hopping charge transfer characterizing by an appropriate temperature dependences of the conductivity. In a metal, the VB and CB overlap, so negligible thermal energy is needed for an electron to move into a vacant state. Highly doped polymer systems also demonstrate complex mixture of the charge transfer mechanisms, which contribution depends on the system doping level and homogeneity. Besides, metallic behavior of the conductivity can be realized for the highly doped polymers as well.

The conductivity of a conducting polymer due to dynamics of  $N$  spin charge carriers can be calculated from the modified Einstein relation,

$$\sigma_{1,3D}(T) = Ne^2 \mu = \frac{Ne^2 D_{1,3D} c_{1,3D}^2}{k_B T}, \quad (37)$$

where  $\mu$  is the charge carrier mobility and  $c_{1,3D}$  is the respective lattice constant.

Several models have been proposed to describe a temperature dependence of experimentally obtained conducting polymer conductivity.

Kivelson proposed<sup>194</sup> a phenomenological model for phonon-assisted hopping of electrons between soliton sites in undoped and slightly doped PA. In the frames of this model, charged solitons are coulombically bound to charged impurity sites. The excess charge on the soliton site makes a phonon-assisted transition to a neutral soliton moving along another chain. If this neutral soliton is located near charged impurity at the moment of charge carrier transfer, the energy

of the charge carrier remains unchanged before and after the hop. The temperature dependency of the conductivity is then defined by the probability of that the neutral soliton is located near the charged impurity and the initial and the final energies are within  $k_B T$ , hence both the *dc* and *ac* conductivities can be determined as<sup>194</sup>

$$\sigma_{dc}(T) = \frac{k_1 e^2 \gamma(T) \xi \langle y \rangle}{k_B T N_i R_0^2} \exp\left(\frac{2k_2 R_0}{\xi}\right) = \sigma_0 T^n, \quad (38)$$

$$\sigma_{ac}(T) = \frac{N_i^2 e^2 \langle y \rangle \xi_{||}^3 \xi_{\perp}^2 \omega_e}{384 k_B T} \left[ \ln \frac{2\omega_e L}{\langle y \rangle \gamma(T)} \right]^4 = \frac{\sigma_0 \omega_e}{T} \left[ \ln \frac{k_3 \omega_e}{T^{n+1}} \right]^4, \quad (39)$$

where  $k_1 = 0.45$ ,  $k_2 = 1.39$ , and  $k_3$  are constants,  $\gamma(T) = \gamma_0 (T/300 \text{ K})^{n+1}$  is the transition rate of a charge between neutral and charged soliton states,  $\langle y \rangle = y_n y_{ch} (y_n + y_{ch})^{-2}$ ,  $y_n$ , and  $y_{ch}$  are, respectively, the concentrations of neutral and charged carriers per monomer unit,  $R_0 = (4\pi N_i/3)^{-1/3}$  is the typical separation between impurities which concentration is  $N_i$ ;  $\xi = (\xi_{||} \xi_{\perp}^2)^{1/3}$ ,  $\xi_{||}$ , and  $\xi_{\perp}$  are dimensionally averaged, parallel, and perpendicular decay lengths for a charge carrier, respectively;  $L$  is a number of monomer units per a polymer chain. In this case a weak coupling of the charge with the polymer lattice is realized when hops between the states of a large radius take place. Note that this mechanism of charge transfer can be realized not only in conducting polymers but also in modified convenient polymers, e.g., in MnCl<sub>2</sub>-filled polyvinyl alcohol films.<sup>195</sup>

If the coupling of the charge with the lattice is stronger, multiphonon processes dominate. The mobility ultimately becomes simply activated when the temperature exceeds the phonon temperature characteristic of the highest energy phonons with which electron states interact appreciably. In this case the strong temperature dependency of the hopping conductivity is more evidently displayed in *ac* conductivity.

A comparatively strong temperature dependency for polymer conductivity can be described in the frames of the Elliot model of a thermal activation of charge carriers over energetic barrier  $E_a$  from widely separated localized states in the gap to close localized states in the VB and CB tails.<sup>196</sup> Both  $\sigma_{dc}$  and  $\sigma_{ac}$  terms of a total conductivity are defined mainly by a number of charge carriers excited to the band tails; therefore,

$$\sigma_{dc}(T) = \sigma_0 \exp\left(-\frac{E_a}{k_B T}\right), \quad (40)$$

$$\sigma_{ac}(T) = \sigma_0 T \nu_e^\gamma \exp\left(-\frac{E_a}{k_B T}\right), \quad (41)$$

where  $0 \leq \gamma \leq 1$  is a constant reflecting the dimensionality of a system under study and  $E_a$  is the energy for activation of charge carrier to extended states. As the doping level increases, the dimensionality of the polymer system rises and activation energy of charge transfer decreases. An approximately linear dependency of  $\gamma$  on  $E_a$  was registered<sup>197</sup> for some conjugated polymers. At the same time Parneix and El Kadiri<sup>198</sup> showed  $\gamma = 1 - \alpha k_B T/E_a$  ( $\alpha = 6$ ,

$E_a = 1.1 \text{ eV}$ ) dependency for, e.g., lightly doped poly(3-methylthiophene). Therefore,  $\gamma$  value can be varied in 0.3–0.8 range and it reflects the dimensionality of a system under study.

$E_a$  value can depend on the conjugation length and conformation of the polymer chains. For example,  $E_a \propto n_d$  and  $E_a \propto n_d^{1/2}$  dependencies were obtained<sup>199,200</sup> for *trans*-PA with different doping levels (here  $n_d$  is the concentration of  $sp^3$ -defects in a sample) whereas  $E_a \propto (n_\pi + 1)/n_\pi^2$  dependency was estimated<sup>201</sup> for relatively short  $\pi$ -conducting systems having  $n_\pi$  delocalized electrons. In order to reduce the band gap, the planarity of the chains in polymer matrix can be increased,<sup>38,202</sup> for example, by introducing an additional hexamerous ring to a monomer unit.<sup>203</sup>

Mott<sup>204</sup> developed the VRH model to describe electron conduction in amorphous metals. Mott balances the likelihood of tunneling between random energy electron potential wells with the likelihood of gaining enough thermal energy to move to a nearby site. In this hopping conduction process, each state can have only one electron of one spin direction. If the carrier localization is very strong, the charge will hop to the nearest state with the probability proportional to  $\exp(-E_{12}/k_B T)$ , where  $E_{12}$  is the difference between the energies of the two states. At smaller localization of charge carriers in conducting polymer, this model seems to be more suitable. As the temperature decreased, fewer states fall within the allowed energy range and the average hopping distance increases. This results in the dependence of the *dc* and *ac* conductivities of a *d*-dimensional system on temperature as<sup>205,206</sup>

$$\sigma_{dc}(T) = \sigma_0 \exp\left[-\left(\frac{T_0}{T}\right)^{\frac{1}{d+1}}\right], \quad (42)$$

$$\sigma_{ac}(T) = \frac{1}{3} \pi e^2 k_B T n^2(\varepsilon_F) \langle L \rangle^5 \omega_e \left[ \ln \frac{\omega_0}{\omega_e} \right]^4 = \sigma_0 T, \quad (43)$$

where  $\sigma_0 = 0.39 \omega_0 e^2 [n(\varepsilon_F) \langle L \rangle / (k_B T)]^{1/2}$  and  $T_0 = 16/k_B n(\varepsilon_F) z \langle L \rangle$  at  $d = 1$ ,  $\sigma_0 = \omega_0 e^2 [9/8 \pi k_B T n^{3/2}(\varepsilon_F) / \langle L \rangle]^{1/2}$  and  $T_0 = 18.1/k_B n(\varepsilon_F) \langle L \rangle^3$  at  $d = 3$  in equation for *dc* conductivity,  $\omega_0$  is a hopping attempt frequency,  $z$  is the number of nearest-neighbor chains,  $\langle L \rangle = (L_{||} L_{\perp}^2)^{1/3}$ ,  $L_{||}$ , and  $L_{\perp}$  are the averaged length of charge wave localization function and its projection in parallel and perpendicular directions, respectively, and  $T_0$  is the percolation constant or effective energy separation between localized states depending on disorder degree in amorphous regions. The conductivity is essentially determined by the phonon bath and by the distributional disorder of electron states in space and energy, respectively, above and below  $T_0$ . The distance  $R$  and average energy  $W$  of the charge carriers hopping are  $R^{-4} = 8\pi k_B T n(\varepsilon_F) / 9 \langle L \rangle$  and  $W^{-1} = 4\pi R^3 n(\varepsilon_F) / 3$ , respectively. In Mott's model, as the temperature falls to zero, the conductivity rises also to zero.

It is important to note that VRH theory was originally developed for amorphous semiconductors and does not consider specific nature of non-linear charge carriers in conducting polymers. For homogeneous systems, the localization length  $\langle L \rangle$  is greater than the disordered length scale, e.g.,

greater than the structural coherence length  $\zeta$  in a polymer which has both crystalline and amorphous regions. Since Mott's power  $T^{-1/(d+1)}$  law is usually observed in a homogeneously disordered insulating systems, the observation of a similar temperature dependence of conductivity at low temperatures in conducting polymers can evidence for presence of homogeneous disordering. For inhomogeneous systems with inhomogeneous doping, phase segregation of doped and undoped regions, partial dedoping and large-scale morphological disorder, etc., should also be taken into consideration.

Kivelson and Heeger have proposed<sup>78</sup> the model of the charge carrier scattering on the lattice optical phonons in metal-like clusters embedded into conjugated polymer matrix. In the framework of this model, the total conductivity of the polymers can be expressed in the form<sup>78,207</sup>

$$\begin{aligned}\sigma_{ac}(T) &= \frac{Ne^2 c_{1D}^2 M t_0^2 k_B T}{8\pi\hbar^3 \alpha^2} \left[ \sinh\left(\frac{E_{ph}}{k_B T}\right) - 1 \right] \\ &= \sigma_0 T \left[ \sinh\left(\frac{E_{ph}}{k_B T}\right) - 1 \right],\end{aligned}\quad (44)$$

where  $M$  is the mass of the polymer unit,  $t_0$  is the transfer integral, for the  $\pi$ -electron equal approximately to 2.5–3 eV,  $E_{ph}$  is the energy of the optical phonons, and  $\alpha$  is the constant of electron-phonon interaction, for *trans*-PA equal to  $\alpha = 4.1 \times 10^8$  eV cm<sup>-1</sup>.<sup>78</sup>

So, two main conception of charge transfer in highly doped PANI and other conducting polymers are now actual. The first of them considers an elemental charge transfer by polaron along and between individual polymer chains even in heavily doped polymers.<sup>86,94,208</sup> According to the other approach, the doping leads to the increase of number and size of metal-like domains embedded into amorphous a polymer backbone in which the polarons are considered to be localized and the charge is transferred by 3D delocalized electrons.<sup>71,72,209</sup> The formation of such Q3D crystal domains in the polymer is confirmed by the increase of its Pauli susceptibility during the polymer doping. In the framework of the latter approach the electronic and dynamics properties of the polymer are determined mainly by Q3D intradomain and Q1D interdomain charge transfer. As in case of other conducting polymers, the energy levels of polarons in crystal phase of polymer are merged into metal-like band leading to formation of polaron lattice.<sup>43,56</sup> If diamagnetic bipolarons and/or anti-ferromagnetic interacting polaron pairs each possessing two elemental charges are

formed in heavily doped polymer, it can be considered as disordered system on the metal-insulator boundary in which the charge is transferred according to the modified Drude model.<sup>56</sup> Such a system is characterized as a Fermi glass, in which the electronic states at the Fermi energy  $\varepsilon_F$  are localized due to disorder and the charge is transferred by the phonon-assisted Mott VRH between exponentially localized states near the Fermi level  $\varepsilon_F$ .<sup>210</sup>

Thus, the numerous transport mechanisms with different temperature dependencies can be realized in conducting polymers. These mechanisms are directly associated with the evolution of both crystalline and electron structures of the systems. The formation of the polaron- and bipolaron-type charge carrier states in conducting polymers leads to a variety in transport phenomena, including the contribution of such mobile non-linear excitations to the conductivity.

### III. MAGNETIC, RELAXATION, AND DYNAMICS PARAMETERS OF CHARGE CARRIERS IN POLYANILINE AS FUNCTION OF STRUCTURE AND CONCENTRATION OF DOPANT

Figure 7 shows 3-cm and 2-mm waveband EPR spectra of an initial, PANI-EB sample, and PANI slightly doped with different numbers of sulfuric acid molecules. At the 3-cm waveband PANI-EB demonstrates a Lorentzian three-component EPR signal consisting of asymmetric ( $R_1$ ) and symmetric ( $R_2$ ) spectra of paramagnetic centers which should be attributed, respectively, to localized and delocalized PC.  $R_2$  PC keep line symmetry at higher doping levels. At the 2-mm waveband the PANI EPR spectra became Gaussian and broader compared with 3-cm waveband ones (Fig. 7), as is typical of PC in other conducting polymers.<sup>88,118</sup> At this waveband delocalized PC demonstrate an asymmetric EPR spectrum at all doping levels. The analysis of EPR spectra obtained at both wavebands EPR showed that the line asymmetry of  $R_2$  PC in undoped and slightly doped PANI samples can be attributed to anisotropy of the  $g$ -factor which becomes more evident at the 140 GHz waveband EPR. The linewidth of these PC weakly depends on the temperature.

Therefore, the  $R_1$  with strongly asymmetric EPR spectrum can be attributed to a -(Ph-NH-Ph)- radical with  $g_{xx} = 2.006032$ ,  $g_{yy} = 2.003815$ ,  $g_{zz} = 2.002390$ ,  $A_{xx} = A_{yy} = 4.5$  G, and  $A_{zz} = 30.2$  G ( $R_1$ ), localized on a short polymer chain. The magnetic parameters of this radical differ weakly

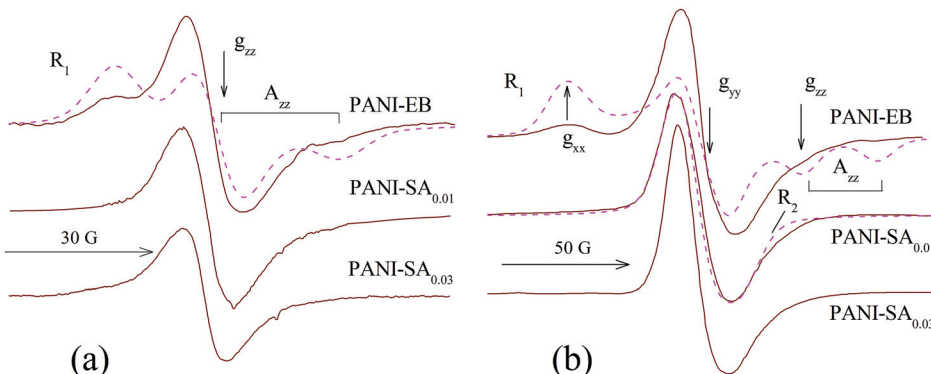


FIG. 7. Typical room temperature 3-cm (a) and 2-mm (b) waveband EPR absorption spectra of PANI-EB and this sample slightly doped by sulfuric acid. The absorption spectra calculated with  $g_{xx} = 2.006032$ ,  $g_{yy} = 2.003815$ ,  $g_{zz} = 2.002390$ ,  $A_{xx} = A_{yy} = 4.5$  G,  $A_{zz} = 30.2$  G ( $R_1$ ), and with  $g_{\perp} = 2.004394$  and  $g_{\parallel} = 2.003763$  ( $R_2$ ) are shown by dashed lines.

from those of the Ph-NH-Ph radical,<sup>139,140</sup> probably because of a smaller delocalization of an unpaired electron on the nitrogen atom ( $\rho_N^\pi = 0.39$ ) and of the more planar conformation of the latter. Assuming a McConnell proportionality constant for the hyperfine interaction of the spin with nitrogen nucleus  $Q = 23.7$  G,<sup>139,140</sup> a spin density on the heteroatom nucleus of  $\rho_N(0) = (A_{xx} + A_{yy} + A_{zz})/(3Q) = 0.55$  is estimated. At the same time another radical  $R_2$  is formed in the system with  $g = 2.004394$  and  $g_{\parallel} = 2.003763$  which can be attributed to PC  $R_1$  delocalized on more polymer units of a longer chain. Indeed, the model spectra presented in Fig. 7 well fit both the PC with different mobility. The lowest excited states of the localized PC were determined from Eq. (3) at<sup>211</sup>  $\rho_N^\pi = 0.56$  to be  $\Delta E_{n\pi^*} = 2.9$  eV and  $\Delta E_{\sigma\pi^*} = 7.1$  eV.

### A. Polyaniline chemically modified by sulfuric and hydrochloric acids

In PANI-HCA, the  $R_1$  also demonstrates the strongly anisotropic spectrum with the canonic components  $g_{xx} = 2.00522$ ,  $g_{yy} = 2.00401$ , and  $g_{zz} = 2.00228$  of  $g$  tensor, and hyperfine coupling constant  $A_{zz} = 22.7$  G (Fig. 7). Radicals  $R_2$  are registered at  $g = 2.00463$  and  $g_{\parallel} = 2.00223$ .

It was shown earlier<sup>170,171</sup> that  $g_{xx}$  and  $A_{zz}$  values of nitroxide radicals localized in a polymer are sensitive to changes in the radical microenvironmental properties, for example, polarity and dynamics. The shift of the PC  $R_2$  spectral X component to higher fields with y and/or a temperature increase may be interpreted not only by the growth of the polarity of the radical microenvironment but also by the acceleration of the radical dynamics near its main molecular X axis. The effective  $g$ -factors of both PC are near to one another, i.e.,  $\langle g_1 \rangle = 1/3(g_{xx} + g_{yy} + g_{zz}) \approx \langle g_2 \rangle = 1/3(2g + g_{\parallel})$ . This indicates that the mobility of a fraction of radicals  $R_1$  along the polymer chain increases with the polymer doping. Such a depinning of the mobility results in an exchange between the spectral components of the PC and, hence, to a decrease in the anisotropy of its EPR spectrum. In other words, radical  $R_1$  transforms into radical  $R_2$ , which can be considered as a

polaron diffusing along a polymer chain with a minimum diffusion rate,<sup>212,213</sup>

$$D_{1D}^0 \geq \frac{(g_{\perp} - g_{\parallel})\mu_B B_0}{\hbar}, \quad (45)$$

equal to  $6.5 \times 10^8$  rad/s.

As in case of other conducting polymers, at the 2-mm waveband in both in-phase and  $\pi/2$ -out-of-phase components of the dispersion EPR signal of neutral and slightly doped PANI, the bell-like contribution with Gaussian spin packet distributions due to the adiabatically fast passage of the saturated spin packets by a modulating magnetic field is registered (Fig. 7). This effect was not observed earlier in studies of PANI at lower registration frequencies.<sup>86,157</sup> It can be used for determining of relaxation and dynamics parameters of these PC.

Relaxation times of an initial and slightly doped PANI-SA and PANI-HCA samples calculated from Eqs. (24) to (27) are shown in Fig. 8 as functions of temperature. The figure demonstrates that the increase in the doping level of the polymer leads to shortening of the effective relaxation times of PC, which can be due to an intensification of the spin exchange with the lattice and with other spins stabilized on neighboring polymer chains of highly conducting domains. It should be noted that spin relaxation in the polymer at high temperatures are mainly determined by the Raman interaction of the charge carries with lattice optical phonons. The probability and rate of such a process are dependent on the concentration  $n$  of the PC localized, e.g., in ionic crystals ( $W_R \propto T_1^{-1} \propto n^2 T^7$ ) and in  $\pi$ -conjugated polymers ( $W_R \propto T_1^{-1} \propto nT^2$ ).<sup>214</sup> The available data suggest that the  $T_1^{-1}$  values of PC in slightly (up to  $y \leq 0.03$ ) doped PANI are described by a dependence of the type  $T_1^{-1} \propto nT^{-k}$ , where  $k = 3 - 4$ . The  $k$  exponent decreases with the  $y$  increase. This indicates the appearance of an additional channel of the energy transfer from the spin ensemble to the lattice at the polymer doping, as is the case in classical metals. At a medium degree of oxidation  $y \geq 0.21$ , the electronic relaxation times become comparable and only slightly temperature dependent because of an intense spin-spin exchange

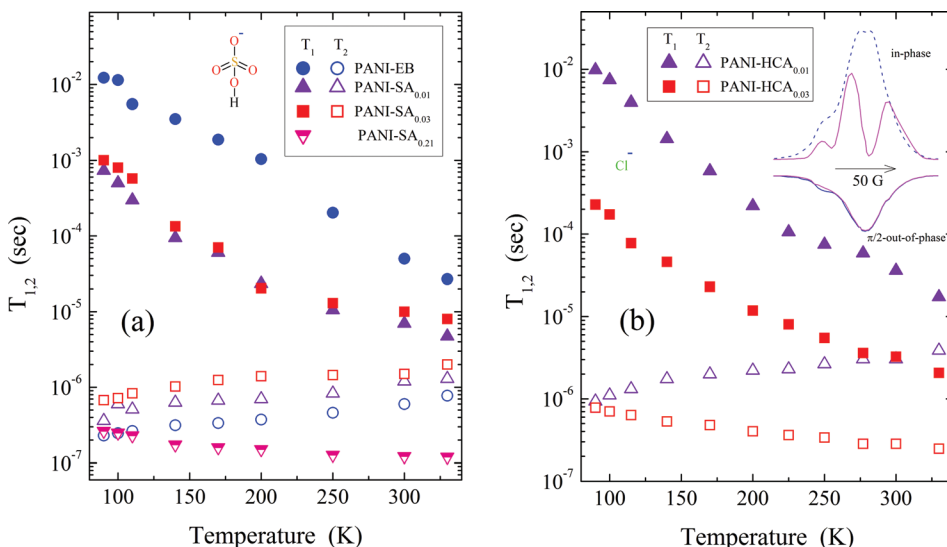


FIG. 8. Temperature dependences of spin-lattice and spin-spin relaxation times of polarons in emeraldine base form of PANI, PANI-EB, as well as in emeraldine base form of PANI, doped with sulfuric (PANI-SA (a)) and hydrochloric (PANI-HCA (b)) acids with different doping levels  $y$  calculated using Eqs. (24)–(27). In the inset, solid and dashed lines show 2-mm waveband EPR in-phase and  $\pi/2$ -out-of-phase dispersion spectra of PANI-EB registered at 300 and 200 K, respectively.

in metal-like domains of higher effective dimensionalities. Providing that  $T_1 = T_2$  for the PANI sample with  $y = 0.21$ , an effective rate of Q1D and Q2D spin motions in this polymer can be evaluated as well. It seems that both the rates calculated in the frameworks of such spin diffusions should be near to one another.

The shape of  $\pi/2$ -out-of-phase dispersion signal of PC localized in PANI-EB changes with the temperature (Fig. 8) indicating the defrosting of anisotropic macromolecular librations in this polymer. The correlation of such motions was determined from Eq. (31) with  $\tau_{c0}^x = 5.4 \times 10^{-8}$  s and  $\alpha = 4.8$  to be  $\tau_c^x = 3.5 \times 10^{-5} \exp(0.015 \text{ eV}/k_B T)$ . Similar dependencies were also obtained for slightly doped samples. The activation energy of the polymer chains librations lies near to that determined for PANI-HCA.<sup>119</sup> Upper limit for correlation time, calculated using Eq. (29) with  $\vartheta = 45^\circ$ ,  $B_1 = 0.1$  G,  $g_{xx}$  and  $g_{zz}$  values measured for  $R_1$  PC, is equal to  $1.3 \cdot 10^{-4}$  s and corresponds to  $u_3^x/u_3^y = 0.22$  [see Eq. (29)] at 125 K.

The relaxation times of electron and proton spins in PANI should vary depending on the spin precession frequency as  $T_{1,2} \propto n^{-1} \omega_e^{1/2}$ .<sup>95</sup> This is a case for PANI-SA and PANI-HCA; therefore, the experimental data obtained for these polymers can be explained by a modulation of electronic relaxation by Q1D diffusion of  $R_2$  radicals along the polymer chain, and by Q3D hopping of these centers between chains with the diffusion coefficients  $D_{1D}$  and  $D_{3D}$ , respectively.

Figure 9 shows the temperature dependences of dynamic parameters  $D_{1D}$  and  $D_{3D}$  calculated for both types of PC in several PANI samples from the data presented in Fig. 8 using Eqs. (34)–(36) at  $L \cong 5$ .<sup>184</sup> It seems to be justified that the anisotropy of the spin dynamics is maximum in the initial PANI sample, and decreases as  $y$  increases.

It was found at  $\omega_e/2\pi \leq 10$  GHz<sup>95</sup> that the high anisotropy of the spin dynamics is retained in PANI-HCA with  $y = 0.6$  even at room temperature. However, our experimental data indicate that the anisotropy of the motion of the charge carriers is high only in PANI-HCA and PANI-SA with  $y < 0.21$ . Such a discrepancy is likely due to the

limitations appearing at the study of spin dynamics at low frequencies. At  $y \geq 0.21$ , the system dimensionality seems to grow in PANI-ES, and at high temperatures the spin motion tends to become almost isotropic. The increase in the dimensionality at the polymer doping is accompanied by a decrease in the number of electron traps, which reduces the probability of electron scattering by the lattice phonons and results in the virtually isotropic spin motion and relatively slight temperature dependences of both the electronic relaxation and diffusion rates of PC, as is the case for amorphous inorganic semiconductors.<sup>205,215</sup>

By assuming that the diffusion coefficients  $D$  of spin and diamagnetic charge carriers have the same values, one can obtain from Eq. (37)  $\sigma_{1D} = 0.1$  S/cm and  $\sigma_{3D} = 1 \times 10^{-5} - 5 \times 10^{-3}$  S/cm at room temperature for the PANI-HCA sample with  $0 < y < 0.03$ . At  $D_{1D} = D_{3D}$ , these values were determined to be  $\sigma_{1D} = 50 - 180$  and  $\sigma_{3D} = 30 - 100$  S/cm. Thus, the conclusion can be drawn that  $\sigma_{3D}$  grows more strongly with  $y$  that is the evidence for the growth of a number and a size of 3D quasi-metal domains in PANI-ES.

Let us consider the charge transfer mechanisms in the initial and slightly doped PANI samples. The fact that the spin-lattice relaxation time of PANI is strongly dependent on the temperature (see Fig. 8) means that, in accordance with the energy conservation law, electron hops should be accompanied by the absorption or emission of a minimum number of lattice phonons. Multiphonon processes become predominant in neutral PANI because of a strong spin-lattice interaction. For this reason, an electronic dynamics process occurring in the polymer should be considered in the framework of Kivelson's formalism<sup>194,216,217</sup> of isoenergetic electron transfer between the polymer chains involving optical phonons, because spin and spinless charge carriers probably exist even in an undoped polymer (see Fig. 7). Figure 10 shows that the experimental data for  $\sigma_{1D}$  of the initial PANI sample is fitted well by Eq. (39) with  $\sigma_0 = 2.7 \times 10^{-10}$  S K s cm<sup>-1</sup>,  $k_3 = 3.1 \times 10^{12}$  s K<sup>9.5</sup>, and  $n = 8.5$ . In contrast to undoped *trans*-PA, some quantity of charged carriers exist even in the initial, PANI-EB sample, so the above Kivelson

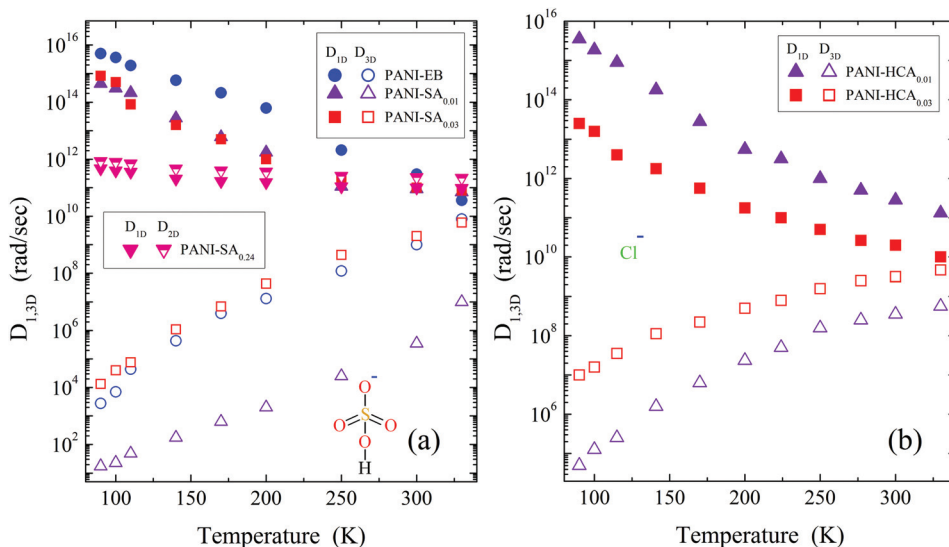


FIG. 9. Temperature dependences of coefficients of the intrachain and inter-chain polaron diffusion in undoped, PANI-EB as well as in PANI-SA (a) and PANI-HCA (b) samples with different doping levels calculated using Eqs. (34)–(36). Counter-ions SA and HCA are shown schematically.

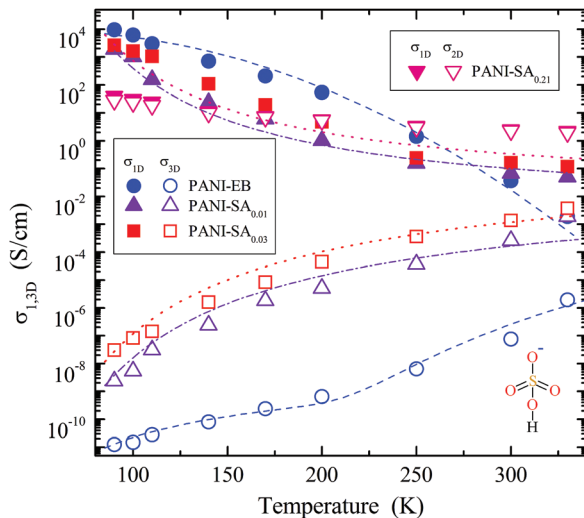


FIG. 10. Temperature dependency of the *ac* conductivity due to polaron motion along ( $\sigma_{1D}$ , filled symbols) and between ( $\sigma_{3D}$ , open symbols) polymer chains in the PANI-EB and slightly doped PANI-SA samples as well as an effective rate of spin diffusion in PANI-SA<sub>0.21</sub> calculated, respectively, in the framework of Q1D (closed symbols) and Q2D (semi-filled symbols) spin transport. The lines show the dependence calculated from Eq. (39) with  $\sigma_0 = 2.7 \times 10^{-10} \text{ S K}^{-1} \text{ s cm}^{-1}$ ,  $k_3 = 3.1 \times 10^{12} \text{ s K}^{-0.5}$ , and  $n = 8.5$  (upper dashed line), those calculated from Eq. (44) with  $\sigma_0 = 3.95 \times 10^{-6} \text{ S cm}^{-1} \text{ K}^{-1}$  and  $E_{ph} = 0.12 \text{ eV}$  (upper dashed-dotted line),  $\sigma_0 = 1.75 \times 10^{-6} \text{ S cm}^{-1} \text{ K}^{-1}$  and  $E_{ph} = 0.11 \text{ eV}$  (upper dotted line), and those calculated from Eq. (41) with  $\sigma_0 = 8.2 \times 10^{-21} \text{ S K}^{-1} \text{ s}^{0.8} \text{ cm}^{-1}$  and  $E_a = 0.033 \text{ eV}$  (low temperature region) and  $\sigma_0 = 3.9 \times 10^{-12} \text{ S K}^{-1} \text{ s}^{0.8} \text{ cm}^{-1}$  and  $E_a = 0.41 \text{ eV}$  (high temperature region) (lower dashed line),  $\sigma_0 = 4.5 \times 10^{-14} \text{ S K}^{-1} \text{ s}^{0.8} \text{ cm}^{-1}$  and  $E_a = 0.102 \text{ eV}$  (lower dashed-dotted line),  $\sigma_0 = 3.1 \times 10^{-13} \text{ S K}^{-1} \text{ s}^{0.8} \text{ cm}^{-1}$  and  $E_a = 0.103 \text{ eV}$  (lower dotted line).

mechanism can determine its conductivity. Such an approach is not evident for PANI doped up to  $0.01 \leq y \leq 0.03$  with less strong temperature dependence. The model of charge carrier scattering on optical phonons of the lattice of metal-like domains described above seems to be more convenient for the explanation of the behavior of their conductivity.

The concentration of mobile spins in PANI-HCA<sub>0.01</sub> sample is  $y_p = 6.1 \times 10^{-5}$  per one benzoid ring. Taking into account that each bipolaron possesses dual charge,  $y_{bp} = 1.2 \times 10^{-3}$  and  $\langle y \rangle = 2.3 \times 10^{-2}$  can be obtained. The concentration of impurity is  $N_i = 2.0 \times 10^{19} \text{ cm}^{-3}$ , so then the separation between them  $R_0 = (4\pi N_i/3)^{-1/3} = 2.28 \text{ nm}$  is obtained for this polymer. The prefactor  $\gamma_0$  in Eqs. (38) and (39) is evaluated from the  $\sigma_{dc}(T)$  dependence to be  $3.5 \times 10^{19} \text{ s}^{-1}$ . Assuming spin delocalization over five polaron sites along the polymer chain,<sup>184</sup>  $\zeta_{||} = 1.19 \text{ nm}$  is obtained as well. The decay length of a carrier wave function perpendicular to the chain can be determined from the relation,<sup>216,217</sup>

$$\zeta_{\perp} = \frac{b}{\ln(\Delta_0/t_{\perp})}, \quad (46)$$

where  $2\Delta_0$  is the band gap and  $t$  is the hopping matrix element estimated as<sup>218</sup>

$$t_{\perp}^2 = \frac{\hbar^4 \omega_{ph}^3 D_{3D}}{2\pi E_p} \exp\left(\frac{2E_p}{\hbar\omega_{ph}}\right), \quad (47)$$

where  $E_p$  is the polaron formation energy. Using  $2\Delta_0 = 3.8 \text{ eV}$ ,<sup>219</sup> typical for  $\pi$ -conjugated polymers  $E_p \approx 0.1 \text{ eV}$ ,<sup>218</sup>

$D_{3D} = 3.6 \times 10^8 \text{ rad/s}$  determined for PANI-HCA<sub>0.01</sub>,  $t = 7.1 \times 10^{-3} \text{ eV}$ ,  $\xi = 0.079 \text{ nm}$ , and  $\zeta = 0.20 \text{ nm}$  are obtained for this sample. The similar procedure gives  $\langle y \rangle = 7.9 \times 10^{-2}$ ,  $\gamma_0 = 2.1 \times 10^{17} \text{ s}^{-1}$ ,  $\xi = 0.087 \text{ nm}$ , and  $\zeta = 0.21 \text{ nm}$  for PANI-HCA<sub>0.03</sub> sample with  $y_p = 1.1 \times 10^{-3}$  and  $y_{bp} = 1.2 \times 10^{-2}$ .

As can be seen in Fig. 10, the  $\sigma_{1D}(T)$  dependence for the PANI-SA<sub>0.01</sub> and PANI-SA<sub>0.03</sub> samples is fairly well fitted using Eq. (44) with  $E_{ph} = 0.12$  and  $0.11 \text{ eV}$ , respectively. These values are near to energy (0.19 eV) of the polaron pinning in heavily doped PANI-ES.<sup>220</sup> The strong temperature dependence  $\sigma_{3D}$  of the initial sample can probably be interpreted in the framework of the model for the activation charge transfer between the polymer chains described by Eq. (41) with  $E_a$  equal to 0.033 and 0.41 eV for low- and high-temperature regions, respectively (Fig. 10). The activation energy of interchain charge transfer in slightly doped samples is  $E_a = 0.102 \text{ eV}$  for PANI-SA<sub>0.01</sub> and  $E_a = 0.103 \text{ eV}$  for PANI-SA<sub>0.03</sub> (Fig. 10).

Note that the spin diffusion coefficients and consequently the conductivities, calculated from the spin relaxation of PANI-ES with  $y = 0.21$ , in frameworks of one- and two-dimensional spin diffusion are near to one another (Figs. 9 and 10). This fact can possibly be interpreted as the result of the increase of system dimensionality above the percolation threshold lying around  $y \approx 0.1$ . However, this can be also due to the decrease in accuracy of the saturation method at high doping levels. In this case, the dynamics parameters of both spin and spinless charge carriers can be evaluated from the Dyson-like EPR spectrum of PANI with  $y \geq 0.21$  using the method described above.

The *g*-factor of PC  $R_2$  in PANI-SA with  $y \geq 0.21$  becomes isotropic and decreases from  $g_{R2} = 2.00418$  down to  $g_{iso} = 2.00314$ . This is accompanied by a narrowing of the  $R_2$  line (Fig. 11). Such effects can be explained by a further depinning of Q1D spin diffusion along the polymer chain, and therefore spin delocalization, and by the formation of areas with high spin density in which a strong exchange of spins on neighboring chains occurs. This is in agreement with the supposition<sup>60,63,71–74</sup> of formation in amorphous PANI-EB of high-conductive massive domains with 3D delocalized electrons.

Figure 11 shows the dependency of linewidth of the PANI-SA on the temperature and doping level. The predominance of extremal  $\Delta B_{pp}(T)$  curves evidences for the dipole-dipole exchange of PC in the system described by Eq. (10). The reason of such exchange can be an interaction of PC localized on neighboring polymer chains modulated by macromolecular librations. Assuming activation character of this chain motion, the dependences presented in Fig. 11 were fitted by Eq. (11) with the parameters summarized in Table II. The activation energy of spin-spin interaction  $E_a$  decreases at the increase of polarizing magnetic field and lies near activation energy of the macromolecular librations (0.015 eV) determined above. This is an evidence of the dependency of the spin-spin interaction on an external magnetic field and its correlation with macromolecular dynamics in the system. The  $\Delta B_{pp}(T)$  dependences presented evidence also of different charge transport mechanisms in this

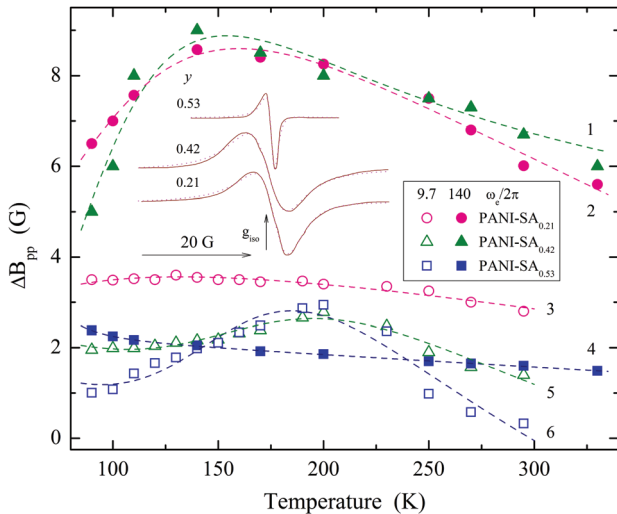


FIG. 11. Temperature dependence of linewidth of PC in PANI-SA with different doping levels registered at 3-cm and 2-mm wavebands. The dependences calculated from Eq. (11) with  $\omega_{\text{hop}}^0 = 5.1 \times 10^{16} \text{ s}^{-1}$ ,  $E_a = 0.021 \text{ eV}$ ,  $J_{\text{ex}} = 0.59 \text{ eV}$  (1),  $\omega_{\text{hop}}^0 = 9.5 \times 10^{15} \text{ s}^{-1}$ ,  $E_a = 0.018 \text{ eV}$ ,  $J_{\text{ex}} = 0.19 \text{ eV}$  (2),  $\omega_{\text{hop}}^0 = 7.5 \times 10^{15} \text{ s}^{-1}$ ,  $E_a = 0.021 \text{ eV}$ ,  $J_{\text{ex}} = 0.72 \text{ eV}$  (3),  $\omega_{\text{hop}}^0 = 9.3 \times 10^{17} \text{ s}^{-1}$ ,  $E_a = 0.024 \text{ eV}$ ,  $J_{\text{ex}} = 0.66 \text{ eV}$  (4),  $\omega_{\text{hop}}^0 = 1.7 \times 10^{17} \text{ s}^{-1}$ ,  $E_a = 0.051 \text{ eV}$ ,  $J_{\text{ex}} = 0.64 \text{ eV}$  (5), and  $\omega_{\text{hop}}^0 = 1.9 \times 10^{17} \text{ s}^{-1}$ ,  $E_a = 0.052 \text{ eV}$ ,  $J_{\text{ex}} = 0.49 \text{ eV}$  (6) are shown by dashed lines. Inset—RT 2-mm waveband absorption spectra of PC in PANI-SA with different doping levels  $y$ . Top-down dotted lines present the spectra calculated from Eqs. (15) to (17) with respective  $D/A = 0.895$ ,  $\Delta B_{\text{pp}} = 1.48 \text{ G}$ ,  $D/A = 0.16$ ,  $\Delta B_{\text{pp}} = 7.10 \text{ G}$ , and  $D/A = 0.53$ ,  $\Delta B_{\text{pp}} = 5.86 \text{ G}$ . The position of isotropic  $g$ -factor,  $g_{\text{iso}}$ , is shown.

polymer with different doping levels. The mechanism affecting the linewidth, however, depends also on the electron precession frequency, so then the linewidth does not directly reflects the relaxation and dynamics parameters of PC in this polymer.

The doping of the PANI with sulfuric acid leads to an inverted  $\Lambda$ -like temperature dependence of an effective paramagnetic susceptibility (see Fig. 12), as occurs in the case of polyaniline perchlorate.<sup>114</sup> However, this does not lead to a strong narrowing of the PC line (Fig. 11). As in the case of, e.g., PANI treated with ammonia, this should indicate a strong antiferromagnetic spin interaction due to a singlet-triplet equilibrium in the PANI-SA which total paramagnetic susceptibility can be described by Eq. (4). Indeed, Fig. 12 shows that the paramagnetic susceptibility experimentally determined for the PANI-SA samples is well reproduced by Eq. (4) with the parameters also presented in Table II. The  $J_{\text{af}}$  value is close to that (0.078 eV) obtained for the ammonia treated PANI.<sup>114</sup> Note that  $n(\varepsilon_F)$  determined for PANI-SA, consistent with those determined earlier for PANI heavily doped with other counter-ions.<sup>45,55,221</sup> With the assumption of a metallic behavior one can estimate that the energy of  $N_P$  Pauli spins in, e.g., PANI-ES, with  $0.21 \leq y \leq 0.53$  at the Fermi level<sup>215</sup>  $\varepsilon_F = 3N_P/2n(\varepsilon_F)$  is to be 0.1–0.51 eV.<sup>125</sup> This value lies near to that (0.4 eV) obtained, e.g., for PANI-CSA.<sup>54</sup> From this value, the number of charge carriers with mass  $m_c = m_e$  in heavily doped PANI-SA,<sup>215</sup>  $N_c = (2m_c\varepsilon_F/\hbar^2)^{3/2}/3\pi^2 \approx 1.7 \times 10^{21} \text{ cm}^{-3}$  is evaluated. The  $N_c$  value is close to a total spin concentration in PANI-SA.

TABLE II. The  $\Delta B_{\text{pp}}^0$  (in G),  $\omega_{\text{hop}}^0$  (in  $10^{16} \text{ rad/s}$ ),  $E_a$  (in eV),  $J_{\text{ex}}$  (in eV) parameters calculated from Eq. (11), and the  $\chi_P$  (in emu/mol one ring),  $n(\varepsilon_F)$  (in states/eV one ring),  $C$  (in emu K/mol one ring),  $k_1$  (in emu K/mol one ring), and  $J_{\text{af}}$  (in eV) values determined from Eq. (4) for different PANI samples.

| Polymer                                  | $\Delta B_{\text{pp}}^0$ | $\omega_{\text{hop}}^0$ | $E_a$ | $J_{\text{ex}}$ | $\chi_P$             | $n(\varepsilon_F)$ | $C$                  | $k_1$                | $J_{\text{af}}$ |
|--|--------------------------|-------------------------|-------|-----------------|----------------------|--------------------|----------------------|----------------------|-----------------|
| PANI-SA <sub>0.21</sub> <sup>a</sup>     | 4.5                      | 0.75                    | 0.021 | 0.72            |                      |                    |                      |                      |                 |
| PANI-SA <sub>0.21</sub> <sup>b</sup>     | 4.6                      | 0.96                    | 0.018 | 0.19            | $3.1 \times 10^{-5}$ | 0.65               | $1.2 \times 10^{-2}$ | 4.2                  | 0.051           |
| PANI-SA <sub>0.42</sub> <sup>a</sup>     | 3.1                      | 17                      | 0.051 | 0.64            |                      |                    |                      |                      |                 |
| PANI-SA <sub>0.42</sub> <sup>b</sup>     | 2.7                      | 5.1                     | 0.021 | 0.59            |                      | 0.90               |                      |                      |                 |
| PANI-SA <sub>0.53</sub> <sup>a</sup>     | 2.5                      | 17                      | 0.052 | 0.49            |                      |                    |                      |                      |                 |
| PANI-SA <sub>0.53</sub> <sup>b</sup>     | 2.4                      | 93                      | 0.024 | 0.66            | $1.4 \times 10^{-3}$ | 1.4                | $1.6 \times 10^{-2}$ | 48.6                 | 0.057           |
| PANI-HCA <sub>0.50</sub>                 |                          |                         |       |                 | 1.9                  |                    |                      |                      |                 |
| PANI-AMPSA <sub>0.4</sub> <sup>a,c</sup> |                          |                         |       |                 | $9.8 \times 10^{-7}$ |                    | $4.5 \times 10^{-4}$ | $1.5 \times 10^{-2}$ | 0.001           |
| PANI-AMPSA <sub>0.4</sub> <sup>a,d</sup> |                          |                         |       |                 | $1.1 \times 10^{-4}$ | 0.42               | $7.2 \times 10^{-3}$ | $1.1 \times 10^{-2}$ | 0.005           |
| PANI-AMPSA <sub>0.6</sub> <sup>a,c</sup> |                          |                         |       |                 | $2.2 \times 10^{-5}$ |                    | $1.7 \times 10^{-2}$ | $1.7 \times 10^{-2}$ | 0.004           |
| PANI-AMPSA <sub>0.6</sub> <sup>a,d</sup> |                          |                         |       |                 | $5.3 \times 10^{-3}$ | 3.5                | $6.5 \times 10^{-1}$ | $1.2 \times 10^{-2}$ | 0.006           |
| PANI-CSA <sub>0.5</sub> <sup>a,c</sup>   |                          |                         |       |                 | $5.2 \times 10^{-7}$ |                    | $2.3 \times 10^{-4}$ | $9.1 \times 10^{-3}$ | 0.005           |
| PANI-CSA <sub>0.5</sub> <sup>a,d</sup>   |                          |                         |       |                 | $2.7 \times 10^{-4}$ | 1.2                | $2.7 \times 10^{-2}$ | 1.58                 | 0.004           |
| PANI-CSA <sub>0.6</sub> <sup>a,c</sup>   |                          |                         |       |                 | $8.5 \times 10^{-7}$ |                    | $4.2 \times 10^{-4}$ | $6.6 \times 10^{-3}$ | 0.014           |
| PANI-CSA <sub>0.6</sub> <sup>a,d</sup>   |                          |                         |       |                 | $7.1 \times 10^{-5}$ | 1.8                | $2.2 \times 10^{-2}$ | 2.13                 | 0.004           |
| PANI-PTSA <sub>0.5</sub> <sup>a,e</sup>  |                          |                         |       |                 | $7.9 \times 10^{-6}$ | 0.6                | $1.3 \times 10^{-3}$ | 1.44                 | 0.099           |
| PANI-PTSA <sub>0.5</sub> <sup>b,e</sup>  |                          |                         |       |                 | $3.3 \times 10^{-6}$ | 0.12               | $1.1 \times 10^{-3}$ | 0.29                 | 0.041           |
| PANI-PTSA <sub>0.5</sub> <sup>a,f</sup>  | 12.2                     | $1.3 \times 10^{19}$    | 0.102 | 0.36            |                      | 9.1                |                      |                      |                 |
| PANI-PTSA <sub>0.5</sub> <sup>b,f</sup>  | 1.7                      | $9.6 \times 10^{17}$    | 0.058 | 0.28            | $5.6 \times 10^{-4}$ | 27                 | $3.9 \times 10^{-2}$ |                      |                 |

<sup>a</sup>Determined at 3-cm waveband EPR.

<sup>b</sup>Determined at 2-mm waveband EPR.

<sup>c</sup>Determined for PC  $R_1$ .

<sup>d</sup>Determined for PC  $R_2$ .

<sup>e</sup>In nitrogen atmosphere.

<sup>f</sup>In air atmosphere.

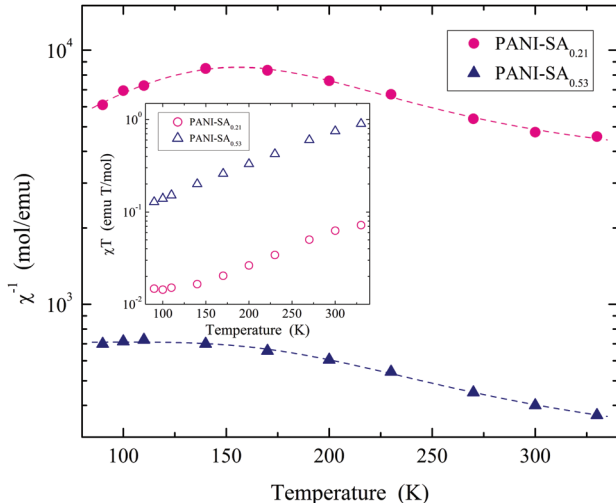


FIG. 12. Temperature dependence of inversed paramagnetic susceptibility and  $\chi T$  product (inset) of PANI-SA samples with different doping levels. Upper and lower dashed lines show the dependences calculated from Eq. (4) with respective  $\chi_p = 3.1 \times 10^{-5}$  emu/mol,  $C = 1.2 \times 10^{-2}$  emu K/mol,  $k_1 = 4.2$  emu K/mol,  $J_{af} = 0.051$  eV, and  $\chi_p = 1.4 \times 10^{-3}$  emu/mol,  $C = 1.6 \times 10^{-2}$  emu K/mol,  $k_1 = 48.6$  emu K/mol,  $J_{af} = 0.057$  eV.

This fact leads to the conclusion that all PC take part in the polymer conductivity. For heavily doped PANI-SA samples, the concentration of spin charge carriers is less than that of spinless ones, due to the possible collapse of pairs of polarons into diamagnetic bipolarons. The velocity of the charge carrier near the Fermi level can be calculated,<sup>215</sup> as  $v_F = 2c_{1D}/\pi\hbar n(\varepsilon_F) = (3.3\text{--}7.2) \times 10^7$  cm/s that is typical for other conducting polymers.<sup>88,118</sup>

Both the *dc* and *ac* conductivities of the PANI-SA and PANI-HCA samples are presented in Fig. 13 as function of temperature. The analysis shown that the *dc* conductivity in PANI-HCA and PANI-SA samples can be described in the framework of the models of Q1D VRH of charge carriers between crystalline high-conducting regions through amorphous bridges<sup>205</sup> and their scattering on the lattice optical phonons in metal-like clusters. (*dc* conductivities at  $T \geq 90$  K are shown in the figure). *DC* conductivity of the samples is a combination of Eqs. (42) and (44)

$$\sigma_{dc}^{-1}(T) = k_1^{-1} T^{\pm 0.5} \exp \left[ \left( \frac{T_0}{T} \right)^{\frac{1}{d+1}} \right] + k_2^{-1} T^{-1} \left[ \sinh \left( \frac{E_{ph}}{k_B T} \right) - 1 \right]^{-1}. \quad (48)$$

The parameters of Eq. (48) determined from the fitting of experimental data are summarized in Table III. It is seen from the table that both the percolation constant and lattice phonon energy of PANI-ES decrease at the increase of polymer doping level. A transition from localization to delocalization of charge carriers occurs when  $\pi^2 t / 32^{1/2} T_0$  is equal to a unit.<sup>61</sup> This value was calculated for PANI-SA<sub>0.21</sub>, PANI-SA<sub>0.42</sub>, PANI-SA<sub>0.53</sub>, and PANI-HCA<sub>0.50</sub> using  $t = 0.29$  eV and  $T_0$  determined to be 0.31, 0.53, 2.1, and 3.1 eV, respectively. An increase in this value with  $y$  means increasing the charge-carrier delocalization as a result of an

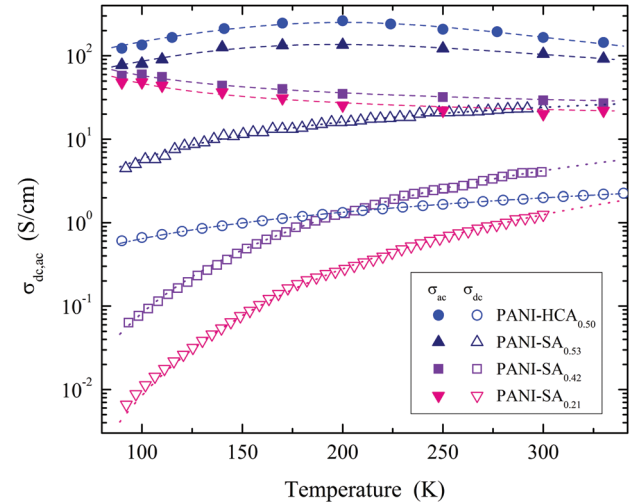


FIG. 13. Temperature dependency of *ac* (filled symbols) and *dc* (open symbols) conductivity calculated from Dyson-like EPR spectra of the PANI-HCA and PANI-SA samples with different doping levels  $y$ . Top-down dotted lines present the dependences calculated from Eq. (48) with respective  $k_1 = 9.2 \times 10^3$  S K<sup>0.5</sup>/cm,  $T_0 = 2.8 \times 10^3$  K,  $k_2 = 0.53$  S/K cm,  $E_{ph} = 0.042$  eV,  $k_1 = 3.5 \times 10^4$  S K<sup>0.5</sup>/cm,  $T_0 = 1.1 \times 10^4$  K,  $k_2 = 1.3 \times 10^{-2}$  S/K cm,  $E_{ph} = 0.062$  eV,  $k_1 = 7.3 \times 10^5$  S K<sup>0.5</sup>/cm,  $T_0 = 1.9 \times 10^4$  K,  $k_2 = 9.2 \times 10^{-3}$  S/K cm,  $E_{ph} = 0.063$  eV, and  $d = 1$ . Dashed-dotted line shows the dependence calculated from the same equation with  $k_1 = 8.4 \times 10^2$  S K<sup>0.5</sup>/cm,  $T_0 = 3.6 \times 10^3$  K,  $k_2 = 0.51$  S/K cm,  $E_{ph} = 0.048$  eV and  $d = 1$ . Top-down dashed lines show the dependences calculated from Eq. (50) with respective  $\sigma_{01} = 1.47$  S cm<sup>-1</sup> K<sup>-1</sup>,  $\sigma_{02} = 2.1 \times 10^{-2}$  S cm<sup>-1</sup> K<sup>-1</sup>, and  $E_{ph}^1 = 0.12$  eV,  $\sigma_{01} = 0.86$  S cm<sup>-1</sup> K<sup>-1</sup>,  $\sigma_{02} = 4.3 \times 10^{-2}$  S cm<sup>-1</sup> K<sup>-1</sup>, and  $E_{ph}^1 = 0.087$  eV,  $\sigma_{01} = 0.48$  S cm<sup>-1</sup> K<sup>-1</sup>,  $\sigma_{02} = 8.5 \times 10^{-3}$  S cm<sup>-1</sup> K<sup>-1</sup>, and  $E_{ph}^1 = 0.049$  eV and  $\sigma_{01} = 0.41$  S cm<sup>-1</sup> K<sup>-1</sup>,  $\sigma_{02} = 5.7 \times 10^{-3}$  S cm<sup>-1</sup> K<sup>-1</sup>,  $E_{ph} = 0.052$  eV, and  $\kappa = -1$ .

increase in the interchain coherence. This value is higher than unity for heavily doped PANI-HCl,<sup>222</sup> and decreases down to 0.1–0.4 for heavily doped derivatives of polyaniline, namely, poly(*o*-toluidine) and poly(*o*-ethylaniline).<sup>223</sup> One can conclude that the insulator-to-metal transition in PANI-SA is of localization-to-delocalization type, driven by the increased structural order between the chains and through an increased interchain coherence. PANI-SA<sub>0.53</sub> and PANI-HCA<sub>0.50</sub> possess a more metallic behavior, and the properties of PANI-SA  $y \leq 0.42$  demonstrate it to be near an insulator/metal boundary. The inherent disorder present in slightly doped PANI keeps the electron states localized on individual chains. At low  $y$ , the structural disorder in polyaniline localizes the charge to single chains (Curie-like carriers) and the higher doping leads to the appearance of delocalized electron states (Pauli-like carriers). This holds typically for the formation in PANI-ES with  $y \geq 0.21$  metal-like domains, according to the island model proposed by Wang and co-workers.<sup>60,63</sup> This is consistent with that drawn earlier on the basis of data obtained with TEM and X-ray-diffraction methods.<sup>116</sup>

The energy of phonons interacting with a polaron determined from Eq. (48) is near to that of superslow anisotropic librations obtained above from ST-EPR. This means that macromolecular dynamics plays an important role in interacting processes taking place in spin reservoir. The lattice librations modulate the interacting spin exchange and consequently the charge transfer integral. Assuming that polaron

TABLE III. The  $k_1$  (in  $\text{S K}^{\pm 0.5}/\text{cm}$ ),  $T_0$  (in K),  $k_2$  (in  $\text{S/K cm}$ ),  $\hbar\omega_{\text{ph}}$  (in eV) values determined from the fitting of  $\sigma_{\text{dc}}$  by Eq. (48), and  $\sigma_{0_1}$  (in  $\text{S/K cm}$ ),  $\sigma_{0_2}$  (in  $\text{S/K cm}$ ), and  $\hbar\omega_{\text{ph}}^{\perp}$  (in eV) ones determined from the fitting of  $\sigma_{\text{ac}}$  by Eq. (50) for different PANI samples.

| Polymer                               | $k_1$             | $T_0$             | $k_2$                | $E_{\text{ph}}$ | $\sigma_{0_1}$ | $\sigma_{0_2}$       | $E_{\text{ph}}^{\perp}$ |
|---------------------------------------|-------------------|-------------------|----------------------|-----------------|----------------|----------------------|-------------------------|
| PANI-SA <sub>0.21</sub>               | $7.3 \times 10^5$ | $1.9 \times 10^4$ | $9.2 \times 10^{-3}$ | 0.063           | 0.41           | $5.7 \times 10^{-3}$ | 0.052                   |
| PANI-SA <sub>0.42</sub>               | $3.5 \times 10^4$ | $1.1 \times 10^4$ | $1.3 \times 10^{-2}$ | 0.062           | 0.48           | $8.5 \times 10^{-3}$ | 0.049                   |
| PANI-SA <sub>0.53</sub>               | $9.2 \times 10^3$ | $2.8 \times 10^3$ | 0.53                 | 0.042           | 0.86           | $4.3 \times 10^{-2}$ | 0.087                   |
| PANI-HCA <sub>0.50</sub>              | $8.4 \times 10^2$ | $3.6 \times 10^3$ | 0.51                 | 0.048           | 1.5            | $2.1 \times 10^{-2}$ | 0.12                    |
| PANI-AMPSA <sub>0.4</sub>             | $1.2 \times 10^3$ | 209               | 0.31                 | 0.022           | 1.68           | 1.57                 | 0.037                   |
| PANI-AMPSA <sub>0.6</sub>             | $1.1 \times 10^3$ | 277               | 0.18                 | 0.020           | 1.62           | 0.76                 | 0.039                   |
| PANI-CSA <sub>0.5</sub>               | $5.6 \times 10^3$ | 521               | 1.7                  | 0.028           | 1.99           | 0.68                 | 0.039                   |
| PANI-CSA <sub>0.6</sub>               | $5.5 \times 10^3$ | 753               | 0.29                 | 0.024           | 2.27           | 0.64                 | 0.036                   |
| PANI-PTSA <sub>0.5</sub> <sup>a</sup> |                   |                   |                      |                 | 13.3           | 0.25                 | 0.027                   |
| PANI-PTSA <sub>0.5</sub> <sup>b</sup> | 26                | $4.6 \times 10^4$ | 0.19                 | 0.027           | 24.9           | 10.8                 | 0.022                   |

<sup>a</sup>Determined at 3-cm waveband EPR.

<sup>b</sup>Determined at 2-mm waveband EPR.

is covered by both electron and excited phonon clouds, we can propose that both spin relaxation and charge transfer should be accompanied with the phonon dispersion. Such cooperating charge-phonon processes seem to be more important for the doped polymers the high-coupled chains of which constitute 3D metal-like clusters.

Aasmundtveit *et al.*<sup>106</sup> have shown that 3-cm waveband linewidth and consequently the spin-spin relaxation rate of PC in PANI depend directly on its *dc* conductivity. The comparison of  $\Delta B_{\text{pp}}(T)$  and  $\sigma_{\text{ac}}(T)$  functions presented in Figs. 11 and 13 demonstrates the additivity of these values at least for the higher doped polymers. Besides, Khazanovich<sup>224</sup> have found that spin-spin relaxation depends on the number of spins on each polymer chain  $N_s$  and on the number of neighboring chains  $N_c$  with which these spins interact as follows:

$$T_2^{-1} = \frac{4\langle\Delta\omega^2\rangle}{5\omega_0 N_s} \left[ 21 \ln \frac{\omega_0}{\omega_e} + 18 \ln N_c \right]. \quad (49)$$

Using  $T_2 = 1.7 \times 10^{-7}$  s,  $\Sigma_{ij} = 1.2 \times 10^{45} \text{ cm}^{-6}$ , and  $\omega_0 = 6.1 \times 10^{13} \text{ s}^{-1}$  determined from experiment, a simple relation  $N_c \approx 55 \exp(N_s)$  of these values is obtained from Eq. (49). This means that at  $L_{||} = 7.0 \text{ nm}$  at least seven interacting spins exist on each chain as spin-packet and interact with  $N_c = 20$  chains, i.e., spin and charge 3D hopping does not exceeds distance more than  $3c_{3D} < L$ .

Figure 13 also exhibits the temperature dependence of the *ac* conductivity of highly doped PANI-SA and PANI-HCA samples determined from their Dysonian 2-mm EPR spectra using Eqs. (15)–(17). The shape of the temperature dependences presented demonstrates non-monotonous temperature dependence with a characteristic point  $T_c \approx 200 \text{ K}$ . Such a temperature dependency can be attributed to the above-mentioned interacting charge carriers with lattice phonons at high temperatures (the metallic regime) and by their Mott VRH at low temperatures (the semiconducting regime). In this case the charge transfer should consist of two successive processes, so then the *ac* conductivity should be expressed as a combination of Eqs. (42) and (44).

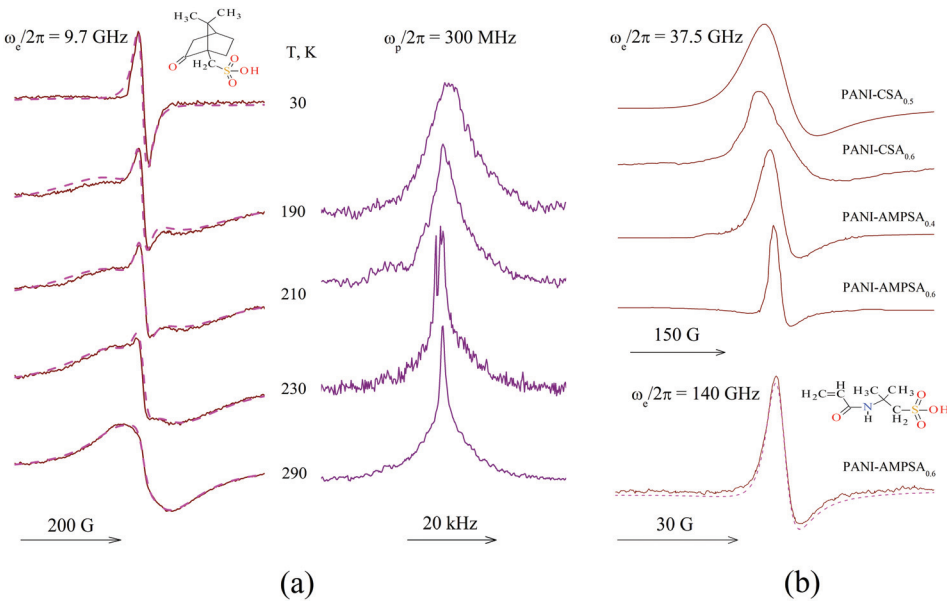
$$\sigma_{\text{ac}}^{\kappa}(T) = (\sigma_{0_1} T)^{\kappa} + \left\{ \sigma_{0_2} T \left[ \sinh \left( \frac{E_{\text{ph}}^{\perp}}{k_B T} \right) - 1 \right] \right\}^{\kappa}. \quad (50)$$

Figure 13 shows that the experimental  $\sigma_{\text{ac}}$  values obtained for PANI-SA and PANI-HCA are fitted well by Eq. (50) with the appropriate parameters listed in Table III. The energy determined for phonons in PANI sample lies near to that (0.066 eV) evaluated from the data obtained by Wang *et al.*<sup>60,63</sup>

RT  $\sigma_{\text{ac}}$  of heavily doped PANI-SA and PANI-HCA, estimated from the contribution of spin charge carriers, does not exceed 140 S/cm. This value is much smaller than  $\sigma_{\text{ac}}(\omega_e \rightarrow \infty) \cong 10^7 \text{ S/cm}$  calculated theoretically,<sup>225</sup> however, it lies near that obtained for metal-like domains in PANI at 6.5 GHz.<sup>77</sup> The  $\sigma_{\text{ac}}/\sigma_{\text{dc}}$  ratio for these domains can be evaluated to be 80 for PANI-HCA<sub>0.50</sub> and 18, 7, and 4 for PANI-SA with  $y = 0.21, 0.42$ , and 0.53, respectively. Taking into account that the  $\sigma_{\text{ac}} = \sigma_{\text{dc}}$  condition should be fulfilled for classic metals,<sup>215</sup> one can conclude a better structural ordering of these domains in PANI-SA. Charge carriers diffuse along these polymer chains with the constant  $D_{1D}$  can be determined from relation  $\sigma_{\text{ac}} = e^2 n(\varepsilon_F) D_{1D} c_{1D}^2$  to vary within  $5 \times 10^{13} - 1.1 \times 10^{14} \text{ rad/s}$  at room temperature that exceeds at least by an order of magnitude  $D_{1D}$  determined above for slightly doped samples. The RT mean free path  $l_i = \sigma_{\text{ac}} m_c v_F / (Ne^2)$  calculated for the highly doped PANI-SA and PANI-HCA lies near to 0.5 and 6.0 nm, respectively. These values are smaller than that estimated for oriented *trans*-PA,<sup>78</sup> but holds for extended electron states in these polymers. The energy of lattice phonons  $\hbar\omega_{\text{ph}}^{\perp}$  obtained from *ac* data lies near the energy  $J_{\text{af}}$  of the interaction between spins (see Table II) that shows the modulation of spin-spin interaction by macromolecular dynamics in the system.

## B. Polyaniline chemically modified by camphorsulfonic and 2-acrylamido-2-methyl-1-propanesulfonic acids

The shape of EPR spectrum of PANI-ES depends on the nature of counter-ion. Figure 14 presents EPR spectra of highly doped film-like PANI-CSA and PANI-AMPSA



samples registered at different polarizing frequencies. For the comparison, NMR spectra of PANI-CSA<sub>0.5</sub> registered at different temperatures are presented as well. In order to determine correctly all main magnetic resonance parameters, linewidth, paramagnetic susceptibility, *g*-factor, of PC with Dysonian contribution, all double spectra presented should be calculated using the above mentioned method. Kon'kin *et al.* pointed<sup>124</sup> that in case of PANI-CSA and PANI-AMPSA the Dysonian line asymmetry factor *A/B* and therefore the ratio *D/A* depends more on the  $2d/\delta$  ratio in Eqs. (18) and (19). The *D/A*( $2d/\delta$ ) dependences calculated for these polymer presented in Fig. 15. It was shown the applicability of these functions for the analysis of Dysonian EPR spectra of PC in an initial and also in two, three, and four times incrassate PANI films (Fig. 15).

EPR spectra of PANI-CSA and PANI-AMPSA were then analyzed as sum of two different PC coexisting in these

polymers with Dysonian shape, namely, narrow EPR spectrum of PC *R*<sub>1</sub> with *g* = 2.0028 localized in amorphous polymer matrix and broader EPR spectrum of PC *R*<sub>2</sub> with *g* = 2.0020 and higher mobility in crystalline phase of the polymers. The cooling of the samples leads to the decrease in the relative concentration of PC *R*<sub>2</sub> and to the monotonous increase in its linewidth, as it is seen in Figs. 14 and 16. In the same time, the linewidth of PC *R*<sub>1</sub> decreases monotonously and the sum spin concentration increases at the temperature decrease. Besides, NMR linewidth decreases at such a sample cooling (Fig. 14) due possible to the decrease of interaction of electron and proton spins. The RT  $\Delta B_{pp}$  value of PC *R*<sub>2</sub> in, e.g., PANI-AMPSA<sub>0.6</sub> decreases from 54 down to 20 and then down to 5.3 G at the increase of registration frequency  $\omega_e/2\pi$  from 9.7 up to 36.7 and then up to 140 GHz (Fig. 14), so one can express this value as  $\Delta B_{pp}(\omega_e) = 1.5 + 2.2 \times 10^9 \omega_e^{-0.84}$  G. Such extrapolation

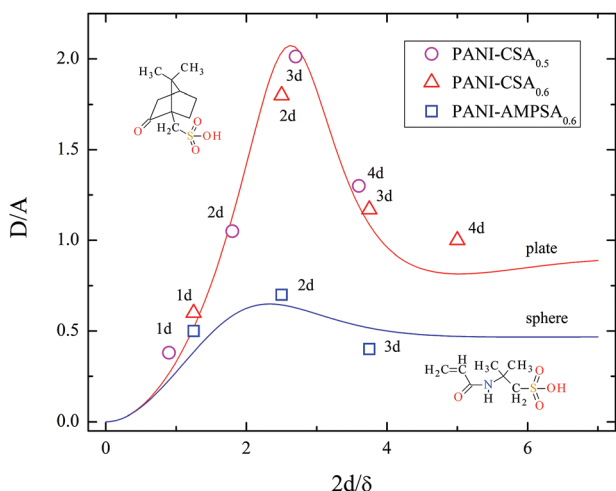


FIG. 15. The theoretical  $D/A(2d/\delta)$  dependencies calculated<sup>124</sup> and experimentally determined for the PANI-CSA and PANI-AMPSA films with different plate thickness (*nd*) at 3-cm waveband EPR and 300 K. The structures of CSA and AMPSA are shown schematically.

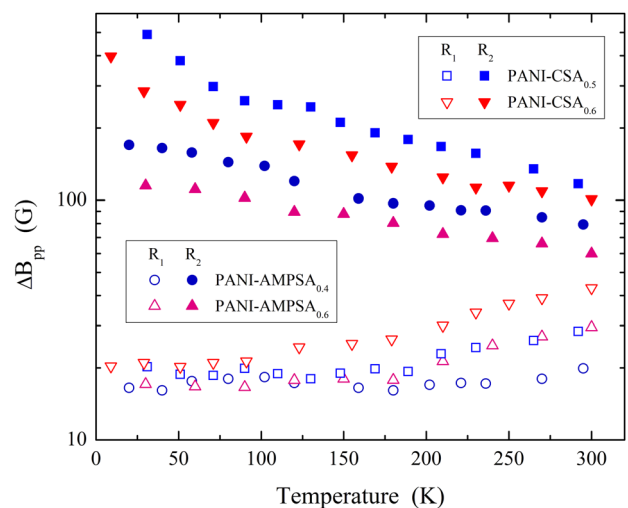


FIG. 16. Temperature dependence of linewidth of the *R*<sub>1</sub> (open points) and *R*<sub>2</sub> (filled points) PC stabilized in the PANI-CSA and PANI-AMPSA samples with different doping levels *y* determined from their 3-cm waveband EPR spectra with the Dysonian contribution.

reveals the dependence of spin-spin relaxation time on the registration frequency and allows estimating correct linewidth at  $\omega_e \rightarrow 0$  limit to be 1.5 G.

The narrowing of the line on raising the PANI temperature can be explained by averaging of the local magnetic field caused by HFI between the localized spins whose energy levels lie near the Fermi level. The EPR line of PANI-CSA and PANI-AMPSA may also be broadened to some extent by relaxation due to the spin-orbital interaction responsible for linear dependence of  $T_1^{-1}$  on temperature;<sup>92</sup> however, this interaction seems to be rather weak in our case. It is significant that for both types of PC the linewidths are appreciably larger than those obtained previously for the fully oxidized powder-like and film-like PANI-CSA (0.35 and 0.8 G, respectively),<sup>92</sup> which indicates a higher conductivity of the samples under study. Comparison of the  $\Delta B_{pp}$  values obtained for different PANI-CSA samples and presented in Fig. 16 suggested that a crystalline phase is formed in the amorphous phase of the polymer, beginning with the oxidation level  $y = 0.3$ , and that the paramagnetic centers of this newly formed phase exhibit a broader EPR spectrum. In the amorphous phase of the polymer, the PC  $R_1$  are characterized by less temperature-dependent linewidth and are likely not involved in the charge transfer being, however, as probes for whole conductivity of the sample. At the same time, the magnetic resonance parameters of radicals of the  $R_2$  type should reflect the charge transport in the crystalline domains of PANI-CSA and PANI-AMPSA. The linewidth of PANI appreciably decreases on replacement of the CSA anion by the AMPSA anion (see Fig. 16), which is likely due to the shortening of spin-spin relaxation time of both PC.

Figure 17 depicts the effective paramagnetic susceptibility of both the  $R_1$  and  $R_2$  PC as a function of temperature. The  $J_{af}$  values obtained are much lower of the corresponding energy (0.078 eV) obtained for ammonia-doped PANI.<sup>114</sup> It is seen that at low temperatures when  $T \leq T_c \approx 100$  K the Pauli and Curie terms prevail in the total paramagnetic susceptibility  $\chi$  of both type PC in all PANI samples. At  $T \geq T_c$ , when the energy of phonons becomes comparable with the value  $k_B T_c \approx 0.01$  eV, the spins interact leading to the last term of Eq. (4) in sum susceptibility as a result of the equilibrium between the spins with triplet and singlet states in the system. It is evident that the  $R_1$  signal susceptibility obeys mainly the Curie law typical for localized isolated PC, whereas the  $R_2$  susceptibility consists of the Curie-like and Pauli-like contributions.

The  $n(\varepsilon_F)$  values obtained for the charge carriers in PANI-CSA and PANI-AMPSA are also summarized in Table II. This value increases in series PANI-AMPSA<sub>0.4</sub> → PANI-CSA<sub>0.5</sub> → PANI-CSA<sub>0.6</sub> → PANI-AMPSA<sub>0.6</sub>. This density of stated polarons in PANI-CSA is in agreement with that obtained previously in the optical<sup>49</sup> (0.06–6 eV) and EPR<sup>92</sup> studies of this polymer. The Fermi energy of the Pauli-spins was calculated to be  $\varepsilon_F \approx 0.2$  eV. This value is lower than the Fermi energy obtained for highly CSA-(0.4 eV)<sup>54</sup> and sulfur- (0.5 eV)<sup>87,125</sup> doped PANI. Assuming again that the charge carrier mass in heavily doped polymer is equal to the mass of free electron ( $m_c = m_e$ ), the number of charge carriers in such a quasi-metal,<sup>215</sup>  $N_c \approx 4.1 \times 10^{20} \text{ cm}^{-3}$

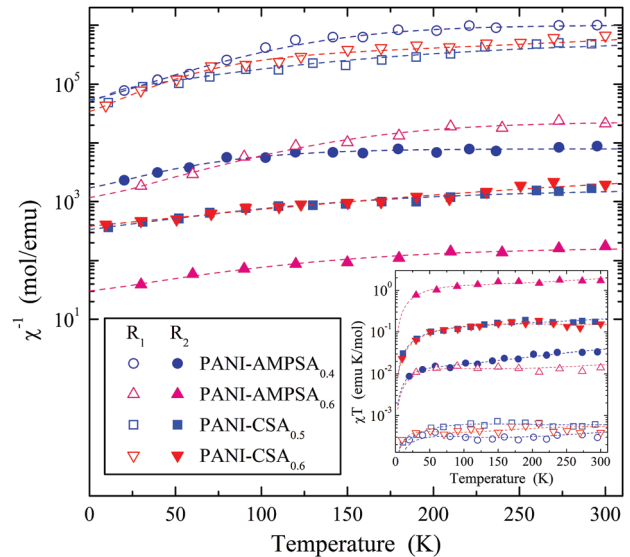


FIG. 17. Temperature dependence of inverted effective paramagnetic susceptibility  $\chi$  and  $\chi T$  product (inset) of the  $R_1$  (open points) and  $R_2$  (filled points) PC stabilized in the PANI-CSA and PANI-AMPSA samples with different doping levels  $y$ . Top-down dashed lines show the dependences calculated from Eq. (4) with respective  $\chi_P = 9.8 \times 10^{-7}$  emu/mol,  $C = 4.5 \times 10^{-4}$  emu K/mol,  $k_1 = 1.5 \times 10^{-2}$  emu K/mol,  $J_{af} = 0.001$  eV,  $\chi_P = 8.5 \times 10^{-7}$  emu/mol,  $C = 4.2 \times 10^{-4}$  emu K/mol,  $k_1 = 6.6 \times 10^{-3}$  emu K/mol,  $J_{af} = 0.014$  eV,  $\chi_P = 5.2 \times 10^{-7}$  emu/mol,  $C = 2.3 \times 10^{-4}$  emu K/mol,  $k_1 = 9.1 \times 10^{-3}$  emu K/mol,  $J_{af} = 0.005$  eV,  $\chi_P = 2.2 \times 10^{-5}$  emu/mol,  $C = 1.7 \times 10^{-2}$  emu K/mol,  $k_1 = 1.7 \times 10^{-3}$  emu K/mol,  $J_{af} = 0.004$  eV,  $\chi_P = 1.1 \times 10^{-4}$  emu/mol,  $C = 7.2 \times 10^{-3}$  emu K/mol,  $k_1 = 1.1 \times 10^{-2}$  emu K/mol,  $J_{af} = 0.005$  eV,  $\chi_P = 7.1 \times 10^{-5}$  emu/mol,  $C = 2.2 \times 10^{-3}$  emu K/mol,  $k_1 = 2.13$  emu K/mol,  $J_{af} = 0.004$  eV,  $\chi_P = 2.7 \times 10^{-4}$  emu/mol,  $C = 2.7 \times 10^{-2}$  emu K/mol,  $k_1 = 1.58$  emu K/mol,  $J_{af} = 0.004$  eV,  $\chi_P = 5.3 \times 10^{-3}$  emu/mol,  $C = 6.5 \times 10^{-1}$  emu K/mol,  $k_1 = 1.2 \times 10^{-2}$  emu K/mol,  $J_{af} = 0.006$  eV.

was determined. This is close to the spin concentration in this polymer; therefore, one can conclude that all delocalized PC are involved in the charge transfer in PANI-CSA<sub>0.6</sub>. The velocity of charge carriers near the Fermi  $v_F$  level was calculated to be  $3.8 \times 10^7$  cm/s for PANI-CSA that is close to those evaluated for this polymer from the EPR magnetic susceptibility data  $(2.8\text{--}4.0) \times 10^7$  cm/s,<sup>226,227</sup> and  $6.2 \times 10^7$  cm/s for PANI-AMPSA.

Thus, main PC in the highly doped PANI-CSA and PANI-AMPSA samples are localized at  $T \leq T_c$ . This is the reason for the Curie type of susceptibility of the sample and should lead to the VRH charge transfer between the polymer chains. The spin-spin exchange is stimulated at  $T \geq T_c$  due likely to the activation librations of the polymer chains. The activation energies of these librations lie within the energy range characteristic of PANI-CSA,<sup>228</sup> PANI-HCA,<sup>119,121</sup> and poly(tetrathiafulvalenes).<sup>118,229</sup> The  $E_a$  value depends on the effective rigidity and planarity of the polymer chains that are eventually responsible for the electrodynamic properties of the polymer.

*DC* and *ac* conductivities of the highly doped PANI-CSA and PANI-AMPSA determined, respectively, by the *dc* conductometry method<sup>124</sup> and from the Dysonian spectra of the  $R_2$  PC are given in Fig. 18 as a function of temperature. Charge carrier hops through amorphous part of the sample and then diffuses through its crystalline domain, so then the

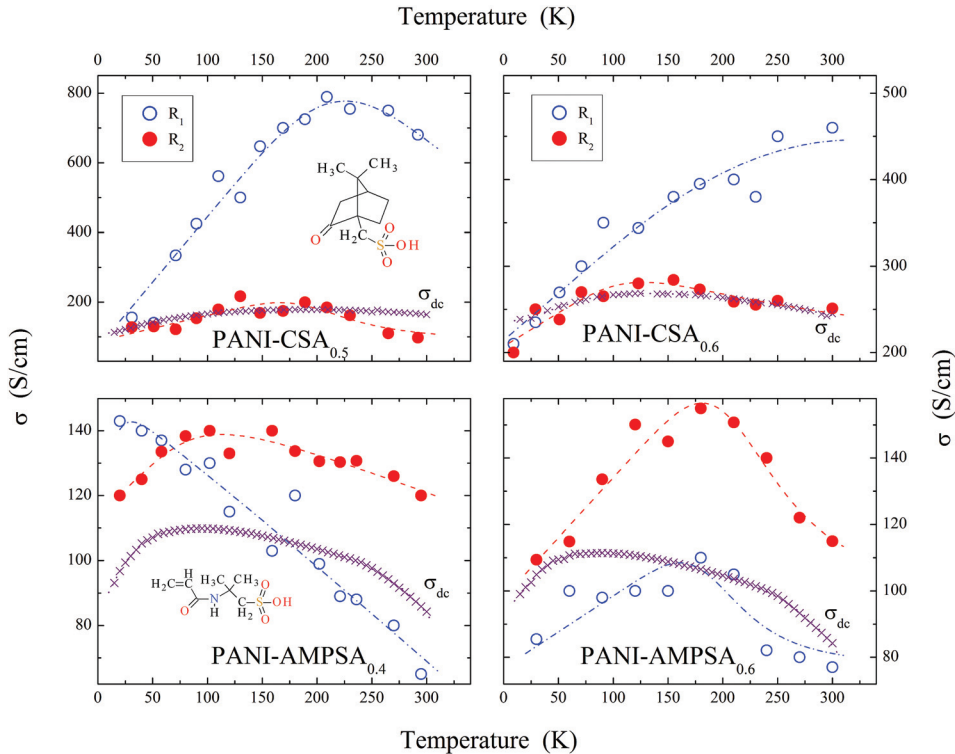


FIG. 18. Temperature dependence of *dc* (marked by the  $\times$  symbol) and *ac* conductivity determined from Dysonian spectra of the  $R_1$  (open circles) and  $R_2$  (filled circles) PC stabilized in the PANI-CSA<sub>0.5</sub> (a), PANI-CSA<sub>0.6</sub> (b), PANI-AMPSA<sub>0.4</sub> (c), and PANI-AMPSA<sub>0.6</sub> (d) films. Dotted lines show the dependences calculated from Eq. (48) with  $d=1$  and  $k_1=5.6 \times 10^3 \text{ S K}^{0.5}/\text{cm}$ ,  $T_0=521 \text{ K}$ ,  $k_2=1.7 \text{ S/K cm}$ ,  $\hbar\omega_{\text{ph}}=0.028 \text{ eV}$  (a),  $k_1=5.5 \times 10^3 \text{ S K}^{0.5}/\text{cm}$ ,  $T_0=753 \text{ K}$ ,  $k_2=0.29 \text{ S/K cm}$ ,  $\hbar\omega_{\text{ph}}=0.024 \text{ eV}$  (b),  $k_1=1.2 \times 10^3 \text{ S K}^{0.5}/\text{cm}$ ,  $T_0=209 \text{ K}$ ,  $k_2=0.31 \text{ S/K cm}$ ,  $\hbar\omega_{\text{ph}}=0.022 \text{ eV}$  (c),  $k_1=1.1 \times 10^3 \text{ S K}^{0.5}/\text{cm}$ ,  $T_0=277 \text{ K}$ ,  $k_2=0.18 \text{ S/K cm}$ ,  $\hbar\omega_{\text{ph}}=0.020 \text{ eV}$  (d). Dashed-dotted and dashed lines show the dependences calculated from Eq. (50) with, respectively,  $\sigma_{01}=3.8 \text{ S/K cm}$ ,  $\sigma_{02}=9.1 \times 10^{-2} \text{ S/K cm}$ ,  $\hbar\omega_{\text{ph}}=0.12 \text{ eV}$  and  $\sigma_{01}=8.5 \times 10^{-4} \text{ S/K cm}$ ,  $\sigma_{02}=0.75 \text{ S/K cm}$ ,  $\hbar\omega_{\text{ph}}=0.14 \text{ eV}$  (a),  $\sigma_{01}=1.1 \text{ S/K cm}$ ,  $\sigma_{02}=1.5 \text{ S/K cm}$ ,  $\hbar\omega_{\text{ph}}=0.045 \text{ eV}$  and  $\sigma_{01}=0.78 \text{ S/K cm}$ ,  $\sigma_{02}=0.11 \text{ S/K cm}$ ,  $\hbar\omega_{\text{ph}}=0.042 \text{ eV}$  (b),  $\sigma_{01}=0.79 \text{ S/K cm}$ ,  $\sigma_{02}=0.22 \text{ S/K cm}$ ,  $\hbar\omega_{\text{ph}}=0.009 \text{ eV}$  and  $\sigma_{01}=0.32 \text{ S/K cm}$ ,  $\sigma_{02}=0.11 \text{ S/K cm}$ ,  $\hbar\omega_{\text{ph}}=0.027 \text{ eV}$  (c),  $\sigma_{01}=0.22 \text{ S/K cm}$ ,  $\sigma_{02}=1.1 \times 10^{-4} \text{ S/K cm}$ ,  $\hbar\omega_{\text{ph}}=0.14 \text{ eV}$  and  $\sigma_{01}=0.32 \text{ S/K cm}$ ,  $\sigma_{02}=4.4 \times 10^{-4} \text{ S/K cm}$ ,  $\hbar\omega_{\text{ph}}=0.15 \text{ eV}$  (d), and  $\kappa=-1$ .

*dc* term of the total conductivity of the samples should be determined by 1D VDH between metal-like domains accompanied by the charge carriers scattering on the lattice phonons in these domains described by Eqs. (42) and (44). These processes occur parallel, so the effective conductivity can be expressed by Eq. (48). Indeed, Fig. 18 shows that *dc* conductivity of the polymers experimentally obtained is fitted well by Eq. (48) whose fitting parameters are also summarized in Table III. The  $v_F$  value was calculated for the PANI-CSA and PANI-AMPSA systems, to be  $2.4 \times 10^7$  and  $6.0 \times 10^7 \text{ cm/s}$ , respectively.<sup>124</sup> In contrast with other conducting polymers, lower  $T_0$  parameter is characteristic for these samples. (Note that the 3D VRH model gives abnormal low  $T_0$  value for all the samples.) This is evidence of the longer averaged length of charge wave localization function in the samples. Indeed,  $\langle L \rangle$  value was determined for PANI-CSA<sub>0.6</sub>, PANI-CSA<sub>0.5</sub>, PANI-AMPSA<sub>0.6</sub>, and PANI-AMPSA<sub>0.4</sub>, to be 17, 37, 264, and 239 nm, respectively. The  $n(\varepsilon_F)$  increases in series PANI-AMPSA<sub>0.4</sub> → PANI-CSA<sub>0.5</sub> → PANI-CSA<sub>0.6</sub> → PANI-AMPSA<sub>0.6</sub>.

*AC* conductivity of the polymers is also reflects the above mentioned successive mechanisms, so the experimental data can be circumscribed by Eq. (50). Indeed, it is seen from Fig. 18 that the  $\sigma_{\text{ac}}(T)$  dependences obtained experimentally for mobile  $R_2$  PC are fitted well by Eq. (50) with the parameters summarized in Table III. The energy

determined for phonons in these PANI samples lies near to that obtained for other polymers<sup>87,88</sup> and evaluated (66 meV) from the data determined by Wang *et al.* for HCl-doped PANI.<sup>60,63</sup> It is evident that  $E_{\text{ph}}^\parallel$  and  $E_a$  obtained above for the PANI-CSA<sub>0.5</sub> sample lie near. This means that protons situated in crystalline domains indeed sense electron spin dynamics. The data obtained can be evidence of the contribution of the  $R_1$  and  $R_2$  PC in the charge transfer through, respectively, amorphous and crystalline parts of the polymers. RT  $\sigma_{\text{ac}}$  values determined from Dysonian spectra of  $R_2$  PC lies near respective  $\sigma_{\text{dc}}$  values, which is characteristic for classic metals. The  $\langle L \rangle$  and  $E_{\text{ph}}$  values determined above for mediatory doped samples correlate. This means that the higher the  $\langle L \rangle$  value, the stronger interaction of PC with phonons in metal-like crystallites. There is some tendency in the increase of RT  $\sigma_{\text{dc}}$  and  $\sigma_{\text{ac}}$  conductivities in the series PANI-AMPSA<sub>0.6</sub> → PANI-AMPSA<sub>0.4</sub> → PANI-CSA<sub>0.5</sub> → PANI-CSA<sub>0.6</sub> “feeling” by the  $R_2$  PC. The data obtained can be evidence of indirect contribution of the  $R_1$  PC and direct contribution of the  $R_2$  PC in the charge transfer through, respectively, amorphous and crystalline parts of the polymers. RT  $\sigma_{\text{ac}}$  values determined from Dysonian spectra of  $R_2$  PC lies near respective  $\sigma_{\text{dc}}$  values that is characteristic for classic metals.

Thus, main PC in the highly doped PANI-CSA and PANI-AMPSA samples are localized at low temperatures.

This originates the Curie type of susceptibility of the samples and the VRH charge transfer between their polymer chains. The spin-spin exchange is stimulated at high temperature region due likely to the activation librations of the polymer chains.<sup>230,231</sup> Both pinned and delocalized PC are formed simultaneously in the regions with different crystallinity. An anti-ferromagnetic interaction in crystalline domains is stronger than that in amorphous regions of PANI-CSA and PANI-AMPSA. Charge transport between crystalline metal-like domains occurs through the disordered amorphous regions where the charge/spin carriers are more localized. The assumption that higher purity PANI coupled with homogeneous doping would give rise to no EPR signal, characteristic of a purely bipolaronic matrix, is in contradiction with the increase of *ac* conductivity with spin concentration in polymer systems. Both PANI-CSA and PANI-AMPSA reveal better electronic properties over PANI-SA and PANI-HCA, as shown by their electrical conductivity which is both greater in magnitude and follows metallic temperature dependence. The change of conductivity with temperature is consistent with a disordered metal close to the critical regime of the metal-insulator transition with the Fermi energy close to the mobility edge.<sup>92,93</sup>

### C. Polyaniline chemically modified by para-toluenesulfonic acid

PANI-PTSA<sub>0.50</sub> sample in nitrogen atmosphere at 3-cm waveband EPR demonstrates Lorentzian exchange-narrowed lines which an asymmetry factor *A/B* is 1.03 (Fig. 19). The exposure of the samples to air was observed to lead to reversible line broadening and an increase in the asymmetry factor up to 1.27. The asymmetry of the EPR line may be due to either unresolved anisotropy of the *g*-factor or the presence in the spectrum of the Dysonian term<sup>112</sup> as in case of other

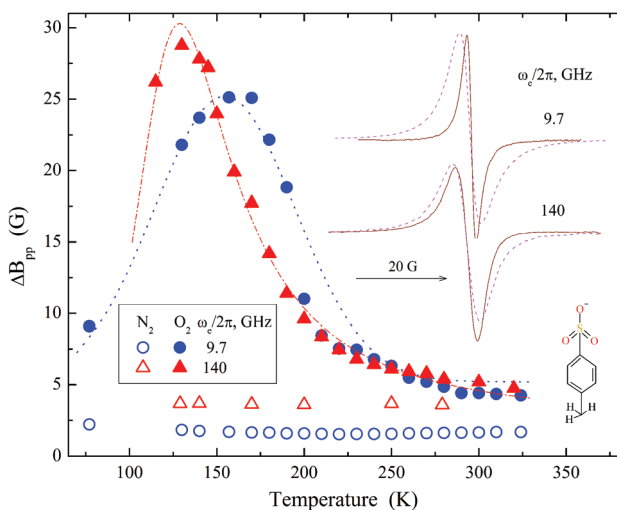


FIG. 19. Inset—3-cm and 2-mm wavebands EPR spectra of the PANI-PTSA<sub>0.50</sub> sample in nitrogen (solid lines) and air (dashed lines) atmospheres. Structure of the PTSA counter-ion is also shown schematically. Temperature dependence of linewidth of PC in the PANI-PTSA<sub>0.50</sub> sample with the presence of nitrogen and oxygen molecules registered at 3-cm and 2-mm wavebands EPR. The lines show the dependences calculated from Eq. (11) with  $\omega_{\text{hop}}^0 = 9.6 \times 10^{17} \text{ s}^{-1}$ ,  $E_a = 0.058 \text{ eV}$ ,  $J_{\text{ex}} = 0.28 \text{ eV}$  (dashed-dotted line),  $\omega_{\text{hop}}^0 = 1.3 \times 10^{19} \text{ s}^{-1}$ ,  $E_a = 0.102 \text{ eV}$ ,  $J_{\text{ex}} = 0.36 \text{ eV}$  (dotted line).

highly doped conducting polymers. To verify these assumptions, the 2-mm waveband EPR spectra of the sample were recorded. It is seen from Fig. 19 that the polymer in this waveband EPR also exhibits a single asymmetric line, where asymmetry factor varies at the exposition to air from 1.68 up to 1.95. This fact indicates substantial interaction of PC even in high fields, the line asymmetry of these PC indeed results from the interaction of a MW field with charge carriers in the skin layer.

Dysonian EPR spectra of the samples were calculated from Eqs. (15) to (17) and the main magnetic parameters were obtained.

As the operating frequency increases from 9.7 up to 140 GHz, the  $\Delta B_{\text{pp}}$  value of PC in the PANI sample increases not more than by a factor of 2 (Fig. 19). Such insignificant line broadening with the operating frequency increase was not observed in studies on other conducting polymers, including PANI. This may be evidence for stronger exchange interaction between PC in the polymer, which is not completely relieved in strong magnetic field. The temperature dependence of the effective absorption linewidth of the sample determined at both the 3-cm and 2-mm wavebands EPR is presented in Fig. 19. It is seen that  $\Delta B_{\text{pp}}$  of PC in the PANI-PTSA<sub>0.50</sub> sample containing nitrogen slightly depends on temperature. Air diffusion into the samples leads to the reversible extremal broadening of its EPR line.

As Fig. 19 evidences, the  $T_c$  value described above characteristic for the  $\Delta B_{\text{pp}}(T)$  dependences presented shifts nearly from 160 K to 130 K at the increase of polarizing frequency from 9.7 GHz up to 140 GHz. Such effect was interpreted as result of exchange interaction of polarons with oxygen molecules possessing sum spin  $S = 1$ . The  $\Delta B_{\text{pp}}(T)$  dependences were fitted by Eq. (11) with appropriate parameters listed in Table II (Fig. 19). It is seen that the experimental data obtained can be rationalized well in terms of this theory. This result reveals that the oxygen biradical act as a nanoscopic probe of the polaron dynamics. The obtained value of  $J_{\text{ex}}$  sufficiently exceeds the corresponding spin-exchange constant for nitroxide radicals with paramagnetic ions,  $J_{\text{ex}} \leq 0.01 \text{ eV}$ .<sup>151</sup>

Figure 20 shows the temperature dependence for the paramagnetic susceptibility of the PANI-PTSA<sub>0.50</sub> sample in the absence and in the presence of oxygen in the polymer. An analysis of the paramagnetic susceptibility of the nitrogen containing sample determined at 3-cm and 2-mm wavebands EPR showed that it can be described by Eq. (4) with the parameters presented in Table II. These data show that the transition of registration frequency from 9.7 GHz to 140 GHz leads to decrease in  $J_{\text{af}}$  determined for nitrogen filled PANI-PTSA<sub>0.5</sub> sample from 0.099 down to 0.041 eV due possible to the field effect. The figure reveals that the effective susceptibility of the PANI-PTSA<sub>0.50</sub> without oxygen, as determined from 3-cm waveband EPR spectra, slightly varies with temperature. However, this value determined from the 2-mm waveband EPR spectra noticeably decreases with a decrease in temperature. The exposure of the polymer to air increases proportionally all components of its magnetic susceptibility. This value of the sample exposed to air increases substantially and exhibits non-monotonic

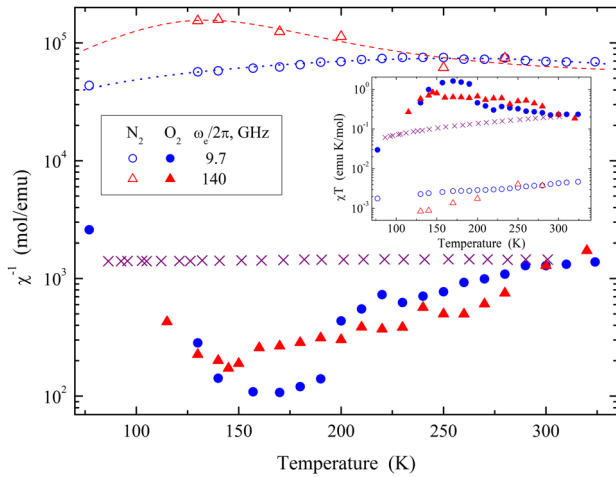


FIG. 20. Temperature dependence of inversed effective paramagnetic susceptibility and  $\chi T$  product (inset) of PC stabilized in PANI-PTSA<sub>0.5</sub> sample exposed to nitrogen (open symbols) and oxygen (filled symbols) determined at different spin precession frequencies. By the  $\times$  symbol is shown the appropriate data<sup>141</sup> obtained for PANI-PTSA<sub>0.5</sub> by using a “force” magnetometer in a dc external magnetic field of  $5 \times 10^3$  Gauss. Dashed and dotted lines show the dependences calculated from Eq. (4) with respective  $\chi_p = 3.3 \times 10^{-6}$  emu/mol,  $C = 1.1 \times 10^{-3}$  emu K/mol,  $k_1 = 0.29$  emu K/mol,  $J_{af} = 0.041$  eV and  $\chi_p = 7.9 \times 10^{-6}$  emu/mol,  $C = 1.3 \times 10^{-3}$  emu K/mol,  $k_1 = 1.44$  emu K/mol,  $J_{af} = 0.099$  eV.

temperature dependence in the 3-cm and 2-mm wavebands EPR with a characteristic temperature maximum at 160 and 150 K, respectively. The nature of this effect is discussed above. The Pauli susceptibility of the sample is close to that<sup>51</sup> determined at  $n(\varepsilon_F) = 22.8 \text{ eV}^{-1}$ . Note that the  $\chi$  measured for PANI-PTSA<sub>0.5</sub> by more direct method<sup>141</sup> exhibits smaller temperature dependency.

The velocity of charge carriers and the Fermi energy was calculated as  $v_F = 2c_{1D}/\pi\hbar n(\varepsilon_F)$  and  $\varepsilon_F = 3N_e/2n(\varepsilon_F)$  to be  $3.1 \times 10^6 \text{ cm/s}$  and  $0.16 \text{ eV}$ , respectively. The latter value is less of Fermi energy obtained earlier for PANI-SA, PANI-CSA, and PANI-AMPSA.

Figure 21 shows the temperature dependence of  $\sigma_{dc}$  determined for the PANI-PTSA<sub>0.50</sub> sample by the *dc* conductometry method. An analysis of these dependences leads to the conclusion that this polymer exhibits 1D VRH at low temperature region, typical of a granular metal. As in case of other PANI, the  $\sigma_{dc}$  value is governed by strong spin-spin interaction at high temperatures. Experimental data is shown from Fig. 21 to be well described by Eq. (48) with the parameters presented in Table III.

The averaged length of charge wave localization  $\langle L \rangle = 11 \text{ nm}$  exceeds the effective radius of a quasi-metallic domains equal to 4 nm.<sup>232</sup> It can be due to closely electronic properties of the metal-like domains in the polymer. It allows to evaluate charge transfer integral  $t$  in such domains from relation connecting  $T_0$  values at 1D VRH,<sup>222</sup>  $T_0^{(3D)} = 256T_0^{(1D)}\ln(2T_0^{(1D)}/\pi t)$ , to be 0.10 eV. The most probable carrier hopping range  $R = (T_0/T)^{1/2}\langle L \rangle/4$  was determined at room temperature to be 34 nm. The hopping energy  $W$  of a charge carrier in the polymer was determined in terms of the VRH theory,  $W = k_B(T_0 T^3)^{1/4}/2$ , to be 0.034 eV, that is of the order of  $k_B T$ . The data make it possible to calculate the velocity of charge carriers  $v_F = 4.0 \times 10^6 \text{ cm/s}$  moving near

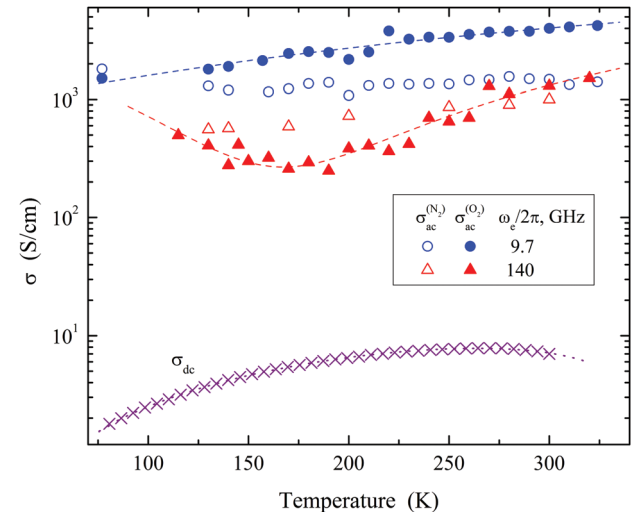


FIG. 21. Temperature dependence of dc and ac conductivity determined from 3-cm and 2-mm waveband EPR Dysonian spectra of the PANI-PTSA<sub>0.5</sub> sample in nitrogen (open symbols) and air (filled symbols) atmospheres. Top-down dashed lines present the dependences calculated from Eq. (50) with respective  $\sigma_{01} = 13.3 \text{ S/K cm}$ ,  $\sigma_{02} = 0.25 \text{ S/K cm}$ ,  $E_{ph}^\dagger = 0.027 \text{ eV}$ ,  $\sigma_{01} = 24.9 \text{ S/K cm}$ ,  $\sigma_{02} = 10.8 \text{ S/K cm}$ ,  $E_{ph}^\dagger = 0.022 \text{ eV}$ ,  $\sigma_{01} = 0.21 \text{ S/K cm}$ ,  $\sigma_{02} = 4.1 \times 10^{-2} \text{ S/K cm}$ ,  $E_{ph}^\dagger = 0.032 \text{ eV}$ ,  $\sigma_{01} = 0.25 \text{ S/K cm}$ ,  $\sigma_{02} = 1.9 \times 10^{-2} \text{ S/K cm}$ ,  $E_{ph}^\dagger = 0.031 \text{ eV}$ , and  $\kappa = 1$ . Dotted line shows the dependences calculated from Eq. (48) with  $k_1 = 26 \text{ S K}^{-0.5}/\text{cm}$ ,  $T_0 = 4.6 \times 10^4 \text{ K}$ ,  $d = 3$ ,  $k_2 = 0.19 \text{ S/K cm}$ ,  $E_{ph} = 0.027 \text{ eV}$ .

the Fermi energy with an energy of  $\varepsilon_F = 0.34 \text{ eV}$ . The latter value lies near to that determined for PANI-CSA (0.4 eV)<sup>54</sup> and PANI-SA (0.5 eV).<sup>122,125</sup> This is in agreement with the supposition earlier made by Pelster *et al.*<sup>232</sup> that the charge transport in PANI-PTSA takes place via two contributions: metallic conduction through a crystalline core of 8 nm and thermally activated tunneling (hopping) through an amorphous barrier of 1–2 nm diameter.

Spin-lattice and spin-spin relaxation times measured by the saturation method at 3-cm waveband EPR for the PANI-PTSA<sub>0.50</sub> by using Eqs. (20) and (21) are, respectively,  $1.2 \times 10^{-7}$  and  $3.1 \times 10^{-8} \text{ s}$  (in the nitrogen atmosphere) and  $1.1 \times 10^{-7}$  and  $1.6 \times 10^{-8} \text{ s}$  (in the air).<sup>127,128</sup> If one supposes that the polarons in this polymer possess mobility and diffuse along and between polymer chains with the diffusion coefficients  $D_{1D}$  and  $D_{3D}$ , respectively,  $D_{1D} = 3.5 \times 10^8$  and  $D_{3D} = 1.1 \times 10^9 \text{ rad/s}$  (in the nitrogen atmosphere) and  $D_{1D} = 8.1 \times 10^{11}$  and  $D_{3D} = 2.3 \times 10^8 \text{ rad/s}$  (in the air) are evaluated from Eqs. (34) to (36). A corresponding conductivities due to so possible polaron mobility calculated from Eq. (37) are, respectively,  $\sigma_{1D} = 2.5 \times 10^{-4} \text{ S/cm}$ ,  $\sigma_{3D} = 2.3 \times 10^{-4} \text{ S/cm}$  and  $\sigma_{1D} = 29 \text{ S/cm}$ ,  $\sigma_{3D} = 2.4 \times 10^{-3} \text{ S/cm}$ . This means that  $D_{1D} < D_{3D}$  in the sample without oxygen; however, the conductivity appears to be practically isotropic in character. The  $D_{1D}/D_{3D}$  ratio for the sample exposed to air increases to  $\sim 10^4$ , which substantially exceeds the value  $D_{1D}/D_{3D} \sim 50$  obtained for highly doped PANI-HCA.<sup>95</sup> The conductivity of this sample also becomes anisotropic,  $\sigma_{1D}/\sigma_{3D} \sim 10^4$ , and is also determined mainly by the diffusion of paramagnetic center along the polymer chain. The data obtained can be compared with those evaluated from the Dysonian EPR spectra.

The  $\sigma_{ac}$  values determined for the PANI-PTSA<sub>0.50</sub> sample from its Dysonian 3-cm and 2-mm waveband EPR spectra by using Eqs. (15)–(17) are shown in Fig. 21 vs. temperature. An intrinsic conductivity of the sample visibly increases at its exposition to air (Fig. 21). RT conductivity obtained for the sample at 3-cm waveband EPR is two orders of magnitude higher than  $\sigma_{1D}$  and  $\sigma_{3D}$  calculated above in terms of Q1D polaron diffusion along the “single conducting chain.”<sup>95</sup> Hence, it may be concluded that the conductivity in this polymer, as in polyaniline with other counter-ions, is mainly governed by the mobility of 3D-delocalized electrons in metal-like domains in which paramagnetic polarons are localized on parallel chains due of their strong exchange interaction. The temperature dependence of intrinsic conductivity can be interpreted in terms of the VRH mechanism of charge carriers and their scattering on the polymer lattice phonons respectively in amorphous and crystalline phases of the samples. Analogous to other PANI, the charge carrier crosses these phases one after another, so the resulting conductivity should be described by Eq. (50). Figure 21 evidences that the  $\sigma_{ac}(T)$  dependence evaluated for the PANI sample exposed to air follows well to Eq. (50) with the parameters listed in Table III. The  $E_{ph}^{\parallel}$  value obtained for the sample correlates with  $E_{ph}$  determined from the fitting of its  $\sigma_{dc}(T)$  dependence in terms of the same charge transport mechanism (Table III). This fact confirms additionally supposition above made on the existing of strong spin dipole-dipole interaction in crystalline domains.

A decrease in  $\sigma_{ac}$  with an increase in the registration frequency may be as result of, e.g., the influence of external magnetic field on the spin-exchange process in the polymer or deeper penetration of MW field into the polymer bulk at 2-mm waveband EPR. Indeed, the intrinsic conductivity should be higher if the skin-layer is formed on metal-like domains with a smaller radius in PANI particles.

In general, as in case of main conducting polymers, two types of PC are formed in PANI, polarons localized on chains in amorphous polymer regions and polarons moving along and between polymer chains. During the polymer doping the number of the mobile polarons increases and the conducting chains become crystallization centers for the formation of the massive metal-like domains of strongly coupled chains with 3D delocalized charge carriers. This process is accompanied by the increase of the electron-phonon interaction, crystalline order, and interchain coupling. The latter factor plays an important role in the stabilizing of the metallic state, when both 1D electron localization and “Peierls instability” are avoided. Above the percolation threshold the interaction between spin charge carriers becomes stronger and their mobility increases, so part of the mobile polarons collapses into diamagnetic bipolarons. Besides, the doping changes the interaction of the charge carriers with the lattice phonons, and therefore the mechanism of charge transfer. It also results in an increase of the number and size of highly conducting domains containing charge carriers of different types and mobilities, which lead to an increase in the conductivity and Pauli susceptibility. This process is modulated by macromolecular dynamics, and is accompanied by an increase in the crystalline order (or dimensionality) and planarity of the system.

In the initial PANI, the charges are transferred isoenergetically between solitary chains in the framework of the Kivelson formalism. The growth of the system dimensionality leads to the scattering of charge carriers on the lattice phonons. The charges 3D and 1D hop between these domains in the medium and heavily doped PANI, respectively. In heavily doped PANI, the charge carriers are transferred according to the Mott VRH mechanism which is accompanied by their scattering on the lattice phonons. This is in agreement with the concept of the presence of 3D metal-like domains in PANI-ES rather than the supposition that 1D solitary conducting chains exist even in heavily doped PANI.

In contrast with PANI-SA and PANI-HCA characterized as a Fermi glass with electronic states localizes at the Fermi energy due to disorder, PANI-CSA, PANI-AMPSA, and PANI-PTSA are disordered metals on the metal-insulator boundary. The metallic quality of ES form of PANI grows in the series PANI-HCA → PANI-SA → PANI-PTSA → PANI-AMPSA → PANI-CSA.

## IV. UTILIZATION OF POLYANILINE IN MOLECULAR ELECTRONICS

### A. Polyaniline-based sensors for solution components

Conjugated polymers are widely used as chemical sensors for different gases and liquids,<sup>26,233</sup> PANI among them. PANI-ES has been shown<sup>234</sup> to be sensitive to vapors of ethanol or acetone, however, such sensor was appeared to be unstable due to polymer partial dedoping. We have showed<sup>115</sup> that the ambient humidity can change magnetic resonance, electronic, and crystalline properties of PANI-ES. This effect can be attributed to formation in polymer matrix water chains with hydrogen binding. Davydov’s solitons<sup>235</sup> formed on such chains can transfer a charge which, therefore, should change polymer magnetic and electronic properties. Transistor structures can also be used as chemical sensors<sup>236</sup> since the potential barrier of the transistor base, and hence the resistance, can alter upon interaction with a medium. We have assumed<sup>237,238</sup> that in this case a PANI-EB layer on the transistor structure could act as mediator changing its response on the sensing components due to existence in this polymer of electron donor (amino-) and acceptor (quinone diimino-) sites. Such methodic approach was used in the study of various organic substances, e.g., ethanol, citric acid, solution of nitroxide stable radical 4-acetylamin-2,2,6,6-piperidine-1-axyl (ATPO), and some others.

#### 1. Ethanol in hexane

Figure 22(a) shows that the “passive” transistor (with or without PANI-EB layer) and the PANI-EB resistive structures are practically insensitive to the change in ethanol concentration in hexane; their characteristics are almost horizontal and non-monotonous. This implies that no appreciable charge transfer between the ethanol and the above structures occurs.

The “active” transistor structure has a noticeable sensitivity but the response is non-linear, with a slope of

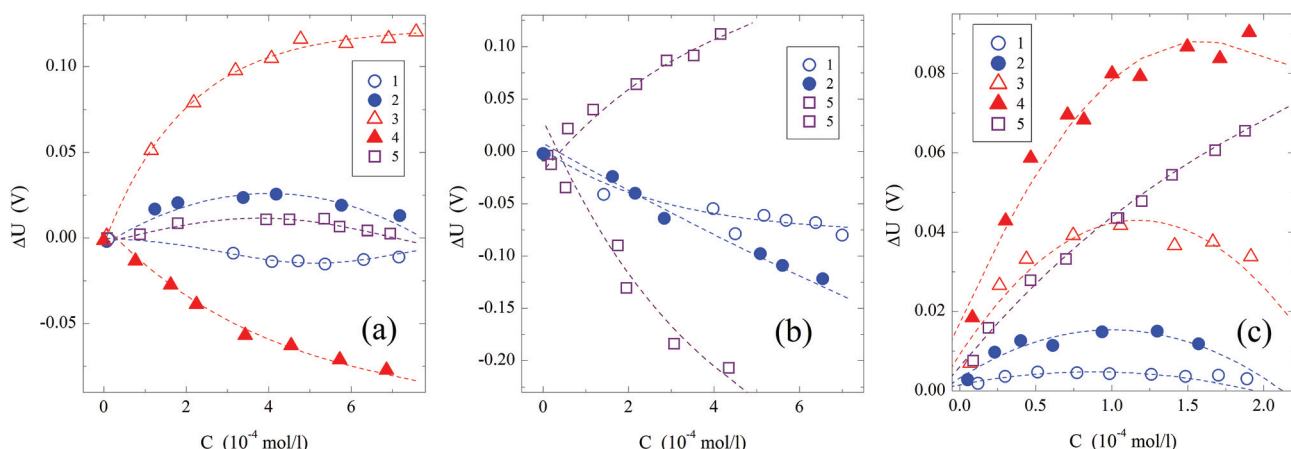


FIG. 22. Concentration dependences of the response of the sensors based on “passive” transistor scheme without (1) and with (2) PANI-EB layer, “active” transistor scheme without (3) and with (4) PANI-EB layer, and PANI-EB deposited onto ceramic plate to ethanol in hexane (a), citric acid in ethanol (b), and nitroxide stable radical ATPO in ethanol (c). Dashed lines connecting the experimental points are painted arbitrarily.

590 V·l/mol in the initial region and a tendency to saturation at concentrations higher than 0.4 mM. PANI-EB casting changes the sign of the response, i.e., the polymer does not act synergetically with the transistor structure. The steepness decreases down to 230 V·l/mol but the characteristic has a lower curvature. The latter sensor possesses 820 V·l/mol response to acetone. This indicates that the PANI-EB film may specifically associate the base of a transistor with polar substances such as ethanol in solution to give changes of the response.

## 2. Citric acid in ethanol

Figure 22(b) evidences that the sensitivity of all the sensors to citric acid is higher than that to ethanol that and is characterized by lower curvature. PANI-EB slightly increases the sensitivity of the “passive” transistor sensor thus acting synergetically with the transistor structure, but both response values are relatively low, no more than 200 V·l/mol.

It is noteworthy that rather a steep (535 V·l/mol) and perfectly linear (for the range of concentrations used) response is attained for a simple resistive PANI-EB sensor. This should be due to the protonic acid doping of the PANI-EB forming PANI-ES coils in polymer matrix and, therefore, increases sum conductivity of the system. This supposition is confirmed by the narrowing of the PANI EPR spectrum under its modification by different dopants (see above).

## 3. Nitroxide radical ATPO in ethanol

As in the case of ethanol in hexane, “passive” transistors with or without PANI-EB are practically insensitive to the presence of nitroxide radical ATPO in ethanol (Fig. 22(c)). The characteristic of the “active” transistor (without PANI-EB), being rather steep initially (1200 V·l/mol), becomes horizontal at concentrations higher than 0.06 mM. PANI-EB acts synergetically increasing the steepness of the response up to 1830 V·l/mol in the initial concentration range and keeps the characteristic increasing to at least 0.15 M. The response of the resistive PANI sensor is less steep

(800 V·l/mol) but has a lower curvature over the whole range of concentrations studied. Comparing the results obtained for ATPO and ethanol one can conclude another type of interaction of the N-O<sup>•</sup> active radical group with the sensoric matrix due, probably, to interaction this radical with polarons stabilized in the PANI-EB matrix.

## B. Spin-assisted charge transfer in polyaniline composites

Conjugated polymers gain an additional particular interest because the existence of a spin charge carriers in such organic semiconductors allows one to construct more efficient molecular electronic devices than using spineless ones.<sup>239</sup> For instance, a unique capability of spin orientation in external magnetic field and its very weak interaction with own environment in semiconductors open an undoubted imperative to developing new spin electronic (magneto-electronic, spintronic) devices simultaneously exploiting both charge and spin of electrons in the same device and appropriate cutting-edge spectroscopic methods suitable for registration of spin polarization and its controlled manipulation.<sup>240</sup>

Electron spin plays a crucial role in organic semiconductor devices in which a charge is transferred by polarons with spin  $S = 1/2$ . Injection of charge carriers into, e.g., organic light-emitting diodes or light illumination of polymer/fullerene solar cells leads to the formation of excitons in these organic semiconductors. Excitons can be transformed into polaron pairs or donor-acceptor complexes which then can collapse into radical pairs, positively charged polarons on polymer chains and negatively charged fullerene anion radicals. Moreover, the triplet state of fullerene characterized by high electron spin polarization can also be easily photoexcited in bulk heterojunction which it forms with a polymer backbone. However, these processes themselves are not trivial phenomena whose microscopic details still remain unknown. For example, one would not necessarily expect the recombination of a charge carrier with the first opposite charged carrier. Because both the charge carriers exchangeable spin-flip, their further recombination becomes dependent on their dynamics, number, polarization, and mutual separation. For large separations, when thermal energy exceeds

the interaction potential, the charges can be considered as non-interacting. Once the carriers become nearer than the inverted Coulombic interaction potential, their wave functions overlap and exchange interactions become non-negligible. This can lead to the formation of singlet or triplet excitons in organic semiconductors. Introduction of galvinoxyl radical into polymer/fullerene bulk heterojunctions allowed one to suppress recombination of photoinduced charge carriers and thereby to improve of light conversion efficiency of such solar cells.<sup>241,242</sup> Such effect was explained by resonant exchange interaction of charged acceptors with spin adducts, which converts the bipolaronic spin state from singlet to triplet.

These excited states can be detected in organic systems using optical (fluorescence and phosphorescence) and/or magnetic resonance.<sup>243</sup> However, other absorbing species are generally present in such systems, namely, polaronic charge carriers, which themselves introduce efficient subgap optical transitions. Thus, a clear assignment to triplet excitations is not always possible. EPR was proved<sup>243</sup> to be the most effective direct tool able to reveal the underlying nature of spin carriers excited in such systems. This method allows one to study various materials with weak spin-orbit coupling, where the differences in lifetime between the three excited-state triplet sublevels give rise to a spin-dependent buildup of macroscopic polarization,<sup>244</sup> including spin charge carriers stabilized in conjugated polymers<sup>86,88</sup> and photoinduced in their fullerene-based compositions for photovoltaic applications.<sup>245,246</sup>

So, to handle charge transfer by spin carriers, another spin reservoir should be introduced into organic polymer system. In this case the interaction between spin charge carriers one can expect to affect electronic properties of this system as it is shown schematically in the inset of Fig. 6(a). PANI-PTSA seems to be the most suitable systems for the study of spin-assisted charge transfer in organic semiconductors.<sup>130</sup> Polarons diffusing along its chains appeared to be accessible for triplet excitations injected into its bulk. It was shown above that the collision of diffusing domestic and guest spins dramatically changing magnetic, relaxation, and electron dynamics parameters of this polymer. Such effect was not registered in PANI-ES highly doped by other counterions.<sup>87,88,119,124,129</sup> Such principal difference can probably be explained by the increase in a PANI-PTSA matrix ordering. Indeed, this polymer, similarly to PANI-CSA,<sup>56</sup> can also be considered as disordered metal on the boundary of the metal-insulator transition, whereas, e.g., PANI-SA is Fermi glass in which the electronic wave functions are localized. So-called Anderson localization arises from the severe disorder observed in the latter initiating in such a system electron VRH between exponentially localized states with energies near  $\epsilon_F$ . However, PANI-PTSA demonstrates better material quality and therefore more metallic behavior with extended states near  $\epsilon_F$ . Thus, PANI-PTSA is disordered metal on metallic side of the metal-insulator boundary in contrast to PANI-SA with localized electronic states at  $\epsilon_F$  due to disorder. This predestined the use of both these PANI-ES as reservoirs of stabilized spins in our comparative experiments.

Poly(3-alkylthiophene) (P3AT) can be used as another spin ensemble. Illumination of bulk heterojunction formed

by P3AT with fullerene derivative, e.g., [6,6]-phenyl-C<sub>61</sub>-butyric acid methyl ester (PCBM) provokes the turnover exciton to the donor-acceptor complex which collapses into positively charged polaron and a methanofullerene radical anion.<sup>247</sup> Since the former shows high mobility along a polymer backbone, the radicals are scattered in this radical pair in such a way that two respective non-interacting spins are stabilized in bulk heterojunction. A long spatial distance lowers the probability of their collision and recombination that provides longer lifetime. Earlier we showed<sup>246</sup> that the rate, anisotropy, and mechanism of charge transfer photoinitiated in different polymer/fullerene composites are governed by structure, nanomorphology, and concentration of their ingredients. Therefore, we selected poly(3-dodecylthiophene) (P3DDT) previously used as an effective polymer matrix of organic solar cells<sup>248–252</sup> as a second spin reservoir.

### 1. EPR and light-induced EPR (LEPR) spectra of PANI-ES/P3DDT/PCBM composite

To analyze the nature of all paramagnetic centers in both the PANI-SA/P3DDT/PCBM and PANI-PTSA/P3DDT/PCBM composites, first related study of spin properties of their ingredients should be done.

Initial PANI-SA and PANI-PTSA samples exhibit single 3-cm waveband EPR spectra presented in Figs. 23(a) and 23(b), respectively attributed to polarons P<sub>1</sub><sup>+</sup> stabilized in their backbones. Their g-factors remain almost unchanged within all temperature range used that is characteristic of paramagnetic centers in crystalline high-conductive solids<sup>87,88,118</sup> As-prepared P3DDT/PCBM sample does not demonstrate any EPR spectrum without light irradiation (Fig. 23(c)). When illuminated by visible light, positively charged polaron is formed on a polymer backbone due to electron transfer to methanofullerene (see Fig. 23(c)). Various experimental methods have shown the reversibility of this process and its stability over time.<sup>245,246</sup> As in our previous studies,<sup>251,252</sup> two partly overlapping LEPR lines are observed at low temperatures (Fig. 23(c)). Such doublet was attributed to radical pairs of positively charged diffusing polarons P<sub>2</sub><sup>+</sup> with isotropic (effective)  $g_{\text{iso}} = 2.0018$  and negatively charged radical anions C<sub>61</sub><sup>•-</sup> with effective  $g_{\text{iso}} = 1.9997$  pseudorotating near the main axis. These values are close to those obtained for spin charge carriers photoinduced in other polymer/fullerene bulk heterojunctions.<sup>246,253,254</sup> The EPR line shape due to dipole or hyperfine broadening is normally Gaussian. For spin 3D motion in metal-like crystallites of PANI-ES or exchange of different spin packets, the line shape becomes close to Lorentzian shape, corresponding to an exponential decay of transverse magnetization. The effective LEPR doublet presented in Fig. 23(c) is characterized by a Lorentzian distribution of mobile radical pairs P<sub>2</sub><sup>+</sup> – mC<sub>61</sub><sup>•-</sup> (Fig. 23(d)) of mobile polarons P<sub>2</sub><sup>+</sup> and fullerene methanofullerene radical anions mC<sub>61</sub><sup>•-</sup> as well as a Gaussian contribution of polarons pinned by deep traps appeared in a polymer matrix under its illumination (shown in Fig. 23(e)). Both mobile charge carriers recombine with the probability increasing with temperature, and their effective spectrum shown in Fig. 23(d) becomes too

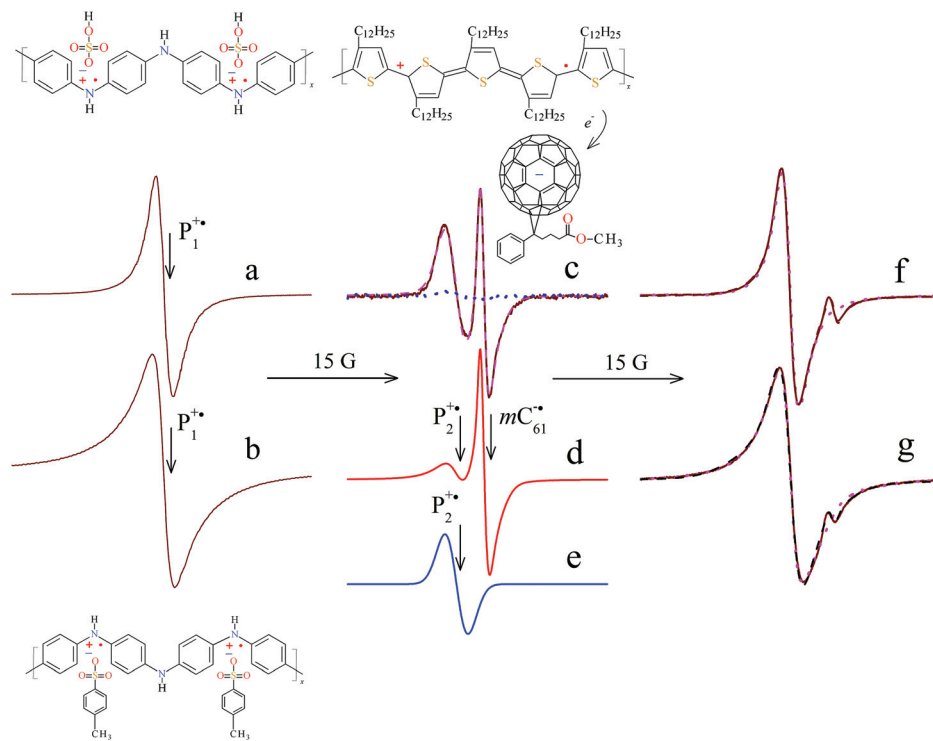


FIG. 23. EPR spectra of polarons  $P_1^+$  in the polyaniline emeraldine salts PANI-SA (a) and PANI-PTSA (b), P3DDT/PCBM bulk heterojunctions illuminated by white light (c) with contributions due to mobile polaron-methanofullerene radical pairs  $P_2^+ - mC_{61}^-$  (d) and localized polarons  $P_2^+$  pinned by deep traps (e) as well as PANI-SA/P3DDT/PCBM (f) and PANI-PTSA/P3DDT/PCBM (g) composites illuminated by white light in MW cavity at 77 K. Dashed line in (c) and deconvoluted lines (d) and (e) show EPR spectra calculated using  $\Delta B_{pp}^P = 2.67$  G,  $\Delta B_{pp}^F = 1.17$  G, and  $[P_2^+]/[mC_{61}^-] = 2.0$ . In (c), (f), and (g), dotted lines exhibit “dark” EPR spectra of paramagnetic centers stabilized in appropriate composites, whereas the spectra calculated at their illumination by white light at 77 K are shown by dashed lines. The positions of all paramagnetic charge carriers are also shown. Schematic structures of the PANI-ES with appropriate SA and PTSA counter-ions as well as P3DDT with PCBM cage are shown as well. The appearance of positive charged polaron in the P3DDT backbone due to the photoinitiated charge separation and transfer to the fullerene cage is also shown.

weak to be registered at  $T \geq 200$  K at a reasonable signal/noise ratio. Captured polarons  $P_2^+$  are characterized by higher stability, and their spectrum can be observed for several hours even at high temperatures. Nevertheless, these carriers indirectly participate in collective charge transfer through bulk heterojunctions.

It is evident that LEPR spectra of both PANI-SA/P3DDT/PCBM and PANI-PTSA/P3DDT/PCBM composites presented in Figs. 23(f) and 23(g), respectively, can be considered as a sum of P3DDT/PCBM and appropriate PANI-ES contributions. As an illumination is turned off, the spectra originated from the polarons  $P_1^+$  stabilized in PANI-ES (shown in Figs. 23(a) and 23(b)) and polarons  $P_2^+$  pinned in P3DDT/PCBM (shown in Fig. 23(e)) can only be registered (see Figs. 23(f) and 23(g)). In order to study charge-separated states and spin-spin interactions in these systems more precisely, their spectra were tentatively deconvoluted, as it was successfully done for analogous spin-modified systems.<sup>252,255–259</sup> This allowed to obtain separately magnetic resonance parameters of all paramagnetic centers stabilizing in initial polymers and appropriate composites and analyze their interaction in bulk heterojunctions.

## 2. EPR linewidth of charge carriers in PANI-ES/P3DDT/PCBM composites

Figure 24(a) shows temperature dependences of effective absorption peak-to-peak linewidth  $\Delta B_{pp}$  of polarons  $P_1^+$

stabilized in the PANI-SA,  $P_2^+$  photoinitiated in P3DDT/PCBM bulk heterojunctions, and these values obtained for darkened and illuminated PANI-SA/P3DDT/PCBM composite. It is seen that the EPR linewidth for both polarons stabilized in these systems depends on structure of a polymer matrix. Indeed, the heating of the initial PANI-SA samples is accompanied by a monotonic decrease in  $\Delta B_{pp}$  of polarons  $P_1^+$  stabilized on their chains. However, this parameter for polarons  $P_2^+$  photoinitiated in the P3DDT/PCBM bulk heterojunctions evidences an opposite temperature dependence as compared with that for polarons  $P_1^+$  (Fig. 24). This effect can be explained by different interaction of these polarons with appropriate polymer lattice. The formation of the PANI-SA/P3DDT/PCBM composite does not noticeably changes the linewidth for paramagnetic centers  $P_1^+$ . However, this originates the change in the temperature dependence of  $P_2^+$  charge carriers photoinitiated in the P3DDT matrix (see Fig. 24(a)).

Spin properties of both polaronic reservoirs in the PANI-ES/P3DDT/PCBM composites are strongly governed by the conformation of PANI-ES chains which determines its main electronic properties.<sup>260</sup> As the PANI-SA matrix is replaced by the PANI-PTSA one, both polarons  $P_1^+$  and  $P_2^+$  start to demonstrate above mentioned extreme temperature dependent linewidths characterized by appropriate critical point  $T_{ex} \approx 150$  K. A similar effect was observed in the EPR study of exchange interaction of polarons with guest oxygen biradicals  $\cdot O - O^\bullet$  in PANI-ES highly doped with

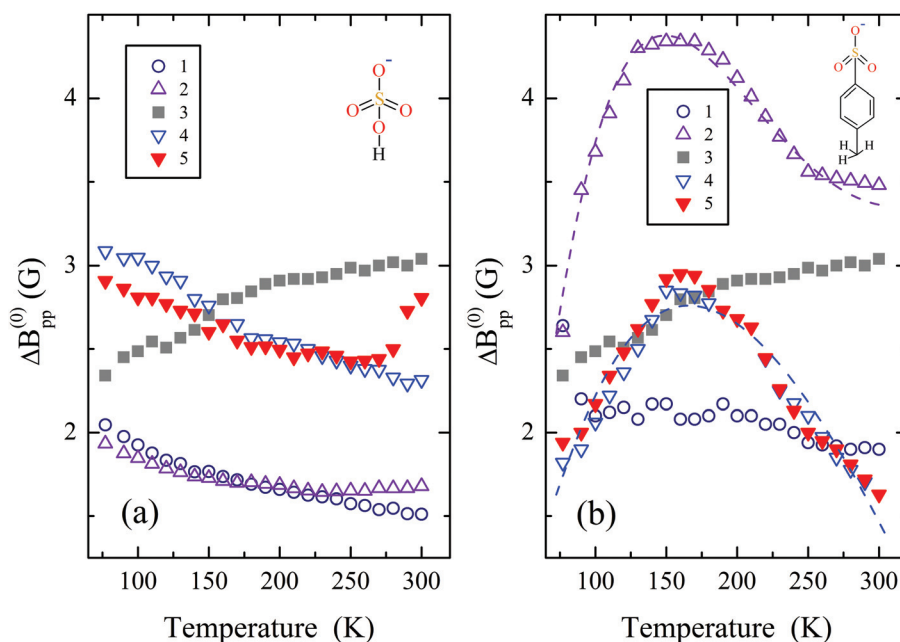


FIG. 24. Temperature dependence of the peak-to-peak linewidth  $\Delta B_{pp}^{(0)}$  determined for domestic polarons  $P_1^+$  stabilized in initial PANI-ES backbones (1), PANI-ES/P3DDT/PCBM composites (2), polarons  $P_2^+$  background photoinitiated by white light in the P3DDT/PCBM composite (3) as well as polarons  $P_2^+$  stabilized in the darkened (4) and irradiated by white light (5) PANI-ES/P3DDT/PCBM composites with SA (a) and PTSAs (b) counter-ions shown in the insets. The upper (0) symbol in  $\Delta B_{pp}^{(0)}$  means that this parameter is measured far from the spectrum MW saturation. Dashed lines show the dependences calculated from Eq. (11) with  $\omega_{hop}^0 = 1.2 \times 10^9 \text{ s}^{-1}$ ,  $E_a = 0.006 \text{ eV}$  (above line),  $\omega_{hop}^0 = 1.3 \times 10^9 \text{ s}^{-1}$ ,  $E_a = 0.012 \text{ eV}$  (below line), and  $J_{ex} = 0.110 \text{ eV}$ .

hydrochloric acid<sup>111</sup> and PTSAs<sup>261,262</sup> (see above) and was attributed to exchange interaction in quasi-pairs formed by guest spins with domestic mobile polarons hopping between sites of polymer chain with rate  $\omega_{hop}$  across activation energy barrier  $E_a$ . So, the data presented in Fig. 24(b) can also be described in terms of the spin-spin exchange interaction of polarons  $P_1^+$  and  $P_2^+$  hopping in the nearly located solitary polymer chains. The collision of both type spins should additionally broaden the absorption term of EPR line by the value described by Eq. (10).

Assuming activation character of polaron motion in both polymer matrices and  $C_g = 1.2 \times 10^{-4}$  obtained for P3DDT/PCBM bulk heterojunctions,<sup>252</sup> the linewidth of the polarons  $P_1^+$  and  $P_2^+$  can be fitted by Eq. (11) with  $E_a = 0.006$  and  $0.012 \text{ eV}$ , respectively, at  $J_{ex} = 0.110 \text{ eV}$  (see Fig. 24(b)).  $J_{ex}$  is less than that determined above for air-filled PANI-PTSA<sup>261,262</sup> due probably to less number of guest radical and higher interpolaron distance.

### 3. Spin susceptibility of charge carriers in PANI-ES/P3DDT/PCBM composites

Figs. 25(a) and 25(b) show the temperature dependence of spin susceptibility  $\chi$  with contributions due to polarons  $P_1^+$ ,  $P_2^+$  and methanofullerene radical anions  $mC_{61}^-$  forming spin pairs in the P3DDT/PCBM bulk heterojunctions stabilized in the darkened and background illuminated PANI-SA/P3DDT/PCBM and PANI-PTSA/P3DDT/PCBM composites. The analysis of the above data was performed using an ensemble of  $N_s/2$  spin pairs with an uniform distribution of intrapair exchange characterized by coefficient  $J$ . In PANI-ES, as in other conducting polymers, most spins are expected to be localized.<sup>86,141</sup> Disorder localizes electron spins and conducting polymer systems exhibit significant disorder. Therefore, for explanation of the data presented in Fig. 25 we used an exchange coupled pairs (ECPs) model.<sup>145,146</sup> This model predicts spin susceptibility change

with the temperature described by Eq. (5). It is seen from the figure that the model calculations provide excellent fits to all the experimental data sets within all temperature range used. The  $C$ ,  $a_d$ , and  $J$  values determined for polarons carrying a charge in the initial PANI-ES and respective PANI-ES/P3DDT/PCBM composites are summarized in Table IV.

Spin susceptibility obtained for  $P_1^+$  is close to that obtained for PANI highly doped by sulfuric<sup>263</sup> and hydrochloric<sup>61</sup> acids. The latter parameter is normally a function of distance. When polymer chains vibrate,  $J$  for polarons diffusing along neighboring chains would oscillate and should be described by a stochastic process.<sup>264</sup> However, such effect appears at low temperatures, when  $k_B T \ll J$ . Thus, it can be neglected within all temperature range used. Nevertheless, this constant increases as polarons  $P_1^+$  start to interact with polarons  $P_2^+$  and, on the side, SA counter ions are replaced by PTSAs ones (see Table IV). This is additional evidence of strong interaction of polarons stabilized in both PANI-ES and P3DDT matrices. When the Fermi energy  $\varepsilon_F$  is close to the mobility edge, the temperature dependence of spin susceptibility gradually changes from Curie-law behavior  $\chi_C \propto 1/T$  to temperature-independent Pauli-type behavior with increasing temperature. Corresponding density of states  $n(\varepsilon_F)$  for both spin directions per monomer unit at  $\varepsilon_F$  can be determined from the analysis of the  $\chi(T)T$  dependence for all polarons stabilized in both polymers (see insets in Fig. 25). It is seen that the PTSAs-treated system is characterized by higher  $n(\varepsilon_F)$  as compared with PANI-SA. This can be explained by the difference in their above mentioned metallic properties and also by on-site electron-electron interaction.<sup>45</sup>

Spin susceptibility obtained for methanofullerene radical anions  $mC_{61}^-$  in both composites demonstrates sharper temperature dependence (Fig. 4). This can be explained by fast recombination of the polaron-methanofullerene radical pairs  $P_2^+ - mC_{61}^-$  whose spectrum is shown in Fig. 23(d). During background illumination of the P3DDT/PCBM bulk

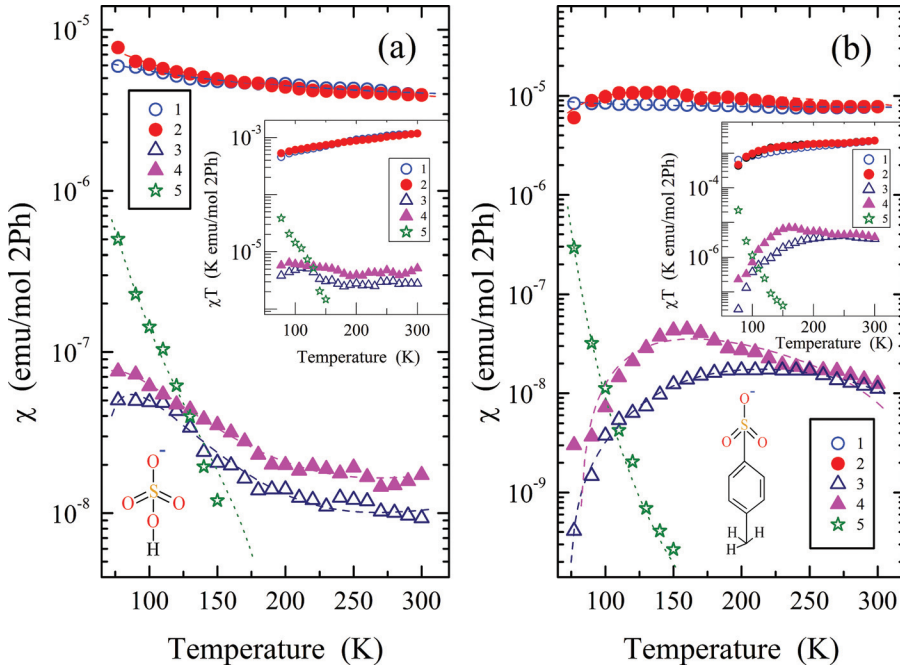


FIG. 25. Temperature dependences of spin susceptibility  $\chi$  and  $\chi T$  product (insets) obtained for domestic polarons  $P_1^+$  stabilized in the initial PANI-ES networks (1) and respective PANI-ES/P3DDT/PCBM composites (2), polarons  $P_2^+$  stabilized in the darkened (3) and illuminated by white light (4) PANI-ES/P3DDT/PCBM composites, as well as methanofullerene anion radicals  $mC_61^-$  (5) photogenerated in these composites with the SA (a) and PTSAs (b) counter-ions shown in the insets. Dashed lines show the dependences calculated from Eq. (51) with  $C$ ,  $a_d$ , and  $J$  presented in Table IV. The dotted lines show the dependences calculated from Eq. (51) with  $E_b = 0.024$  eV (a) and  $0.050$  eV (b).

heterojunctions, two processes are realized simultaneously, namely, photoinitiation and recombination of spin pairs. As a result, we detected only net (effective) spin concentration. Therefore, effective paramagnetic susceptibility of both charge carriers photogenerated in P3DDT/PCBM bulk heterojunction should inversely depend on the probability of their recombination. Such process is also governed by multi-stage activation one-dimensional (1D) polaron hopping between polymer units.<sup>265</sup>

Positive charge on a polaron is not required to be recombined with the first negatively charged methanofullerene radical anion. Activation traveling of a polaron near such a center localized near a polymer chain should interact with its unpaired electron with the above probability  $p$  in Eq. (10). In this case, effective spin susceptibility of such interacting spin sub-pairs can finally be written as<sup>246,252,258,259,266</sup>

$$\chi = \chi_0 \frac{2(1 + \alpha^2)}{\alpha^2} \exp\left(\frac{E_b}{k_B T}\right). \quad (51)$$

The dependences calculated from Eq. (51) with  $E_b = 0.024$  and  $0.050$  eV are also presented in Fig. 25. The latter value is higher than  $E_a = 0.012$  eV obtained from Eq. (11) for polaron diffusion in the respective system. It can probably be explained by more complex exchange interaction of methanofullerene radical anion with polarons in both the PANI-PTSA and P3DDT backbones. Equation (51) fits well the experimental data presented in Fig. 25. Therefore, the decay of long-lived charge carriers originated from initial spin pairs photogenerated in the PANI-ES/P3DDT/PCBM composites can successfully be described in terms of the above model in which the low-temperature recombination rate is strongly governed by temperature and the width of energy distribution of trap sites. This process is also determined by structure and morphology of radical anion and its environment in a polymer backbone.<sup>267</sup>

It is seen from Fig. 25 that spin susceptibility of polarons  $P_1^+$  stabilized in both initial PANI-ES samples is characterized by weak temperature dependence without any

TABLE IV. The values of  $C$ ,  $a_d$ , and  $J$  determined for effective paramagnetic susceptibility  $\chi$  of polarons  $P_1^+$  stabilized in the initial PANI-SA and PANI-PTSA matrices and polarons  $P_2^+$  photoinduced in the P3HT network of respective PANI-ES/P3DDT/PCBM composites fitted using Eq. (5) and the data of Fig. 25.

|           | Parameter         | $P_1^{+a,b}$         | $P_1^{+b,c}$         | $P_2^{+d,e}$         | $P_2^{+d,e}$         |
|-----------|-------------------|----------------------|----------------------|----------------------|----------------------|
| PANI-SA   | $C$ , emu/mol 2Ph | $2.3 \times 10^{-6}$ | $2.2 \times 10^{-6}$ | $1.1 \times 10^{-9}$ | $1.5 \times 10^{-9}$ |
|           | $a_d$             | 0.041                | 0.039                | 0.965                | 0.966                |
|           | $J$ , meV         | 3.8                  | 5.6                  | 11                   | 6.4                  |
| PANI-PTSA | $C$ , emu/mol 2Ph | $5.8 \times 10^{-6}$ | $9.8 \times 10^{-7}$ | $1.1 \times 10^{-8}$ | $1.0 \times 10^{-8}$ |
|           | $a_d$             | 0.88                 | 0.98                 | 0.92                 | 0.98                 |
|           | $J$ , meV         | 3.4                  | 9.8                  | 20                   | 15                   |

<sup>a</sup>Polarons in initial PANI-ES.

<sup>b</sup>In the darkened samples.

<sup>c</sup>Polarons in PANI-ES embedded into the PANI-ES/P3DDT/PCBM composite.

<sup>d</sup>Polarons initiated in P3DDT network of the PANI-ES/P3DDT/PCBM composite.

<sup>e</sup>Background illuminated by white light.

anomaly. This also holds for polarons  $P_2^{+}$  photoinitiated in the PANI-SA/P3DDT/PCBM composite. The shape of  $\chi(T)$  changes dramatically as SA counter ions are replaced by PTSA ones. Such a replacement provokes extremal  $\chi$  vs.  $T$  dependence obtained for polarons  $P_1^{+}$  and  $P_2^{+}$  (see Fig. 25(b)). This is evidence of the above mentioned exchange interaction between these polarons formed on neighboring PANI and P3DDT chains. Such interaction increases the overlapping of their wave functions (which, however, slightly decreases at further light flashing) and the energy barrier which overcomes the polaron crossing a bulk heterojunction. This affects the polaron intrachain mobility and, therefore, probability of its recombination with fullerene anion. However, the character of the  $mC_{61}^{-}$  pseudorotation changes weakly under such a replacement (see Fig. 25).

#### 4. Electron relaxation of polarons in PANI-ES/P3DDT/PCBM composites

Electron relaxationalso get important information about spin localization, matrix dimensionality, and spin-assisted electronic processes carrying out in the system under study. There are several relaxation and dynamic processes in the composites, for example, dipole-dipole, hyperfine, exchange interactions between paramagnetic centers of different spin-packets, etc., which cause the shortening of spin relaxation times and hence the change of the shape of an EPR line. Above, it was demonstrated with the EPR linewidth term  $\delta(\Delta\omega)$  which is opposite proportional to the spin-spin relaxation time. Spin-lattice relaxation shortens the lifetime of a spin state and broadens the line as well. Earlier, we have showed that spin relaxation of spin charge carriers stabilized in, e.g., PANI-SA,<sup>87,125</sup> PANI-PTSA,<sup>128,261,262</sup> and P3DDT<sup>248–252</sup> is strongly defined by structural, conformational, and electronic properties of their microenvironment. So, it is important to analyze also how spin exchange affect spin-lattice relaxation. The interaction of polarons  $P_1^{+}$  stabilized in the PANI-SA matrix was appeared to be depending weakly on the presence of guest spins. Their dominantly contribute in an effective spin susceptibility of the composites under study. So, a spin-lattice relaxation of these charge carriers in the PANI-PTSA and PANI-PTSA/P3DDT/PCBM bulk heterojunctions can be analyzed with more degree of certainty.

Figure 26 exhibits temperature dependencies of  $T_1$  and  $T_2$  values for polarons  $P_1^{+}$  stabilized in shadowed PANI-PTSA and PANI-PTSA/P3DDT/PCBM samples. Spin-spin relaxation was shown to be governed by the spin-spin exchange interaction. Spin-lattice relaxation time of the samples was measured at room temperature to be  $0.45 \times 10^{-7}$  and  $0.33 \times 10^{-7}$  s, respectively. These values are in good agreement with  $T_1 = 0.98 \times 10^{-7}$  s obtained by Wang *et al.*<sup>63</sup> for polyaniline highly doped by hydrochloric acid. It is seen that spin-lattice relaxation of  $P_1^{+}$  stabilized in the initial polymer changes weakly as the temperature increases up to  $\sim 180$  K that is typical for organic ordered systems. This process accelerating suddenly near  $T \sim 210$  K possibly to a phase transition and then plateaus at higher temperatures. The latter value differs from  $T_c$  introduced

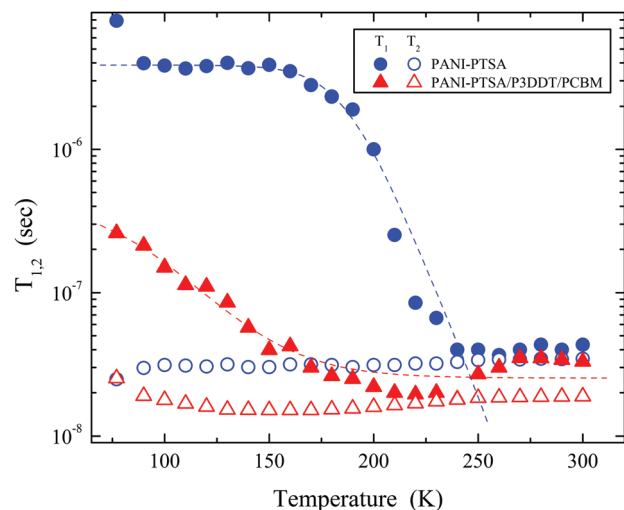


FIG. 26. Temperature dependence of spin-lattice,  $T_1$ , and spin-spin,  $T_2$ , relaxation times determined for polarons  $P_1^{+}$  stabilized in the PANI-PTSA backbone and respective PANI-PTSA/P3DDT/PCBM composite. Dashed lines connecting the experimental points are painted arbitrarily.

above because they characterize different processes. As  $P_1^{+}$  start to interact with other paramagnetic centers in the PANI-PTSA/P3DDT/PCBM composite, their spin-lattice relaxation strongly accelerates and becomes more temperature-dependent (Fig. 26). It is once more evidence of the exchange between polarons stabilized in neighboring polymer chains. Figure 26 demonstrates then  $T_1$  tends to  $T_2$  at high temperatures. This is typical for organic systems of low dimensionality and can be explained by the defrosting of macromolecular dynamics.

So, light excitation of P3DDT/PCBM bulk heterojunctions in the PANI-ES/P3DDT/PCBM composites leads to charge separation and transfer from a P3DDT chain to a methanofullerene molecule. This is accompanied by the excitation of two paramagnetic centers with clearly resolved LEPR spectra, namely, the positively charged polaron  $P_2^{+}$  on the polymer backbone and the negatively charged radical anion  $mC_{61}^{-}$  located between polymer chains. Both radicals are spatially separated due to fast 1D diffusion of the former, so that they become non-interacting. Polarons  $P_2^{+}$  moving in P3DDT solitary chains interact with  $P_1^{+}$  ones stabilized on neighboring PANI-ES chains due to overlapping of their wave functions. Such interaction is governed mainly by nanomorphology of PANI-ES subdomains and defines insulating and conducting forms of PANI-SA and PANI-PTSA, respectively. Spin exchange and transverse relaxation of polarons is governed by 1D activation hopping  $P_2^{+}$  along P3DDT chains and strongly increase as PANI-SA polymer is replaced by PANI-PTSA one in the triple composite. Spin-lattice relaxation of polarons stabilized in PANI-PTSA is also accelerated by their exchange interaction with guest spin ensemble. Paramagnetic susceptibility of these polarons is realized according the model of exchange coupled spin pairs differently distributed in appropriate polymer matrices. This deepens overlapping of wave functions of these charge carriers and leads to the increase in the energy barrier which overcomes the polaron under its crossing through a bulk

heterojunction. It is evident that separate EPR investigation of spin properties of domestic and photoexcited paramagnetic centers in the polymer/polymer/fullerene composite and its ingredients may give a possibility to control its texture and other structural properties over the entire range of temperatures studied. This means that spin charge carriers photoinitiated in the P3DDT-PCBM system act as a nanoscopic probes of the polaron dynamics in the PANI matrix. The data obtained for such model system can contribute to open new horizon in creation of flexible and scalable organic molecular devices with spin-assisted electronic properties. Our results suggest an important role played by interchain coupling of different spin charge carriers on a handling of charge transfer in bulk heterojunction, PANI-ES/P3DDT/PCBM. There seems to be several ways for the charge dynamics operation in this composite. The main way is the interaction of different spin reservoirs above mentioned. Photoinitiation of additional spins seems to handle charge transport more delicate that is a critical strategy in creating systems with spin-assisted charge transfer.

## V. CONCLUDING REMARKS

The data presented show the variety of electronic processes, realized in polyanilines, which are stipulated by the structure, conformation, packing and the degree of ordering of polymer chains, and also by a number and the origin of dopants, introduced into the polymer. Among the general relationships, peculiar to these compounds are the following ones.

Spin and spinless non-linear excitations may exist as charge carriers in PANI-ES. The ratio of these carriers depends on various properties of the polymer and dopant introduced into it. With the increase of doping level the tendency of collapse of polaron pairs into diamagnetic bipolaron is observed. Doping process leads to the change of charge transfer mechanism. Conductivity in neutral or weakly doped samples is defined mainly by interchain charge tunneling in the frames of the Kivelson formalisms, which is characterized by a high enough interaction of spins with several phonons of a lattice and leads to the correlation of Q1D spin motion and interchain charge transfer. These mechanisms ceases to dominate with the increase of doping level and the charge can be transferred by its thermal activation from widely separated localized states in the gap to close localized states in the tails of the VB and CB. Therefore, complex quasi-particles, namely, the molecular-lattice polarons can be formed in some matrices because of libron-phonon interactions analogously to that it is realized in organic molecular crystals. It should be noted that because polyaniline, as other conducting polymers, have *a priori* a lower dimensionality as compared with molecular crystals, dynamics of its charge carriers is appeared to be more anisotropic. In heavily doped samples the dominating is the interchain Mott charge transport, characterized by strong interaction of charge carriers with lattice phonons.

A higher spectral resolution at 2-mm waveband EPR provides a high accuracy of the measurement of magnetic resonance parameters and makes *g*-factor of organic free

radicals an important informative characteristic. This allows the establishment of the correlation between the structure of organic radicals and their *g* tensor canonic values, providing the ability of PC identification in conducting polymers. The multifrequency EPR study allows to obtain qualitatively new information on spin carrier and molecular dynamics as well as on the magnetic and relaxation properties of polymer systems. The data obtained under study of organic conducting polymers allow us to establish the correlations between dynamics, electronic and structural parameters of these systems which can be used for controllable synthesis of various organic novel devices with optimal properties. Since coherent spin dynamics in organic semiconductors is anisotropic, our strategy seems to make it possible obtaining complex correlations of anisotropic electron transport and spin dynamics for the further design of progressive molecular electronics and spintronics.

## ACKNOWLEDGMENTS

The partial support by the Russian Foundation of Basic Researches, Grant No. 12-03-00148, was gratefully acknowledged. The author expresses his gratitude to Professor Dr. G. Hinrichsen, Professor A. P. Monkman, and Dr. B. Wessling for collaboration, to Dr. S. D. Chemerisov and Dr. N. N. Denisov for the assistance in EPR experiments, to Professor Dr. H.-K. Roth, Professor Dr. K. Lüders, and Professor Y. S. Lebedev for fruitful discussion.

## APPENDIX: EXPERIMENTAL

### 1. Sample preparation

Powder-like PANI-SA was synthesized by polymerization via a modification of the general oxidation route with  $(\text{NH}_4)_2\text{S}_2\text{O}_8$  in 1.0 M hydrochloric acid which was doped into aqueous solution of sulfuric acid with an appropriate pH value.<sup>268</sup> The doping level  $y = [\text{S}]/[\text{N}]$  was determined on the base of elemental analysis. PANI-HCA was synthesized by the chemical oxidative polymerization of 1 M aqueous solution of polyaniline sulfate in the presence of 1.2 M ammonium persulfate at 278 K.<sup>269</sup> Film-like high-molecular-weight polyaniline<sup>270,271</sup> synthesized in Durham at 248 K was used as an initial material for PANI-ES doped with CSA and AMPSA as films of  $\sim 50 \mu\text{m}$  thick which were cast from *m*-cresol or dichloroacetic acid solutions onto Si wafers and allowed to dry in air at 313 K.<sup>270,272</sup> The doping levels  $y = [\text{A}]/[\text{N}]$ ; A ≡ acid, N ≡ nitrogen site, ranging between 0.4 and 0.6 were achieved by the stoichiometric addition of acid to polymer. As this process occurs in solution, the doping achieved is both homogeneous and reproducibly stoichiometric. It was studied also powder-like initial Ormecon PANI-PTSA with  $y = 0.5$  doping level, 30% crystalline volume fraction and RT *dc* conductivity of 7.5 S/cm.<sup>51</sup> In the study of spin-assisted charge transfer in organic two-spin-system this powder-like polymer was mixed in chlorobenzene with heterojunctions formed by soluble regioregular P3DDT and PCBM taken at a 1:1 wt. ratio with concentration ca. 1 wt. %.

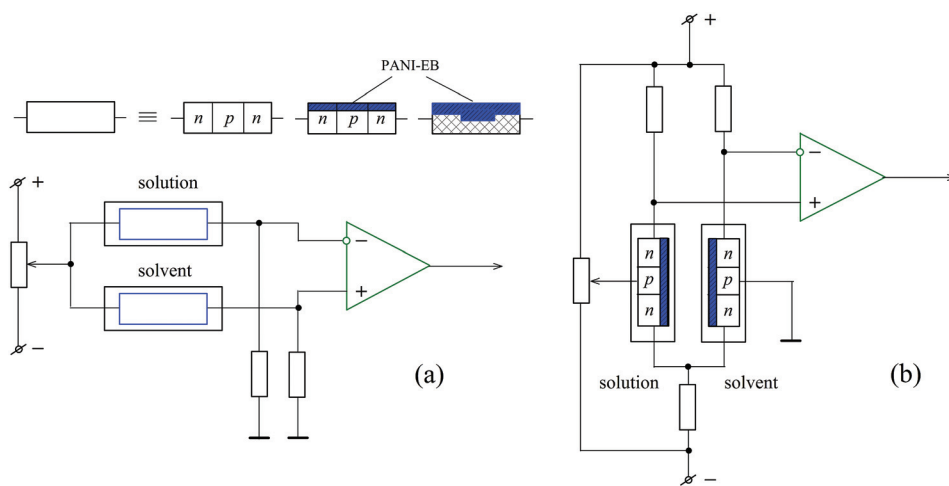


FIG. 27. “Passive” (a) and “active” (b) differential schemes used for the response of PANI-EB-based sensors on Si-transistors for solution components.

## 2. Sample characterization

### a. EPR spectroscopy

The growth of sensitivity and resolution of EPR method should, in principle, be realized at transition to stronger magnetic fields and higher registration frequencies.<sup>81,212</sup> Indeed, the minimal number of registered spins  $N_{\min}$ , i.e., the sensitivity of the method depends on operating frequency  $\omega_e$  as  $N_{\min} \propto \omega_e^{-\alpha}$ , where  $\alpha = 11/4$ , assuming constant both a  $B_1$  value and a sample size, taking into account the fact that the resonator size is inversely proportional to  $\omega_e$ , and considering only resistive losses in the cavity.<sup>81</sup> In practice, however, this relation is not fulfilled for high-field/high-frequency EPR spectrometers, depending on their modification, experimental conditions, and properties of a sample, e.g., size, conductivity, and polarity.<sup>81</sup> The spectral resolution of EPR method is characterized by  $\delta B/B_0$  ratio, where  $\delta B$  is the minimal splitting between two lines registered. This expression is conveniently written as  $\delta B/B_0 \cong \Delta g/g_e$  where  $\Delta g$  is the difference in  $g$ -factors of different paramagnetic centers with equal linewidth. The magnetic resonance condition (2) implies that these values depend linearly on registration frequency  $\omega_e$ . It should, however, be emphasized that such simple relation cannot be realized in practice for some radicals whom magnetic resonance and relaxation parameters contain field-dependent terms, variously called  $g$ -strain and A-strain,<sup>273</sup> limiting increase in resolution at higher registration frequency. EPR measurements were mainly performed using X-band (3-cm, 9.7 GHz) PS-100X, Q-band (8-mm, 36.7 GHz), and D-band (2-mm, 140 GHz) EPR5-01 (Ref. 274) spectrometers with maximal MW power of 150, 50, and 20 mW, respectively, and 100 kHz field ac modulation for phase-lock detection. Quartz tube with a sample placed in the center of the MW cavity was blown with dry nitrogen gas which temperature was controlled within the 90–340 K region using calibrated Cu/Cu:Fe thermocouple with high sensitivity (15 mK/V/K at 20 K) and stability (0.5 K) situated near the sample. The signal-to-noise ratio of EPR spectra was improved by signal averaging at several (typical 4–6) acquisitions. The total spin concentration in the samples was determined using  $\text{Cu}_2\text{S}\text{O}_4 \cdot 5\text{H}_2\text{O}$  single crystal standard, whereas  $\text{Mn}^{2+}$  with  $g_{\text{eff}} = 2.00102$  and  $a = 87.4$  G was used

for the determination of  $g$ -factors as well as for the magnetic field sweep scale calibration at D-band EPR. Another single microcrystal standard, diphenylpicrylhydrazyl (DPPH), with  $g_{\text{iso}} = 2.00360$  was used for estimation of  $g$ -factors at X-band EPR. Absorption EPR spectra were doubly integrated far from MW saturation conditions when the magnetic term  $B_1$  of the MW field and amplitude  $B_m$  of ac modulation in the cavity center did not exceed 5  $\mu\text{T}$  and 0.1 mT, respectively. All relaxation parameters of PC stabilized in the samples were determined separately using the steady-state saturation methods.<sup>160,173</sup>

### b. DC conductometry

The dc conductivity of the pellet-like low- or high-conductive samples was measured at 6–300 K temperature region in an inert atmosphere using the two- or forth-probe methods, respectively.<sup>124</sup> In order to increase the sensitivity of the method, differential “active” scheme was appeared to be more suitable. Such scheme used for the study of PANI-based sensors for solution components is shown in Fig. 27.<sup>238</sup> PANI-EB was besieged from appropriate solution onto two identical silicon transistor structures KT827 (analog of 2N6057) with “active” and “passive” connection and an insulating plate with two copper electrodes spaced by a 1 mm-wide gap. Both so prepared sensors were connected by a differentiating circuit with a multistage amplifier. Relativial sensor was placed into a pure solvent, whereas metrical one—into a solution of the sample under study. The resulting signal was measured as difference between responses of these sensors.

<sup>1</sup>J. M. Williams, J. R. Ferraro, R. J. Thorn, K. D. Carlson, U. Geiser, H. H. Wang, A. M. Kini, and M. H. Whangbo, *Organic Superconductors (Including Fullerenes): Synthesis, Structure, Properties, and Theory* (Prentice-Hall, Inc., Englewood Cliffs, New Jersey, 1992), p. 400.

<sup>2</sup>J. D. Wright, *Molecular Crystals*, 2 ed. (Cambridge University Press, Cambridge, New York, Melbourne, 1995), p. 236.

<sup>3</sup>H. S. Nalwa (John Wiley & Sons, Chichester, New York, 1997), p. 3334.

<sup>4</sup>S. Roth and D. Carroll, *One-Dimensional Metals: Conjugated Polymers, Organic Crystals, Carbon Nanotubes*, 2 ed (Wiley-VCH, Weinheim, 2004), 264 p.

<sup>5</sup>Z. V. Todres, *Ion-Radical Organic Chemistry: Principles and Applications*, 2 ed. (CRC Press, Boca Raton, 2008), p. 496.

- <sup>6</sup>*Fullerenes: Chemistry, Physics, and Technology*, edited by K. M. Kadish and R. S. Ruoff (Wiley-Interscience, New York, 2000), 978 p.
- <sup>7</sup>*Handbook of Advanced Electronic and Photonic Materials and Devices*, edited by H. Nalwa (Academic Press, Maryland Heights, 2001), 3366 p.
- <sup>8</sup>*Fullerene-Based Materials: Structures and Properties*, edited by K. Prassides (Springer, 2004), p. 285.
- <sup>9</sup>A. B. Sorokin, "Phthalocyanine metal complexes in catalysis," *Chem. Rev.* **113**(10), 8152–8191 (2013).
- <sup>10</sup>*Dye-Sensitized Solar Cells*, edited by K. Kalyanasundaram (EFPL Press, 2010), p. 320.
- <sup>11</sup>*Metal Filled Polymers*, edited by S. K. Bhattacharya (CRC Press, Boca Raton, 1986), p. 376.
- <sup>12</sup>*Metal-Filled Polymers—Properties and Applications*, edited by S. K. Bhattacharya (Marcel Dekker, New York, 1986), p. 360.
- <sup>13</sup>*Physical Properties of Polymers Handbook*, 2 ed., edited by J. E. Mark (Springer, New York, 2007), p. 1076.
- <sup>14</sup>L. M. Veca, W. Wang, Y. Lin, M. J. Meziani, L. Tian, J. W. Connell, S. Ghose, C. Y. Kong, and Y.-P. Sun, "Thermal conductive materials based on carbon nanotubes and graphene nanosheets," in *Handbook of Carbon Nano Materials*, edited by F. D'Souza and K. M. Kadish (World Scientific Publishing, Singapore, 2011), Vol. 2, p. 972.
- <sup>15</sup>J. Ma, Q. Meng, I. Zaman, S. Zhu, A. Michelmore, N. Kawashima, C. H. Wang, and H.-C. Kuan, "Development of polymer composites using modified, high-structural integrity graphene platelets," *Compos. Sci. Technol.* **31**, 82–90 (2014).
- <sup>16</sup>*Fullerene Polymers and Fullerene Polymer Composites*, edited by P. C. Eklund and A. M. Rao (Springer, 2000), p. 395.
- <sup>17</sup>Z. Pan, H. Gu, M.-T. Wu, Y. Li, and Y. Chen, "Graphene-based functional materials for organic solar cells," *Optical Materials Express* **2**(6), 816–824 (2012).
- <sup>18</sup>C. Zhang and T. X. Liu, "A review on hybridization modification of graphene and its polymer nanocomposites," *Chin. Sci. Bull.* **57**(23), 3010–3021 (2012).
- <sup>19</sup>*Conjugated Polymers: The Novel Science and Technology of Highly Conducting and Nonlinear Optically Active Materials*, edited by J. L. Brédas and R. Silbey (Kluwer Academic, Dordrecht, 1991), p. 624.
- <sup>20</sup>*Intrinsically Conducting Polymers: An Emerging Technology*, edited by M. Aldissi (Kluwer Academic, Dordrecht, London, 1992), p. 223.
- <sup>21</sup>R. Menon, "Charge transport in conducting polymers," in *Handbook of Organic Conductive Molecules and Polymers*, edited by H. S. Nalwa (John Wiley & Sons, Chichester, 1997), Vol. 4, pp. 47–145.
- <sup>22</sup>*Handbook of Conducting Polymers*, edited by T. Skotheim, R. Elsenbaumer, and J. Reynolds (Marcel Dekker, Inc., New York, 1998), p. 1105.
- <sup>23</sup>*Conducting Polymers, Fundamentals and Applications: A Practical Approach*, edited by P. Chandrasekhar (Kluwer Academic Publishers, Boston, Massachusetts, 1999), p. 718.
- <sup>24</sup>*Semiconducting Polymers: Chemistry, Physics and Engineering*, 2 ed., edited by G. Hadjioannou and P. F. van Hutten (Wiley, Weinheim, 2000), p. 768.
- <sup>25</sup>*Handbook of Polymers in Electronics*, edited by B. D. Malhotra (Rapra Technology Ltd., Shawbury, UK, 2002), p. 488.
- <sup>26</sup>*Conjugated Polymers: Processing and Applications*, edited by T. A. Skotheim and J. Reynolds (CRC Press, Boca Raton, 2006), p. 656.
- <sup>27</sup>*Handbook of Conducting Polymers*, edited by T. E. Scotheim and J. R. Reynolds (CRC Press, Boca Raton, 2007), p. 1680.
- <sup>28</sup>M. X. Wan, *Conducting Polymers with Micro or Nanometer Structure* (Springer, Berlin, Heidelberg, New York, 2008), p. 170.
- <sup>29</sup>A. J. Heeger, N. S. Sariciftci, and E. B. Namdas, *Semiconducting and Metallic Polymers* (Oxford University Press, London, 2010), p. 288.
- <sup>30</sup>G. Inzelt, *Conducting Polymers: A New Era in Electrochemistry*, 2 ed. (Springer, 2012), p. 309.
- <sup>31</sup>J.-P. Launay and M. Verdaguier, *Electrons in Molecules: From Basic Principles to Molecular Electronics* (Oxford University Press, Oxford, New York, 2013), p. 512.
- <sup>32</sup>W. A. Little, "Possibility of synthesizing an organic superconductor," *Phys. Rev.* **134**(6A), 1416–1424 (1964).
- <sup>33</sup>V. Saxena and B. D. Malhotra, "Prospects of conducting polymers in molecular electronics," *Curr. Appl. Phys.* **3**(2–3), 293–305 (2003).
- <sup>34</sup>S. Bhadra, *Polyaniline: Preparation, Properties, Processing and Applications* (Lap Lambert Academic Publishing, 2010), p. 92.
- <sup>35</sup>*Handbook of Nanoscale Optics and Electronics*, edited by G. P. Wiederrecht (Elsevier Academic Press, 2010), p. 401.
- <sup>36</sup>A. A. Syed and M. K. Dinesan, "Polyaniline—A novel polymeric material (Review)," *Talanta* **38**(8), 815 (1991).
- <sup>37</sup>S. Bhadra, S. Chattopadhyay, N. K. Singha, and D. Khastgir, "Improvement of conductivity of electrochemically synthesized polyaniline," *J. Appl. Polym. Sci.* **108**(1), 57–64 (2008).
- <sup>38</sup>M. E. Jozefowicz, R. Laversanne, H. H. S. Javadi, A. J. Epstein, J. P. Pouget, X. Tang, and A. G. MacDiarmid, "Multiple lattice phases and polaron-lattice spinless-defect competition in polyaniline," *Phys. Rev. B* **39**(17), 12958–12961 (1989).
- <sup>39</sup>S. Stafstrom, J. L. Brédas, A. J. Epstein, H. S. Woo, D. B. Tanner, W. S. Huang, and A. G. MacDiarmid, "Polaron lattice in highly conducting polyaniline: Theoretical and optical studies," *Phys. Rev. Lett.* **59**(13), 1464–1467 (1987).
- <sup>40</sup>R. P. McCall, J. M. Ginder, M. G. Roe, G. E. Asturias, E. M. Scherr, A. G. MacDiarmid, and A. J. Epstein, "Massive polarons on large-energy gap polymers," *Phys. Rev. B* **39**(14), 10174–10178 (1989).
- <sup>41</sup>P. Vignolo, R. Farchioni, and G. Grossi, "Tight-binding effective Hamiltonians for the electronic states of polyaniline chains," *Phys. Status Solidi B* **223**(3), 853–866 (2001).
- <sup>42</sup>A. J. Epstein, A. G. MacDiarmid, and J. P. Pouget, "Spin dynamics and conductivity in polyaniline," *Phys. Rev. Lett.* **65**(5), 664–664 (1990).
- <sup>43</sup>J. P. Pouget, M. E. Jozefowicz, A. J. Epstein, X. Tang, and A. G. MacDiarmid, "X-Ray structure of polyaniline," *Macromolecules* **24**(3), 779–789 (1991).
- <sup>44</sup>D. C. Trivedi, "Polyanilines," in *Handbook of Organic Conductive Molecules and Polymers*, edited by H. S. Nalwa (John Wiley, Chichester, 1997), Vol. 2, pp. 505–572.
- <sup>45</sup>J. M. Ginder, A. F. Richter, A. G. MacDiarmid, and A. J. Epstein, "Insulator-to-metal transition in polyaniline," *Solid State Commun.* **63**(2), 97–101 (1987).
- <sup>46</sup>A. J. Epstein and A. G. MacDiarmid, "Polaron and bipolaron defects in polymers: Polyaniline," *J. Mol. Electron.* **4**(3), 161–165 (1988).
- <sup>47</sup>L. M. Dai, J. P. Lu, B. Matthews, and A. W. H. Mau, "Doping of conducting polymers by sulfonated fullerene derivatives and dendrimers," *J. Phys. Chem. B* **102**(21), 4049–4053 (1998).
- <sup>48</sup>A. V. Saprinik, K. R. Brenneman, W. P. Lee, S. M. Long, R. S. Kohlman, and A. J. Epstein, "Li<sup>+</sup> doping-induced localization in polyaniline," *Synth. Met.* **100**(1), 55–59 (1999).
- <sup>49</sup>K. Lee, A. J. Heeger, and Y. Cao, "Reflectance spectra of polyaniline," *Synth. Met.* **72**(1), 25–34 (1995).
- <sup>50</sup>C. Y. Yang, P. Smith, A. J. Heeger, Y. Cao, and J. E. Osterholm, "Electron-diffraction studies of the structure of polyaniline dodecylbenzenesulfonate," *Polymer* **35**(6), 1142–1147 (1994).
- <sup>51</sup>B. Wessling, D. Srinivasan, G. Rangarajan, T. Mietzner, and W. Lennartz, "Dispersion-induced insulator-to-metal transition in polyaniline," *Eur. Phys. J. E: Soft Matter Biol. Phys.* **2**(3), 207–210 (2000).
- <sup>52</sup>M. Reghu, Y. Cao, D. Moses, and A. J. Heeger, "Counterion-Induced processability of polyaniline: Transport of the metal-insulator boundary," *Phys. Rev. B* **47**(4), 1758–1764 (1993).
- <sup>53</sup>C. O. Yoon, M. Reghu, D. Moses, A. J. Heeger, and Y. Cao, "Counterion-induced processability of polyaniline: Thermoelectric power," *Phys. Rev. B* **48**(19), 14080–14084 (1993).
- <sup>54</sup>K. H. Lee, A. J. Heeger, and Y. Cao, "Reflectance of polyaniline protonated with camphor sulfonic acid: Disordered metal on the metal-insulator boundary," *Phys. Rev. B* **48**(20), 14884–14891 (1993).
- <sup>55</sup>K. Lee, A. J. Heeger, and Y. Cao, "Reflectance of conducting polyaniline near the metal-insulator-transition," *Synth. Met.* **69**(1–3), 261–262 (1995).
- <sup>56</sup>K. Lee and A. J. Heeger, "Optical reflectance studies of conducting polymers on the metal-insulator boundary," *Synth. Met.* **84**(1–3), 715–718 (1997).
- <sup>57</sup>E. R. Holland, S. J. Pomfret, P. N. Adams, and A. P. Monkman, "Conductivity studies of polyaniline doped with CSA," *J. Phys.: Condens. Matter* **8**(17), 2991–3002 (1996).
- <sup>58</sup>L. Abell, P. N. Adams, and A. P. Monkman, "Electrical conductivity enhancement of predoped polyaniline by stretch orientation," *Polymer* **37**(26), 5927–5931 (1996).
- <sup>59</sup>L. Abell, S. J. Pomfret, P. N. Adams, A. C. Middleton, and A. P. Monkman, "Studies of stretched predoped polyaniline films," *Synth. Met.* **84**(1–3), 803–804 (1997).
- <sup>60</sup>Z. H. Wang, C. Li, E. M. Scherr, A. G. MacDiarmid, and A. J. Epstein, "3 Dimensionality of metallic states in conducting polymers: Polyaniline," *Phys. Rev. Lett.* **66**(13), 1745–1748 (1991).

- <sup>61</sup>Z. H. Wang, A. Ray, A. G. MacDiarmid, and A. J. Epstein, "Electron localization and charge transport in poly(o-toluidine): A model polyaniline derivative," *Phys. Rev. B* **43**(5), 4373–4384 (1991).
- <sup>62</sup>A. P. Monkman and P. Adams, "Observed anisotropies in stretch oriented polyaniline," *Synth. Met.* **41**(1–2), 627–633 (1991).
- <sup>63</sup>Z. H. Wang, E. M. Scherr, A. G. MacDiarmid, and A. J. Epstein, "Transport and EPR studies of polyaniline: A quasi-one-dimensional conductor with 3-dimensional metallic states," *Phys. Rev. B* **45**(8), 4190–4202 (1992).
- <sup>64</sup>M. Reghu, Y. Cao, D. Moses, and A. J. Heeger, "Metal-insulator-transition in polyaniline doped with surfactant counterion," *Synth. Met.* **57**(2–3), 5020–5025 (1993).
- <sup>65</sup>P. N. Adams, P. J. Laughlin, A. P. Monkman, and N. Bernhoeft, "A further step toward stable organic metals. Oriented films of polyaniline with high electrical-conductivity and anisotropy," *Solid State Commun.* **91**(11), 875–878 (1994).
- <sup>66</sup>J. Joo, Y. C. Chung, H. G. Song, J. S. Baeck, W. P. Lee, A. J. Epstein, A. G. MacDiarmid, and S. K. Jeong, "Charge transport studies of doped polyanilines with various dopants and their mixtures," *Synth. Met.* **84**(1–3), 739–740 (1997).
- <sup>67</sup>B. Wessling, "Metallic properties of conductive polymers due to dispersion," in *Handbook of Organic Conductive Molecules and Polymers*, edited by H. S. Nalwa (John Wiley & Sons, Chichester, 1997), Vol. 3, pp. 497–632.
- <sup>68</sup>P. N. Adams, P. J. Laughlin, and A. P. Monkman, "Synthesis of high molecular weight polyaniline at low temperatures," *Synth. Met.* **76**(1–3), 157–160 (1996).
- <sup>69</sup>A. J. Epstein, J. M. Ginder, F. Zuo, R. W. Bigelow, H. S. Woo, D. B. Tanner, A. F. Richter, W. S. Huang, and A. G. MacDiarmid, "Insulator-to-metal transition in polyaniline," *Synth. Met.* **18**(1–3), 303–309 (1987).
- <sup>70</sup>C. Fite, Y. Cao, and A. J. Heeger, "Magnetic-susceptibility of crystalline polyaniline," *Solid State Commun.* **70**(3), 245–247 (1989).
- <sup>71</sup>F. Zuo, M. Angelopoulos, A. G. MacDiarmid, and A. J. Epstein, "Transport studies of protonated emeraldine polymer: A antigenulocytes polymeric metal system," *Phys. Rev. B* **36**(6), 3475–3478 (1987).
- <sup>72</sup>A. G. MacDiarmid and A. J. Epstein, "Polyanilines: A novel class of conducting polymers," *Faraday Discuss.* **88**, 317 (1989).
- <sup>73</sup>A. J. Epstein and A. G. MacDiarmid, "Structure, order, and the metallic state in polyaniline and its derivatives," *Synth. Met.* **41**(1–2), 601–606 (1991).
- <sup>74</sup>K. R. Cromack, M. E. Jozefowicz, J. M. Ginder, A. J. Epstein, R. P. McCall, G. Du, J. M. Leng, K. Kim, C. Li, Z. H. Wang, M. A. Drury, P. J. Glatkowski, E. M. Scherr, and A. G. MacDiarmid, "Thermal-Process for orientation of polyaniline films," *Macromolecules* **24**(14), 4157–4161 (1991).
- <sup>75</sup>Z. H. Wang, H. H. S. Javadi, A. Ray, A. G. MacDiarmid, and A. J. Epstein, "Electron localization in polyaniline derivatives," *Phys. Rev. B* **42**(8), 5411–5413 (1990).
- <sup>76</sup>P. Grossé, *Freie Elektronen in Festkörpern* (Springer-Verlag, Berlin, Heidelberg, New York, 1979), p. 296.
- <sup>77</sup>J. Joo, E. J. Oh, G. Min, A. G. MacDiarmid, and A. J. Epstein, "Evolution of the conducting state of polyaniline from localized to mesoscopic metallic to intrinsic metallic regimes," *Synth. Met.* **69**(1–3), 251–254 (1995).
- <sup>78</sup>S. Kivelson and A. J. Heeger, "Intrinsic conductivity of conducting polymers," *Synth. Met.* **22**(4), 371–384 (1988).
- <sup>79</sup>*Advanced ESR Methods in Polymer Research*, edited by S. Schlick (John Wiley & Sons, Inc., New York, 2006), p. 368 and references therein.
- <sup>80</sup>G. R. Eaton, S. S. Eaton, D. P. Barr, and R. T. Weber, *Quantitative EPR* (Springer, Wien, New York, 2010), p. 185 and references therein.
- <sup>81</sup>*Multifrequency Electron Paramagnetic Resonance. Theory and Applications*, edited by S. K. Misra (Wiley-VCH, Weinheim, 2011), p. 1056 and references therein.
- <sup>82</sup>A. Lund, M. Shiotani, and S. Shimada, *Principles and Applications of ESR Spectroscopy* (Springer, 2011), p. 430 and references therein.
- <sup>83</sup>*EPR of Free Radicals in Solids I: Trends in Methods and Applications*, 2nd ed., edited by A. Lund and M. Shiotan (Springer Netherlands, 2013), p. 414 and references therein.
- <sup>84</sup>*EPR of Free Radicals in Solids II: Progress in Theoretical Chemistry and Physics*, 2nd ed., edited by A. Lund and M. Shiotan (Springer Netherlands, 2013), p. 387 and references therein. See also other books on EPR spectroscopy.
- <sup>85</sup>V. I. Krinichnyi, *2-mm Wave Band EPR Spectroscopy of Condensed Systems* (CRC Press, Boca Raton, 1995), p. 223.
- <sup>86</sup>K. Mizoguchi and S. Kuroda, "Magnetic properties of conducting polymers," in *Handbook of Organic Conductive Molecules and Polymers*, edited by H. S. Nalwa (John Wiley & Sons, Chichester, New York, 1997), Vol. 3, pp. 251–317.
- <sup>87</sup>V. I. Krinichnyi, "The nature and dynamics of nonlinear excitations in conducting polymers. Polyaniline," *Russ. Chem. Bull.* **49**(2), 207–233 (2000).
- <sup>88</sup>V. I. Krinichnyi, "2-mm Waveband electron paramagnetic resonance spectroscopy of conducting polymers (Review)," *Synth. Met.* **108**(3), 173–222 (2000); see also [hf-epr.awardspace.us](http://hf-epr.awardspace.us).
- <sup>89</sup>C. Menardo, F. Genoud, M. Nechtschein, J. P. Travers, and P. Hani, "On the acidic functions of polyaniline," in *Electronic Properties of Conjugated Polymers, Springer Series in Solid State Sciences*, edited by H. Kuzmany, M. Mehring, and S. Roth (Springer-Verlag, Berlin, 1987), Vol. 76, pp. 244–248.
- <sup>90</sup>M. Lapkowski and E. M. Genies, "Evidence of 2 kinds of spin in polyaniline from in situ EPR and electrochemistry: Influence of the electrolyte-composition," *J. Electroanal. Chem.* **279**(1–2), 157–168 (1990).
- <sup>91</sup>A. G. MacDiarmid and A. J. Epstein, "The polyanilines: Potential technology based on new chemistry and new properties," in *Science and Application of Conducting Polymers*, edited by W. R. Salaneck, D. T. Clark, and E. J. Samuelsen (Adam Hilger, Bristol, 1991), pp. 117–128.
- <sup>92</sup>N. S. Sariciftci, A. J. Heeger, and Y. Cao, "Paramagnetic susceptibility of highly conducting polyaniline: Disordered metal with weak electron-electron interactions (Fermi glass)," *Phys. Rev. B* **49**(9), 5988–5992 (1994).
- <sup>93</sup>N. S. Sariciftci, A. C. Kolbert, Y. Cao, A. J. Heeger, and A. Pines, "Magnetic resonance evidence for metallic state in highly conducting polyaniline," *Synth. Met.* **69**(1–3), 243–244 (1995).
- <sup>94</sup>M. Nechtschein, "Electron spin dynamics," in *Handbook of Conducting Polymers*, edited by T. A. Skotheim, R. L. Elsenbaumer, and J. R. Reynolds (Marcel Dekker, New York, 1997), pp. 141–163.
- <sup>95</sup>K. Mizoguchi, M. Nechtschein, J. P. Travers, and C. Menardo, "Spin dynamics in the conducting polymer. Polyaniline," *Phys. Rev. Lett.* **63**(1), 66–69 (1989).
- <sup>96</sup>K. Mizoguchi, M. Nechtschein, and J. P. Travers, "Spin dynamics and conductivity in polyaniline: Temperature-dependence," *Synth. Met.* **41**(1–2), 113–116 (1991).
- <sup>97</sup>K. Mizoguchi, M. Nechtschein, J. P. Travers, and C. Menardo, "Spin dynamics study in polyaniline," *Synth. Met.* **29**(1), E417–E424 (1989).
- <sup>98</sup>K. Mizoguchi and K. Kume, "Metallic temperature-dependence in the conducting polymer, polyaniline: Spin dynamics study by ESR," *Solid State Commun.* **89**(12), 971–975 (1994).
- <sup>99</sup>K. Mizoguchi and K. Kume, "Metallic temperature-dependence of microscopic electrical-conductivity in HCl-doped polyaniline studied by ESR," *Synth. Met.* **69**(1–3), 241–242 (1995).
- <sup>100</sup>M. Nechtschein, F. Genoud, C. Menardo, K. Mizoguchi, J. P. Travers, and B. Villeret, "On the nature of the conducting state of polyaniline," *Synth. Met.* **29**(1), E211–E218 (1989).
- <sup>101</sup>M. Inoue, M. B. Inoue, M. M. Castillo-Ortega, M. Mizuno, T. Asaji, and D. Nakamura, "Intrinsic paramagnetism of doped polypyroles and poly-thiophenes: Electron spin resonance of the polymers prepared by the use of copper(II) compounds as oxidative coupling agents," *Synth. Met.* **33**, 355–364 (1989).
- <sup>102</sup>M. Iida, T. Asaji, M. Inoue, H. Grijalva, M. B. Inoue, and D. Nakamura, "Electron-spin-resonance study of intrinsic paramagnetism of soluble polyaniline perchlorates," *Bull. Chem. Soc. Jpn.* **64**(5), 1509–1513 (1991).
- <sup>103</sup>T. Ohsawa, O. Kimura, M. Onoda, and K. Yoshino, "An ESR study on polyaniline in nonaqueous electrolyte," *Synth. Met.* **47**(2), 151–156 (1992).
- <sup>104</sup>A. Bartle, L. Dunsch, H. Naarmann, D. Schmeisser, and W. Gopel, "ESR studies of polypyrole films with a two-dimensional microstructure," *Synth. Met.* **61**(1–2), 167–170 (1993).
- <sup>105</sup>M. Nechtschein and F. Genoud, "On the broadening of the ESR line in presence of air or oxygen in conducting polymers," *Solid State Commun.* **91**(6), 471–473 (1994).
- <sup>106</sup>K. Aasmundtveit, F. Genoud, E. Houze, and M. Nechtschein, "Oxygen-induced ESR line broadening in conducting polymers," *Synth. Met.* **69**(1–3), 193–196 (1995).
- <sup>107</sup>P. K. Kahol, A. J. Dyakonov, and B. J. McCormick, "An electron-spin-resonance study of polymer interactions with moisture in polyaniline and its derivatives," *Synth. Met.* **89**(1), 17–28 (1997).

- <sup>108</sup>P. K. Kahol, A. J. Dyakonov, and B. J. McCormick, "An electron-spin-resonance study of polyaniline and its derivatives: Polymer interactions with moisture," *Synth. Met.* **84**, 691–694 (1997).
- <sup>109</sup>Y. S. Kang, H. J. Lee, J. Namgoong, B. Jung, and H. Lee, "Decrease in electrical conductivity upon oxygen exposure in polyanilines doped with HCl," *Polymer* **40**(9), 2209–2213 (1999).
- <sup>110</sup>K. Mizoguchi, N. Kachi, H. Sakamoto, K. Yoshioka, S. Masubuchi, and S. Kazama, "The effect of oxygen on the ESR linewidth in polypyrrole doped by PF<sub>6</sub>," *Solid State Commun.* **105**(2), 81–84 (1998).
- <sup>111</sup>E. Houze and M. Nechtschein, "ESR in conducting polymers: Oxygen-induced contribution to the linewidth," *Phys. Rev. B* **53**(21), 14309–14318 (1996).
- <sup>112</sup>F. J. Dyson, "Electron spin resonance absorption in metals. II. Theory of electron diffusion and the skin effect," *Phys. Rev. B* **98**(2), 349–359 (1955).
- <sup>113</sup>A. P. Monkman, D. Bloor, and G. C. Stevens, "Effects of oxidation-state on the measured g-value in polyaniline," *J. Phys. D* **23** (5), 627–629 (1990).
- <sup>114</sup>M. Iida, T. Asaji, M. B. Inoue, and M. Inoue, "EPR study of polyaniline perchlorates: Spin species-related to charge-transport," *Synth. Met.* **55**(1), 607–612 (1993).
- <sup>115</sup>B. Z. Lubentsov, O. N. Timofeeva, S. L. Saratovskikh, V. I. Krinichnyi, A. E. Pelekh, V. V. Dmitrenko, and M. L. Khidekel, "The study of conducting polymer interaction with gaseous substances. IV. The water-content influence on polyaniline crystal structure and conductivity," *Synth. Met.* **47**(2), 187–192 (1992).
- <sup>116</sup>F. Lux, G. Hinrichsen, V. I. Krinichnyi, I. B. Nazarova, S. D. Chemerisov, and M. M. Pohl, "Conducting islands concept for highly conductive polyaniline—recent results of TEM-measurements, X-ray-diffraction-measurements, EPR-measurements, DC conductivity-measurements and magnetic susceptibility-measurements," *Synth. Met.* **55**(1), 347–352 (1993).
- <sup>117</sup>H. K. Roth and V. I. Krinichnyi, "ESR studies on polymers with particular electronic and magnetic properties," *Makromol. Chem., Macromol. Symp.* **72**, 143–159 (1993).
- <sup>118</sup>V. I. Krinichnyi, "The nature and dynamics of nonlinear excitations in conducting polymers. Heteroaromatic polymers," *Russ. Chem. Rev.* **65**(6), 521–536 (1996).
- <sup>119</sup>V. I. Krinichnyi, S. D. Chemerisov, and Y. S. Lebedev, "EPR and charge-transport studies of polyaniline," *Phys. Rev. B* **55**(24), 16233–16244 (1997).
- <sup>120</sup>V. I. Krinichnyi, S. D. Chemerisov, and Y. S. Lebedev, "Charge transport in slightly doped polyaniline," *Synth. Met.* **84**(1–3), 819–820 (1997).
- <sup>121</sup>V. I. Krinichnyi, S. D. Chemerisov, and Y. S. Lebedev, "Mechanism of spin and charge transport in poly(aniline)," *Polym. Sci., Ser. A* **40**(8), 826–834 (1998).
- <sup>122</sup>V. I. Krinichnyi, I. B. Nazarova, L. M. Goldenberg, and H. K. Roth, "Spin dynamics in conducting poly(aniline)," *Polym. Sci., Ser. A* **40**(8), 835–843 (1998).
- <sup>123</sup>V. I. Krinichnyi, A. L. Konkin, P. Devasagayam, and A. P. Monkman, "Multifrequency EPR study of charge transport in doped polyaniline," *Synth. Met.* **119**, 281–282 (2001).
- <sup>124</sup>A. L. Kon'kin, V. G. Shtyrlin, R. R. Garipov, A. V. Aganov, A. V. Zakharov, V. I. Krinichnyi, P. N. Adams, and A. P. Monkman, "EPR, charge transport, and spin dynamics in doped polyanilines," *Phys. Rev. B* **66**(7), 075203 (2002).
- <sup>125</sup>V. I. Krinichnyi, H. K. Roth, G. Hinrichsen, F. Lux, and K. Lüders, "EPR and charge transfer in H<sub>2</sub>SO<sub>4</sub>-doped polyaniline," *Phys. Rev. B* **65**(15), 155205 (2002).
- <sup>126</sup>V. I. Krinichnyi, H. K. Roth, and G. Hinrichsen, "Charge transfer in heavily H<sub>2</sub>SO<sub>4</sub>-doped polyaniline," *Synth. Met.* **135**(1–3), 431–432 (2003).
- <sup>127</sup>V. I. Krinichnyi and S. V. Tokarev, "Charge transport in polyaniline heavily doped with p-toluenesulfonic acid," *Polym. Sci., Ser. A* **47**(3), 261–269 (2005).
- <sup>128</sup>V. I. Krinichnyi, S. V. Tokarev, H. K. Roth, M. Schrödner, and B. Wessling, "Multifrequency EPR study of metal-like domains in polyaniline," *Synth. Met.* **152**(1–3), 165–168 (2005).
- <sup>129</sup>V. I. Krinichnyi, A. L. Konkin, and A. Monkman, "Electron paramagnetic resonance study of spin centers related to charge transport in metallic polyaniline," *Synth. Met.* **162**(13–14), 1147–1155 (2012).
- <sup>130</sup>V. I. Krinichnyi, E. I. Yudanova, and B. Wessling, "Influence of spin–spin exchange on charge transfer in PANI-ES/P3DDT/PCBM composite," *Synth. Met.* **179**, 67–73 (2013).
- <sup>131</sup>V. I. Krinichnyi, "Relaxation and dynamics of spin charge carriers in polyaniline," in *Advances in Materials Science Research*, edited by M. C. Wythers (Nova Science Publishers, Hauppauge, New York, 2014), Vol. 17, pp. 109–160.
- <sup>132</sup>Y. S. Lebedev, "High-field ESR," in *Electron Spin Resonance*, edited by N. M. Atherton, M. J. Davies, and B. C. Gilbert (Royal Society of Chemistry, Cambridge, 1994), Vol. 14, pp. 63–87.
- <sup>133</sup>W. R. Hagen, "High-frequency EPR of transition ion complexes and metalloproteins," *Coord. Chem. Rev.* **192**, 209–229 (1999).
- <sup>134</sup>G. M. Smith and P. C. Riedi, *Progress in High Field EPR* (RSC, Cambridge, UK, 2000), p. 164.
- <sup>135</sup>D. Marsh, D. Kurad, and V. A. Livshits, "High-field electron spin resonance of spin labels in membranes," *Chem. Phys. Lipids* **116**(1–2), 93–114 (2002).
- <sup>136</sup>E. J. Hustedt and A. H. Beth, "High field/high frequency saturation transfer electron paramagnetic resonance spectroscopy: Increased sensitivity to very slow rotational motions," *Biophys. J.* **86**, 3940–3950 (2004).
- <sup>137</sup>*Very High Frequency (VHF) ESR/EPR (Biological Magnetic Resonance)*, edited by O. Y. Grinberg and L. J. Berliner (Kluwer Academic Plenum Publishers, New York, 2004), p. 592.
- <sup>138</sup>F. Carrington and A. D. McLachlan, *Introduction to Magnetic Resonance with Application to Chemistry and Chemical Physics* (Harrer & Row, Publishers, New York, Evanston, London, 1967), p. 266.
- <sup>139</sup>A. L. Buchachenko and A. M. Vasserman, *Stable Radicals (Russ)* (Khimija, Moscow, 1973), p. 408.
- <sup>140</sup>A. L. Buchachenko, C. N. Turton, and T. I. Turton, *Stable Radicals* (Consultants Bureau, New York, 1995), p. 180.
- <sup>141</sup>A. Raghunathan, P. K. Kahol, J. C. Ho, Y. Y. Chen, Y. D. Yao, Y. S. Lin, and B. Wessling, "Low-temperature heat capacities of polyaniline and polyaniline polymethylmethacrylate blends," *Phys. Rev. B* **58**(24), R15955–R15958 (1998).
- <sup>142</sup>S. V. Vonsovskii, *Magnetism—Magnetic Properties of Dia-, Para-, Ferro-, Antiferro-, and Ferrimagnetics* (John Wiley & Sons, New York, 1974), 1256 p.
- <sup>143</sup>H. Salavagione, G. M. Morales, M. C. Miras, and C. Barbero, "Synthesis of a self-doped polyaniline by nucleophilic addition," *Acta Polym.* **50**(1), 40–44 (1999).
- <sup>144</sup>*Handbook of Magnetism and Advanced Magnetic Materials*, edited by H. Kronmüller and S. Parkin (Wiley, 2007), p. 3064.
- <sup>145</sup>P. K. Kahol and M. Mehring, "Exchange-coupled pair model for the non-curie-like susceptibility in conducting polymers," *Synth. Met.* **16**(2), 257–264 (1986).
- <sup>146</sup>W. G. Clark and L. C. Tippie, "Exchange-coupled pair model for the random-exchange Heisenberg antiferromagnetic chain," *Phys. Rev. B* **20**(7), 2914–2923 (1979).
- <sup>147</sup>H. K. Roth, F. Keller, and H. Schneider, *Hochfrequenzspektroskopie in der Polymerforschung* (Academie Verlag, Berlin, 1984), p. 374.
- <sup>148</sup>L. A. Blumenfeld, V. V. Voevodski, and A. G. Semenov, *Application of Electron Paramagnetic Resonance in Chemistry (Russ)* (Izdat. SO AN SSSR, Novosibirsk, 1962), p. 216.
- <sup>149</sup>J. A. Weil, J. R. Bolton, and J. E. Wertz, *Electron Paramagnetic Resonance: Elementary Theory and Practical Applications* (Wiley-Interscience, New York, 2007), p. 644.
- <sup>150</sup>Y. S. Lebedev and V. I. Muromtsev, *EPR and Relaxation of Stabilized Radicals (Russ)* (Khimija, Moscow, 1972), p. 256.
- <sup>151</sup>Y. N. Molin, K. M. Salikhov, and K. I. Zamaraev, *Spin Exchange* (Springer, Berlin, 1980), p. 260.
- <sup>152</sup>M. A. Butler, L. R. Walker, and Z. G. Soos, "Dimensionality of spin fluctuations in highly anisotropic TCNQ salts," *J. Chem. Phys.* **64**(9), 3592–3601 (1976).
- <sup>153</sup>P. D. Krasicky, R. H. Silsbee, and J. C. Scott, "Studies of a polymeric chromium phosphinate. Electron-spin resonance and spin dynamics," *Phys. Rev. B* **25**(9), 5607–5626 (1982).
- <sup>154</sup>M. J. Hennessy, C. D. McElwee, and P. M. Richards, "Effect of inter-chain coupling on electron-spin resonance in nearly one-dimensional systems," *Phys. Rev. B* **7**(3), 930–947 (1973).
- <sup>155</sup>P. K. Kahol, K. K. S. Kumar, S. Geetha, and D. C. Trivedi, "Effect of dopants on electron localization length in polyaniline," *Synth. Met.* **139**(2), 191–200 (2003).
- <sup>156</sup>Z. Wilamowski, B. Oczkiewicz, P. Kacmar, and J. Blinowski, "Asymmetry of the EPR absorption line in CdF<sub>2</sub> with Y," *Phys. Status Solidi B* **134**, 303–306 (1986).
- <sup>157</sup>P. Bernier, "The magnetic properties of conjugated polymers: ESR studies of undoped and doped systems," in *Handbook of Conducting*

- Polymers*, edited by T. E. Scotheim (Marcel Dekker, Inc., New York, 1986), Vol. 2, pp. 1099–1125.
- <sup>158</sup>A. C. Chapman, P. Rhodes, and E. F. W. Seymour, “The Effect of Eddy currents on nuclear magnetic resonance in metals,” *Proc. Phys. Soc., Sect. B* **70**(4), 345–360 (1957).
- <sup>159</sup>A. Abragam and B. Bleany, *Electron Paramagnetic Resonance of Transition Ions* (Oxford Academ, Oxford, 2012), p. 944.
- <sup>160</sup>C. P. Poole, *Electron Spin Resonance, A Comprehensive Treatise on Experimental Techniques* (John Wiley & Sons, New York, 1983), p. 780.
- <sup>161</sup>A. Lösche, *Kerninduction* (VEB Deutscher Verlag, Berlin, 1957), p. 684.
- <sup>162</sup>J. S. Hyde and L. R. Dalton, “Saturation-transfer spectroscopy,” in *Spin Labeling II: Theory and Application*, edited by L. J. Berliner (Academic, New York, 1979), Vol. 2, pp. 1–70.
- <sup>163</sup>A. A. Bugai, “Passing effects for inhomogeneously broadened EPR lines at high-frequency-modulation of magnetic field,” *Phys. Solid State* **4**, 3027–3030 (1962).
- <sup>164</sup>E. E. Salpeter, “Nuclear induction signals for long relaxation times,” *Proc. Phys. Soc., Sect. A* **63**, 337–349 (1950).
- <sup>165</sup>G. Feher, “Electron spin resonance experiments on donors in silicon. I. Electronic structure of donors by electron nuclear double resonance technique,” *Phys. Rev. B* **114**, 1219 (1959).
- <sup>166</sup>M. Weger, “Passage effects in paramagnetic resonance experiments,” *Bell Syst. Tech. J.* **39**, 1013–1112 (1960).
- <sup>167</sup>C. A. J. Ammerlaan and A. van der Wiel, “The divacancy in silicon: Spin-lattice relaxation and passage effects in electron paramagnetic resonance,” *J. Magn. Reson.* **21**(3), 387–513 (1976).
- <sup>168</sup>S. A. Altshuler and B. M. Kozirev, *Electron Paramagnetic Resonance* (Academic Press, 1964), p. 372.
- <sup>169</sup>V. I. Krinichnyi, “Investigation of biological systems by EPR method of high spectral resolution at 2-mm wave band,” *J. Appl. Spectrosc.* **52**(6), 575–591 (1990).
- <sup>170</sup>V. I. Krinichnyi, “Investigation of biological systems by high-resolution 2-mm wave band ESR,” *J. Biochem. Biophys. Methods* **23**(1), 1–30 (1991).
- <sup>171</sup>V. I. Krinichnyi, “Investigation of biological systems by high resolution 2-mm wave band EPR,” *Appl. Magn. Reson.* **2**(1), 29–60 (1991).
- <sup>172</sup>P. R. Cullis, “EPR in inhomogeneously broadened systems: A spin temperature approach,” *J. Magn. Reson.* **21**(3), 397–418 (1976).
- <sup>173</sup>A. E. Pelekh, V. I. Krinichnyi, A. Y. Brezgunov, L. I. Tkachenko, and G. I. Kozub, “ESR study of relaxational parameters of paramagnetic centers in polyacetylene,” *Polym. Sci. USSR* **33**(8), 1615–1623 (1991).
- <sup>174</sup>V. I. Krinichnyi, A. E. Pelekh, A. Y. Brezgunov, L. I. Tkachenko, and G. I. Kozub, “The EPR study of undoped polyacetylene,” *Mater. Sci. Eng.* **17**(1), 25–29 (1991).
- <sup>175</sup>A. M. Wasserman and T. N. Khazanovich, “New fronties in spin probe and spin label EPR spectroscopy of polymers,” in *Polymer Yearbook*, edited by R. A. Patrick (Taylor & Francis, London, 1995), Vol. 12, pp. 153–184.
- <sup>176</sup>*Spin Labeling: The Next Millennium*, edited by L. J. Berliner (Plenum Press, New York, 1998), p. 444.
- <sup>177</sup>H. Winter, G. Sachs, E. Dormann, R. Cosmo, and H. Naarmann, “Magnetic-properties of spin-labeled polyacetylene,” *Synth. Met.* **36**(3), 353–365 (1990).
- <sup>178</sup>B. H. Robinson and L. R. Dalton, “Anisotropic rotational diffusion studied by passage saturation transfer electron paramagnetic resonance,” *J. Chem. Phys.* **72**, 1312–1324 (1980).
- <sup>179</sup>A. A. Dubinski, O. Y. Grinberg, V. I. Kurochkin, L. G. Oransky, O. G. Poluektov, and Y. S. Lebedev, “Investigation of anisotropy of nitroxide radicals rotation using 2-mm wave band EPR spectra,” *Theor. Exp. Chem.* **17**(2), 180 (1981).
- <sup>180</sup>V. I. Krinichnyi, “High field ESR spectroscopy of conductive polymers,” in *Advanced ESR Methods in Polymer Research*, edited by S. Schlick (Wiley, Hoboken, NJ, 2006), pp. 307–338.
- <sup>181</sup>V. I. Krinichnyi, O. Y. Grinberg, A. A. Dubinskii, V. A. Livshits, Y. A. Bobrov, and Y. S. Lebedev, “Study of anisotropic molecular rotations by saturation transfer EPR spectroscopy at 2-mm wave band,” *Biofizika* **32**(3), 534–535 (1987).
- <sup>182</sup>A. Abragam, *Principles of Nuclear Magnetism* (Clarendon Press, Oxford, 1983), p. 614.
- <sup>183</sup>R. L. Elsenbaume and L. W. Shacklette, “Phenylene-based conducting polymers,” in *Handbook of Conducting Polymers*, edited by T. E. Scotheim (Marcel Dekker, Inc., New York, 1986), Vol. 1, pp. 213–263.
- <sup>184</sup>F. Devreux, F. Genoud, M. Nechtschein, and B. Villeret, “On polaron and bipolaron formation in conducting polymers,” in *Electronic Properties of Conjugated Polymers*, edited by H. Kuzmany, M. Mehring, and S. Roth (Springer-Verlag, Berlin, 1987), Vol. 76, pp. 270–276.
- <sup>185</sup>M. Westerling, R. Osterbacka, and H. Stubb, “Recombination of long-lived photoexcitations in regioregular polyalkylthiophenes,” *Phys. Rev. B* **66**(16), 165220 (2002).
- <sup>186</sup>G. Agostini, C. Corvaja, and L. Pasimeni, “EPR studies of the excited triplet states of C<sub>60</sub>O and C<sub>60</sub>C<sub>2</sub>H<sub>4</sub>N(CH<sub>3</sub>) fullerene derivatives and C-70 in toluene and polymethylmethacrylate glasses and as films,” *Chem. Phys.* **202**(2–3), 349–356 (1996).
- <sup>187</sup>N. N. Denisov, V. I. Krinichnyi, and V. A. Nadtochenko, “Spin properties of paramagnetic centers photogenerated in crystals of complexes between C-60 and TPA,” in *Fullerenes. Recent Advances in the Chemistry and Physics of Fullerenes and Related Materials*, edited by K. Kadish and R. Ruoff (The Electrochemical Society, Inc., Pennington, NJ, 1997), Vol. 4, pp. 139–147.
- <sup>188</sup>D. M. Martino, C. A. Steren, and H. vanWilligen, “Time-resolved EPR study of C-3(60) in solid matrices,” *Res. Chem. Intermed.* **23**(5), 415–429 (1997).
- <sup>189</sup>X. Wei and Z. V. Vardeny, “Spin dynamics of photoexcitations in C-60 and C-70,” *Mol. Cryst. Liq. Cryst. Sci. Technol., Sect. A* **256**, 307–315 (1994).
- <sup>190</sup>M. N. Uvarov, L. V. Kulik, and S. A. Dzuba, “Fullerene C-70 triplet zero-field splitting parameters revisited by light-induced EPR at thermal equilibrium,” *Appl. Magn. Reson.* **40**(4), 489–499 (2011).
- <sup>191</sup>M. N. Uvarov, L. V. Kulik, A. B. Doktorov, and S. A. Dzuba, “Isotropic reorientations of fullerene C-70 triplet molecules in solid glassy matrices revealed by light-induced electron paramagnetic resonance,” *J. Chem. Phys.* **135**(5), 054507 (2011).
- <sup>192</sup>M. I. Klinger, *Problems of Linear Electron (Polaron) Transport Theory in Semiconductors* (Pergamon Press, Oxford, 1979), p. 962.
- <sup>193</sup>*Electronic Processes in Organic Crystals and Polymers*, 2nd ed. (Oxford University Press, Oxford, 1999), p. 1360.
- <sup>194</sup>S. Kivelson, “Electron hopping in a soliton band: Conduction in lightly doped (CH)<sub>x</sub>,” *Phys. Rev. B* **25**(6), 3798–3821 (1982).
- <sup>195</sup>A. Tawansi, A. H. Oraby, H. M. Zidan, and M. E. Dorgham, “Effect of one-dimensional phenomena on electrical, magnetic and ESR properties of MnCl<sub>2</sub>-filled PVA films,” *Physica B* **254**(1–2), 126–133 (1998).
- <sup>196</sup>A. R. Long and N. Balkan, “AC loss in amorphous germanium,” *Philos. Mag. B* **41**(3), 287–305 (1980).
- <sup>197</sup>M. El Kadiri and J. P. Parneix, “Frequency- and temperature-dependent complex conductivity of some conducting polymers,” in *Electronic Properties of Polymers and Related Compounds*, edited by H. Kuzmany, M. Mehring, and S. Roth (Springer-Verlag, Berlin, 1985), Vol. 63, pp. 183–186.
- <sup>198</sup>J. P. Parneix and M. El Kadiri, “Frequency- and temperature-dependent dielectric losses in lightly doped conducting polymers,” in *Electronic Properties of Conjugated Polymers*, edited by H. Kuzmany, M. Mehring, and S. Roth (Springer-Verlag, Berlin, 1987), Vol. 76, pp. 23–26.
- <sup>199</sup>D. Schafer-Siebert, C. Budrowski, H. Kuzmany, and S. Roth, “Influence of the conjugation length of polyacetylene chains on the DC-conductivity,” in *Electronic Properties of Conjugated Polymers*, edited by H. Kuzmany, M. Mehring, and S. Roth (Springer-Verlag, Berlin, 1987), Vol. 76, pp. 38–42.
- <sup>200</sup>D. Schafer-Siebert and S. Roth, “Limitation of the conductivity of polyacetylene by conjugational defects,” *Synth. Met.* **28**, D369–D374 (1989).
- <sup>201</sup>H. Meier, “Application of the semiconductor properties of dyes: Possibilities and problems,” in *Topics in Current Chemistry* (Springer-Verlag, Berlin, 1976), pp. 61–85.
- <sup>202</sup>D. A. Dos Santos, D. S. Galvao, B. Laks, and M. C. dos Santos, “Poly(alkylthiophenes): Chain conformation and thermochromism,” *Synth. Met.* **51**, 203–209 (1992).
- <sup>203</sup>I. Hoogmartens, P. Adreansens, R. Carleer, D. Vanderzande, H. Martens, and J. Gelan, “An investigation into the electronic structure of poly(isothianaphthene),” *Synth. Met.* **51**(1–3), 219–228 (1992).
- <sup>204</sup>N. F. Mott, *Conduction in Non-Crystalline Materials* (Clarendon Press, Oxford, 1987), p. 150.
- <sup>205</sup>N. F. Mott and E. A. Davis, *Electronic Processes in Non-Crystalline Materials* (Clarendon Press, Oxford, 2012), p. 608.
- <sup>206</sup>I. G. Austin and N. F. Mott, “Polaron in crystalline and non-crystalline materials,” *Adv. Phys.* **18**(71), 41–102 (1969).
- <sup>207</sup>L. Pietronero, “Ideal conductivity of carbon  $\tilde{\alpha}$  polymers and intercalation compounds,” *Synth. Met.* **8**, 225–231 (1983).
- <sup>208</sup>M. Nechtschein, “Doped conjugated polymers: Conducting polymers,” in *Organic Conductors Fundamental and Applications*, edited by J. P. Ferges (Marcel Dekker, New York, 1994), pp. 647–689.

- <sup>209</sup>A. J. Epstein and A. G. MacDiarmid, "Novel concepts in electronic polymers: Polyaniline and its derivatives," *Makromol. Chem., Macromol. Symp.* **51**, 217–234 (1991).
- <sup>210</sup>P. W. Anderson "The Fermi glass: theory and experiment," *Comments on Solid State Physics* **2**, 193–198 (1970).
- <sup>211</sup>S. M. Long, K. R. Cromack, A. J. Epstein, Y. Sun, and A. G. MacDiarmid, "ESR of pernigraniline base solutions revisited," *Synth. Met.* **62**(3), 287–289 (1994).
- <sup>212</sup>C. P. Poole, *Electron Spine Resonance* (Int. Sci. Publ., London, 1967), p. 959.
- <sup>213</sup>C. P. Poole, *Electron Spin Resonance: A Comprehensive Treatise on Experimental Techniques* (Dover Publications, 1997), p. 810.
- <sup>214</sup>S. P. Kurzin, B. G. Tarasov, N. F. Fatkullin, and R. M. Aseeva, "The electron spin-lattice relaxation in pyrolyzed poly-2-methyl-5-ethinylpyridine," *Polym. Sci. USSR A* **24**(1), 134–142 (1982).
- <sup>215</sup>J. S. Blakemore, *Solid State Physics*, 2nd ed. (Cambridge University Press, Cambridge, 1985), p. 520.
- <sup>216</sup>S. Kivelson, "Electron hopping conduction in the soliton model of polyacetylene," *Phys. Rev. Lett.* **46**, 1344–1348 (1981).
- <sup>217</sup>S. Kivelson, "Electron hopping conduction in the soliton model of polyacetylene," *Mol. Cryst. Liq. Cryst.* **77**(1–4), 65–79 (1981).
- <sup>218</sup>L. Zuppiroli, S. Paschen, and M. N. Bussac, "Role of the dopant counterions in the transport and magnetic-properties of disordered conducting polymers," *Synth. Met.* **69**(1–3), 621–624 (1995).
- <sup>219</sup>Y. Cao, S. Z. Li, Z. J. Xue, and D. Guo, "Spectroscopic and electrical characterization of some aniline oligomers and polyaniline," *Synth. Met.* **16**(3), 305–315 (1986).
- <sup>220</sup>H. H. S. Javadi, K. R. Cromack, A. G. MacDiarmid, and A. J. Epstein, "Microwave transport in the emeraldine form of polyaniline," *Phys. Rev. B* **39**(6), 3579–3584 (1989).
- <sup>221</sup>P. K. Kahol, N. J. Pinto, and B. J. McCormick, "Charge-transport and electron localization in alkyl ring-substituted polyanilines," *Solid State Commun.* **91**(1), 21–24 (1994).
- <sup>222</sup>P. K. Kahol, N. J. Pinto, E. J. Berndtsson, and B. J. McCormick, "Electron localization effects on the conducting state in polyaniline," *J. Phys.: Condens. Matter* **6**(29), 5631–5638 (1994).
- <sup>223</sup>N. J. Pinto, P. K. Kahol, B. J. McCormick, N. S. Dalal, and H. Wan, "Charge-transport and electron localization in polyaniline derivatives," *Phys. Rev. B* **49**(19), 13983–13986 (1994).
- <sup>224</sup>T. N. Khazanovich, "Theory of nuclear magnetic relaxation in liquid-phase polymers," *Polym. Sci. USSR* **4**(4), 727–736 (1963).
- <sup>225</sup>H. Y. Lim, S. K. Jeong, J. S. Suh, E. J. Oh, Y. W. Park, K. S. Ryu, and C. H. Yo, "Preparation and properties of fullerene doped polyaniline," *Synth. Met.* **70**(1–3), 1463–1464 (1995).
- <sup>226</sup>B. Beau, J. P. Travers, and E. Banka, "NMR evidence for heterogeneous disorder and quasi-1D metallic state in polyaniline CSA," *Synth. Met.* **101**(1–2), 772–775 (1999).
- <sup>227</sup>B. Beau, J. P. Travers, F. Genoud, and P. Rannou, "NMR study of aging effects in polyaniline CSA," *Synth. Met.* **101**(1–2), 778–779 (1999).
- <sup>228</sup>F. L. Pratt, S. J. Blundell, W. Hayes, K. Nagamine, K. Ishida, and A. P. Monkman, "Anisotropic polaron motion in polyaniline studied by muon spin relaxation," *Phys. Rev. Lett.* **79**(15), 2855–2858 (1997).
- <sup>229</sup>V. I. Krinichnyi, N. N. Denisov, H. K. Roth, E. Fanghänel, and K. Lüders, "Dynamics of paramagnetic charge carriers in poly(tetraphiafulvalene)," *Polym. Sci., Ser. A* **40**(12), 1259–1269 (1998).
- <sup>230</sup>V. I. Krinichnyi, "The 140-GHz (D-band) saturation transfer electron paramagnetic resonance studies of macromolecular dynamics in conducting polymers," *J. Phys. Chem. B* **112**(32), 9746–9752 (2008).
- <sup>231</sup>V. I. Krinichnyi, "2-mm Waveband saturation transfer electron paramagnetic resonance of conducting polymers," *J. Chem. Phys.* **129**(13), 134510–134518 (2008).
- <sup>232</sup>R. Pelster, G. Nimtz, and B. Wessling, "Fully protonated polyaniline: Hopping transport on a mesoscopic scale," *Phys. Rev. B* **49**(18), 12718–12723 (1994).
- <sup>233</sup>G. Harsanyi, *Polymer Films in Sensor Applications* (CRC Press, Boca Raton, 1995), p. 465.
- <sup>234</sup>P. N. Bartlett and S. K. Ling-Chung, "Conducting polymer gas sensors," *Sens. Actuators* **20**, 287–292 (1989).
- <sup>235</sup>A. S. Davydov, *Solitons in Molecular Systems (Russ.)* (Naukova Dumka, Kiev, 1984), p. 288.
- <sup>236</sup>W. Heywang, *Sensorik*, 4 ed (Springer-Verlag, Berlin Heidelberg New York, 1993), 231 p.
- <sup>237</sup>V. I. Krinichnyi, O. N. Eremenko, G. G. Rukhman, Y. A. Letuchii, and V. M. Geskin, "Sensors based on conducting organic polymers. Polyaniline," *Polym. Sci. USSR* **31**(8), 1819–1825 (1989).
- <sup>238</sup>V. I. Krinichnyi, O. N. Eremenko, G. G. Rukhman, V. M. Geskin, and Y. A. Letuchii, "Polyaniline based sensors for solution components," *Synth. Met.* **41**(3), 1137–1137 (1991).
- <sup>239</sup>V. A. Dediu, L. E. Hueso, I. Bergenti, and C. Taliani, "Spin routes in organic semiconductors," *Nature Mater.* **8**, 707–716 (2009).
- <sup>240</sup>*Concepts in Spin Electronics*, edited by S. Maekawa (Oxford University Press, Oxford, 2006), p. 416.
- <sup>241</sup>Y. Zhang, T. P. Basel, B. R. Gautam, X. M. Yang, D. J. Mascaro, F. Liu, and Z. V. Vardeny, "Spin-enhanced organic bulk heterojunction photovoltaic solar cells," *Nat. Commun.* **3**, 1043 (2012).
- <sup>242</sup>Y. Zhang, B. R. Gautam, T. P. Basel, D. J. Mascaro, and Z. V. Vardeny, "Organic bulk heterojunction solar cells enhanced by spin interaction," *Synth. Met.* **173**(1), 2–9 (2013).
- <sup>243</sup>J. M. Lupton, D. R. McCamey, and C. Boehme, "Coherent spin manipulation in molecular semiconductors: Getting a handle on organic spintronics," *Chem. Phys. Chem.* **11**(14), 3040–3058 (2010).
- <sup>244</sup>M. Kinoshita, N. Iwasaki, and N. Nishi, "Molecular spectroscopy of the triplet state through optical detection of zero-field magnetic resonance," *Appl. Spectrosc. Rev.* **17**(1), 1–94 (1981).
- <sup>245</sup>*Organic Photovoltaics: Materials, Device Physics, and Manufacturing Technologies*, edited by C. Brabec, U. Scherf, and V. Dyakonov (Wiley-VCH, Weinheim, 2008), p. 575.
- <sup>246</sup>V. I. Krinichnyi, "LEPR spectroscopy of charge carriers photoinduced in polymer/fullerene composites," in *Encyclopedia of Polymer Composites: Properties, Performance and Applications*, edited by M. Lechkov and S. Prandzheva (Nova Science Publishers, Hauppauge, New York, 2009), pp. 417–446.
- <sup>247</sup>V. Dyakonov, "Spectroscopy on conjugated polymer devices," in *Primary Photoexcitations in Conjugated Polymers: Molecular Exciton Versus Semiconductor Band Model*, edited by N. S. Sariciftci (World Scientific, Singapore, 1997), Chap. 10.
- <sup>248</sup>V. I. Krinichnyi, "Dynamics of charge carriers photoinduced in 3 poly(3-dodecylthiophene)/fullerene composite," *Acta Mater.* **56**(7), 1427–1434 (2008).
- <sup>249</sup>V. I. Krinichnyi, "Dynamics of charge carriers photoinduced in poly(3-dodecylthiophene)/fullerene bulk heterojunction," *Sol. Energy Mater. Sol. Cells* **92**(8), 942–948 (2008).
- <sup>250</sup>V. I. Krinichnyi and E. I. Yudanova, "LEPR spectroscopy of charge carriers photoinduced in polymer/fullerene bulk heterojunctions," *J. Renew. Sust. Energ.* **1**(4), 043110 (2009).
- <sup>251</sup>V. I. Krinichnyi and A. A. Balakai, "Light-induced spin localization in poly(3-dodecylthiophene)/PCBM composite," *Appl. Magn. Reson.* **39**(3), 319–328 (2010).
- <sup>252</sup>V. I. Krinichnyi, E. I. Yudanova, and N. G. Spitsina, "Light-induced EPR study of poly(3-alkylthiophene)/fullerene composites," *J. Phys. Chem. C* **114**(39), 16756–16766 (2010).
- <sup>253</sup>R. A. J. Janssen, D. Moses, and N. S. Sariciftci, "Electron and energy transfer processes of photoexcited oligothiophenes onto tetracyanoethylene and C<sub>60</sub>," *J. Chem. Phys.* **101**(11), 9519–9527 (1994).
- <sup>254</sup>K. Marumoto, Y. Muramatsu, N. Takeuchi, and S. Kuroda, "Light-induced ESR studies of polarons in regioregular poly(3-alkylthiophene)-fullerene composites," *Synth. Met.* **135**(1–3), 433–434 (2003).
- <sup>255</sup>K. Takeda, H. Hikita, Y. Kimura, H. Yokomichi, and K. Morigaki, "Electron spin resonance study of light-induced annealing of dangling bonds in glow discharge hydrogenated amorphous silicon: Deconvolution of electron spin resonance spectra," *Jpn. J. Appl. Phys., Part 1* **37**(12A), 6309–6317 (1998).
- <sup>256</sup>V. V. Yanilkin, N. V. Nastapova, V. I. Morozov, V. P. Gubskaya, F. G. Sibgatullina, L. S. Berezhnaya, and I. A. Nuretdinov, "Competitive conversions of carbonyl-containing methanofullerenes induced by electron transfer," *Russ. J. Electrochem.* **43**(2), 184–203 (2007).
- <sup>257</sup>O. G. Poluektov, S. Filippone, N. Martín, A. Sperlich, C. Deibel, and V. Dyakonov, "Spin signatures of photogenerated radical anions in polymer-[70]fullerene bulk heterojunctions: High frequency pulsed EPR spectroscopy," *J. Phys. Chem. B* **114**(45), 14426–14429 (2010).
- <sup>258</sup>V. I. Krinichnyi and E. I. Yudanova, "Structural effect of electron acceptor on charge transfer in poly(3-hexylthiophene)/methanofullerene bulk heterojunctions," *Sol. Energy Mater. Sol. Cells* **95**(8), 2302–2313 (2011).
- <sup>259</sup>V. I. Krinichnyi and E. I. Yudanova, "Light-induced EPR study of charge transfer in P3HT/PC71BM bulk heterojunctions," *J. Phys. Chem. C* **116**(16), 9189–9195 (2012).
- <sup>260</sup>B. Wessling, "New insight into organic metal polyaniline morphology and structure," *Polymers* **2**, 786–798 (2010).

- <sup>261</sup>V. I. Krinichnyi, H. K. Roth, M. Schrödner, and B. Wessling, "EPR study of polyaniline highly doped by *p*-toluenesulfonic acid," *Polymer* **47**(21), 7460–7468 (2006).
- <sup>262</sup>V. I. Krinichnyi, S. V. Tokarev, H. K. Roth, M. Schrödner, and B. Wessling, "EPR study of charge transfer in polyaniline highly doped by *p*-toluenesulfonic acid," *Synth. Met.* **156**(21–24), 1368–1377 (2006).
- <sup>263</sup>P. K. Kahol, "Magnetic susceptibility of polyaniline and polyaniline-polymethylmethacrylate blends," *Phys. Rev. B* **62**(21), 13803–13804 (2000).
- <sup>264</sup>F. J. Adrain and L. Monchick, "Theory of chemically induced magnetic polarization. Effects of  $S-T_{\pm 1}$  mixing in strong magnetic fields," *J. Chem. Phys.* **71**(6), 2600–2610 (1979).
- <sup>265</sup>B. Yan, N. A. Schultz, A. L. Efros, and P. C. Taylor, "Universal distribution of residual carriers in tetrahedrally coordinated amorphous semiconductors," *Phys. Rev. Lett.* **84**(18), 4180–4183 (2000).
- <sup>266</sup>V. I. Krinichnyi and E. I. Yudanova, "Light-induced EPR study of charge transfer in P3HT/*bis*-PCBM bulk heterojunctions," *AIP Adv.* **1**(2), 022131 (2011).
- <sup>267</sup>J. S. Moon, J. Jo, and A. J. Heeger, "Nanomorphology of PCDTBT:PC70BM bulk heterojunction solar cells," *Adv. Energy Mater.* **2**(3), 304–308 (2012).
- <sup>268</sup>F. Lux, "Synthesis and characterization of electrically conductive polyaniline and its mixtures with conventional polymers," Ph.D. thesis (Technical University of Berlin, 1993).
- <sup>269</sup>O. N. Timofeeva, B. Z. Lubentsov, Y. Z. Sudakova, D. N. Chernyshov, and M. L. Khidekel, "Conducting polymer interaction with gaseous substances. I. Water," *Synth. Met.* **40**(1), 111–116 (1991).
- <sup>270</sup>P. N. Adams, P. J. Laughlin, A. P. Monkman, and A. M. Kenwright, "Low temperature synthesis of high molecular weight polyaniline," *Polymer* **37**(15), 3411–3417 (1996).
- <sup>271</sup>P. N. Adams and A. P. Monkman, UK patent application 2287030 (1997).
- <sup>272</sup>P. N. Adams, P. Devasagayam, S. J. Pomfret, L. Abell, and A. P. Monkman, "A new acid-processing route to polyaniline films which exhibit metallic conductivity and electrical transport strongly dependent upon intrachain molecular dynamics," *J. Phys.: Condens. Matter* **10**(37), 8293–8303 (1998).
- <sup>273</sup>J. S. Hyde and W. Froncisz, "The role of microwave frequency in EPR spectroscopy of copper complexes," *Annu. Rev. Biophys. Bioeng.* **11**, 391–417 (1982).
- <sup>274</sup>A. A. Galkin, O. Y. Grinberg, A. A. Dubinskii, N. N. Kabdin, V. N. Krymov, V. I. Kurochkin, Y. S. Lebedev, L. G. Oransky, and V. F. Shuvalov, "EPR spectrometer in 2-mm range for chemical research," *Instrum. Exp. Tech.* **20**(4), 1229–1229 (1977).